THÈSE

L'Université de Pau et des Pays de l'Adour

Ecole doctorale des sciences exactes et de leurs applications
Pour obtenir le grade de

DOCTEUR

Discipline： chimie analytique, environnement et matériaux
Le 25 Septembre 2017

SHUANGLONG WANG

High resolution elemental and molecular mass spectrometry for studies of endogenous metal-containing molecules in living organisms

Développement de méthodes analytiques basées sur la spectrométrie de masse de haute résolution pour l'étude de molécules contenant des métaux chez les organismes vivant

M. CAKMAK Ismail	Professor	Sabanci University, Istanbul, Turkey
M. MARI Stéphane	Researcher director	INRA, Montpellier
M. LOBINSKI Ryszard	Researcher director	CNRS, IPREM, Pau
Mme KRASNODEBSKA-OSTREGA Beata	Assistant professor, HDR	Warsaw University, Warsaw, Poland
Mme SZPUNAR Joanna	Research engineer, HDR	CNRS, Pau, France
M. OUERDANE Laurent	Assistant professor	UPPA, IPREM, Pau

Examination Committee:

To be defended on 25th September 2017

CONTENTS

PART I.

INTRODUCTION AND REASEARCH GOALS

I. INTRODUCTION AND REASEARCH GOALS

Several metal (Fe, Zn, Cu, Mn, Ni, Co, Mo…) ions are essential for a large number of biological processes. The deficiency of some of them or their excess leads to severe growth impairment or cell death. Living organisms often face a significant stress due to the limitation in the bioavailability in their close environment for most of these essential metals. It can be due to their low concentrations, their low solubility, and excess of other metal ions competing for the necessary ligands. To overcome these issues, one of the more efficient strategies is to produce and export particular molecules that will form metal complexes to improve or decrease metal uptake. The resulting chemical forms highly influence the capacity of organisms to handle these metal ions (essential or toxic).

Once in a plant which is used as food, especially staple food, the problem of bioavailability of essential elements to organisms higher in the trophic chain (consumers) is of acute importance. Iron (Fe) is essential for virtually all living organisms. Inadequate intake of iron results in iron-deficiency anemia (IDA), especially in children, and is a serious problem worldwide. The main reason of IDA is the poor availability of iron in foodstuffs of plant origin. Only 5-20% of the iron in maize can be assimilated by man. Therefore, different breeding and genetic engineering strategies were investigated to increase the bioavailability of iron in maize with the goal of increasing the concentration of iron-binding chelators and proteins, decreasing the concentration of absorption inhibitors and increasing the concentration of absorption promoters.

The mechanisms governing the bioavailability are intimately interwoven with the characteristics (speciation) of the chemical forms of metals (coordination complexes) present. Therefore, the understanding of these mechanisms is critically dependent on the knowledge of the metal speciation, the identity and quantity of the individual species present. Further, the description of the bioavailability of iron in food on the molecular level and linking this data with molecular biology approaches is of potential interest.

There exist various analytical methodologies for identification of metal complexes, each having its limitations and advantages [1]. The most widely used methods include nuclear magnetic resonance (NMR) spectroscopy, X-ray crystallography, and liquid chromatography-mass spectrometry (LC-MS). Although NMR has the ability to provide structural information and also has advantage of being non-destructive, quick and easy in terms of sample preparation, the sample purity and amount required can be a practical limitation in many applications [2]. X-ray crystallography has low sensitivity and throughput,

and the need for the sample to be in a purified and crystalline form [1]. Therefore, the combination of liquid chromatography (LC) separation and mass spectrum detection, using elemental (inductively coupled plasma, ICP) or molecular (electrospray ionization) MS has emerged as a principal methodological approach to in-vivo studies because of low detection limits, availability and rapidity [3]. The coupled techniques can overcome the challenge of sample complexity, and produced data on previously unreported molecules.

A number of improvements at different levels of an analytical protocol, eventually enabling direct large-scale identification of metal–metabolite complexes, their semiquantitative determination and the elimination of analytical artifacts, have recently been reported. The pivotal technique is hydrophilic interaction liquid chromatography (HILIC) coupled with mass spectrometry. This coupling was employed for the very first time to achieve the separation and identification of metal complexes for the speciation of nickel in the plant Thlaspi caerulescens [4] and later used for different studies. The technique offers the potential of multispecies separation with online control of metal recovery from the column, potential species transformations and separation efficiency by inductively coupled plasma mass spectrometry (ICP-MS). De novo species identification is possible, by the online detection by high-resolution (> 100 000) Fourier transform mass spectrometry (FTMS) which allowed the elimination of isobaric interferences plaguing earlier studies. Consequently, an unambiguous observation of isotopic patterns and identification of the compounds by accurate (> 1 ppm) molecular mass measurement and the validation of the identification by tandem MS has become possible [5].

The goal of the study was to explore the potential of the hyphenated techniques to two challenging questions regarding metal speciation, in particular iron, in biological systems and attempt of using it for the description of the essential metal bioavailability of the molecular level.

The first of these studies addresses metallophores produced by some bacterial and fungal species under different growth conditions, metallophores many of which are still unknown [6]. In particular, the potential of the high accuracy mass measurement yielding very definitive molecular mass assignments and isotopic patterns of both the iron isotopes and other elements present in the molecule looked promising to be explored for the discovery of novel molecules. The systems studied were two bacteria *Staphylococcus aureus* and *Pseudomonas aeruginosa* well known in terms of genetics and molecular biology perspective which has open a field for an interdisciplinary collaboration in frame of a project funded by the French National

Research Agency (ANR)

The second study was related to the question of iron bioavailability from a staple food, maize. There is no information on the distribution of iron amongst its major chemical constituents (e.g. proteins or polysaccharides) nor on the chemical speciation of iron whereas only few literature works evoked speciation –related information in plants in general: the presence of iron mugineic acid complexes[7], iron – phytate complex which was considered main inhibitors of iron bioavailability , and some other amino acid complexes, especially citrate [8].A particular interest was in the study of well characterized genetically modified maize varieties having shown difference in the in vivo bioavailability [9-11] with an attempt to correlate the chemical information with bioavailability data obtained using the Caco-2 cells method.

References

1. Walker, L.R., et al., *Unambiguous identification and discovery of bacterial siderophores by direct injection 21 Tesla Fourier transform ion cyclotron resonance mass spectrometry.* Metallomics, 2017. **9**(1): p. 82-92.
2. Lin, C.Y., et al., *Evaluation of metabolite extraction strategies from tissue samples using NMR metabolomics.* Metabolomics, 2007. **3**(1): p. 55-67.
3. Tomer, K.B., *Separations Combined with Mass Spectrometry.* Chemical Reviews, 2001. **101**(2): p. 297-328.
4. Ouerdane, L., et al., *Speciation of non-covalent nickel species in plant tissue extracts by electrospray Q-TOFMS/MS after their isolation by 2D size exclusion-hydrophilic interaction LC (SEC-HILIC) monitored by ICP-MS.* Journal of Analytical Atomic Spectrometry, 2006. **21**(7): p. 676-683.
5. Kind, T., et al., *Identification of small molecules using accurate mass MS/MS search.* Mass Spectrometry Reviews, 2017.
6. Ghssein, G., et al., *Biosynthesis of a broad-spectrum nicotianamine-like metallophore in Staphylococcus aureus.* Science, 2016. **352**(6289): p. 1105-1109.
7. Cook, J.D., et al., *Food Iron Absorption Measured by an Extrinsic Tag.* Journal of Clinical Investigation, 1972. **51**(4): p. 805-815.
8. Bou Khouzam, R., et al., *Trace element speciation in food: State of the art of analytical techniques and methods.* Pure and Applied Chemistry, 2012. **84**(2).
9. Weber, G., G. Neumann, and V. Römheld, *Speciation of iron coordinated by phytosiderophores by use of HPLC with pulsed amperometric detection and AAS.* Analytical and bioanalytical chemistry, 2002. **373**(8): p. 767-771.
10. Persson, D.P., et al., *Simultaneous iron, zinc, sulfur and phosphorus speciation analysis of barley grain tissues using SEC-ICP-MS and IP-ICP-MS.* Metallomics, 2009. **1**(5): p. 418-426.
11. Teucher, Olivares, and Cori, *Enhancers of iron absorption: ascorbic acid and other organic acids.* International journal for vitamin and nutrition research, 2004. **74**(6): p. 403-419.

PART II.

LITERATURE OVERVIEW

PART II. LITERATURE OVERVIEW

Chapter 1. Functions of Fe, Co, Ni, Zn and Cu in bacteria and plants

1.1. Essentiality and toxicity

Elements play a vital role in the life cycle of living organisms. They are present as essential macronutrients (such as carbon, oxygen, hydrogen, nitrogen, sulfur, phosphorous, magnesium or calcium), whereas limited contents of iron, manganese, zinc, copper, nickel or molybdenum are considered as essential micronutrients. Some elements, including cobalt, silica, selenium, chromium or vanadium are not essential in plant physiological processes but they are involved in plant growth. Other elements, such as cadmium, lead or aluminum, may be non-essential or even toxic. The brief introduction focused on the most important elements involved in this study is given in the following sections.

Iron. As the second most abundant metal on the earth's crust iron is a significant element involved in the life process of living organisms [1]. Iron is an important component of enzymes, but also an inevitable ion during oxygen transportation. Iron also participates in many bio-oxidation processes benefiting from the mutual conversion between iron (Fe^{2+}) and iron (Fe^{3+}) ions [2].

Fe is essential for plant growth and, consequently, plants tightly control Fe homeostasis and react to Fe deficiency as well as Fe overload [3]. Plants acquire Fe mainly via the rhizosphere from water and soil. The source of iron in surface water is anthropogenic, mainly caused by mining activities, for example the emission of iron (Fe^{2+}) occur as a result of the oxidation of iron pyrite (FeS_2), commonly found in coal seams [1]. The average content in soils depends on the region and varies from 20 to 40 $g \cdot kg^{-1}$ in many cultivated soil[4]. The solubility of crystalline Fe minerals in soil is usually very low; however, the interaction with plant, microbes, and organic substance results in the formation of soluble FeIII complexes and increase the availability of Fe for plant growth. Microbes release siderophores and plant exudates, which can bind and solubilize the Fe present in minerals [5]. The average Fe contents of different cereals range from 31 to 98 $mg \cdot kg^{-1}$ [6]. The existence of cadmium and cobalt has

been reported to exacerbate iron deficiency. Cd can interfere with the movement of Fe from roots to shoots because the cadmium treatment of Brassica napus can lead to a sharp increase in the amount of Fe accumulation in the roots and the Fe deficiency in the shoots. Fe content in the xylem and phloem also significantly decreases the Level rise. This suggests that the presence of Cd attenuates Fe at least in the European rape to obtain phloem rather than ingestion. A similar phenotype was observed in mung bean seedlings with increased Co: Fe uptake, but Fe could not move from the roots to the shoots. In addition, the Fe deficiency reaction in Arabidopsis thaliana is upregulated in Co-treated plants [7]. To increase the bioavailability one obvious approach is to disrupt phytate biosynthesis. Early attempts to reduce phytic acid across the whole plant successfully reduced accumulation in seeds, but these plants often germinated poorly and were more susceptible to stress. A second approach is to overexpress ferritin in seeds. Although the mechanism of dietary ferritin uptake in the human gut is unknown, it is believed that the Fe complexed in ferritin is readily absorbed, and a highly accessible source of Fe [7].

Bacteria obtain iron from transferrin, ferritin, hemoglobin and other iron-containing proteins of their host [8]**.** It is a critical ability for bacteria survival and growth, so successful bacterial pathogens have evolved into competitive iron in host tissue and body fluids. The intracellular concentrations of Fe (II) directly control the expression of a large number of genes by complexion with regulatory proteins. In this way, the biochemical processes of bacteria can be adapted to the host's challenge. Drugs that interfere with the metabolism of iron in bacteria may have a great potential in chemotherapy [8].

Cobalt. Cobalt is a transition metal, which is not essential for plants. It has several possible oxidation states; under physiological conditions, the oxidation state of Co is predominantly II and III, which makes Co a catalyst for Fenton's reaction [9]. The average content of Co in plant varies between 0.05 and 0.30 mg/kg. The beneficial effects of Co supply are related to symbiotic rhizobia in the leguminous nodules and require the activity of several enzymes involved in vitamin B12

(cobalamine) nitrogen fixation [10]**.** Benefits of cobalt include delaying leaf senescence by inhibiting ethylene biosynthesis and increasing seed drought tolerance [11]. Cobalt toxicity is associated with oxidative stress, photosynthesis and inhibition of iron deficiency [11]. It has been reported that cobalt has undermined the stability of iron and competed with iron in many organisms (including plants) to obtain transporters. Once in cells, ferroportins work in Co detoxification and also can transfer Co^{2+} into inside vacuoles of root epidermal and cortical cells **,** so chelated Co can be loaded into xylem and transferred to the shoot thus protecting against Ni over-accumulation during Fe deficiency[12]. Co tolerance and accumulation are still not fully understood[13]**..** It was found that some Co accumulators can also work on copper; some tolerance and / or accumulation mechanisms are considered to be shared by the two metals. A key aspect of Co (hyper)accumulation by some plants is expected to be a means of detoxification preventing the accumulation of free ions that can induce oxidative stress[13].

The knowledge of pathways for transporting cobalt to bacteria is important to study the regulation of bacteria biological processes. It has been shown that the availability of cobalt by methanogenic production of methane produced by methane and sulfate-reducing bacterium Desulfococcus multivorans to limit mercury methylation, and it has been proposed availability of cobalt might influence the composition of phytoplankton assemblages in the open ocean. Marine cyanobacterium *Prochlorococcu*s requires cobalt for growth, and it seems to synthesize and produce aggregated cobalt-binding ligands that enhance cobalt co-enrichment[14]. Cobalt can also be directly associated with a cobalt-dependent enzyme (non-protease) [14]. In order to obtain sufficient cobalt metabolism, the bacteria have a high affinity absorption system to remove Co^{2+} from the environment. When the external metal concentration is very high, Co^{2+} accumulation may become toxic and excess Co^{2+} can be removed from the cell through the efflux system [15].

Nickel. Nickel belongs to the group of micronutrients and in the biological systems its oxidation state is usually Ni(II) but other valences-Ni(I) and Ni(III) are

also possible. It is essential for the growth of temperate cereal crops. The concentrations reported were 40-80 ng/g (dry weight) in barley grains [16]. In a wide range of higher plants nickel is a constituent of the enzyme – urease, where it is bound by N- and O-ligands and is substantial to maintain structure and catalytic function of the enzyme. [17]. Nickel together with urease is involved in nitrogen metabolism which is essential for higher plants and its deficiency may have severe effects on plant growth, ageing, disease resistance, nitrogen metabolism, iron uptake and also the normal grain development. [18]

Since the preliminary study on the Ni-dependent growth of the oxidized bacteria in 1965 [19], the progress of studies of Ni absorption and utilization in bacteria has been accelerating. Several Ni sensors/modifiers have been identified, but their precise mechanisms for interacting with metal ions and their specific regulatory DNA sequences need further study [20]. The progress in understanding the structure and mechanism of nine known Ni enzymes is very advanced, but role of metal ions in catalysis is still unclear. Similarly, the maturation mechanisms of Ni permease systems are beginning to be understood, but the basic questions about the availability of Ni, the basis of specificity, and the role of helper proteins in cells are still there[19].

Copper. Copper is an essential redox-active transition metal that is involved in many physiological processes in plants. Under physiological conditions in vivo it can exist as Cu^{2+} and Cu^{+}. Copper acts as a structural element in regulatory proteins and participates in photosynthetic electron transport, mitochondrial respiration, oxidative stress responses, cell wall metabolism and hormone signaling[21]. Copper ions act as cofactors in many enzymes such as Cu/Zn superoxide dismutase (SOD), cytochrome c oxidase, amino oxidase, laccase, plastocyanin and polyphenol oxidase[22]. At the cellular level, Cu also plays an essential role in signaling of transcription and protein trafficking machinery, oxidative phosphorylation and iron mobilization. Thus, plants require Cu as an essential micronutrient for normal growth and development; when this ion is not available plants develop specific deficiency symptoms, most of which affect young leaves and reproductive organs[22]. The redox properties, that make Cu

an essential element, also contribute to its inherent toxicity. Redox cycling between Cu^{2+} and Cu^{+} can catalyze the production of highly toxic hydroxyl radicals, with subsequent damage to DNA, lipids, proteins and other biomolecules. Thus, at high concentrations (<1μM), Cu can become extremely toxic causing symptoms such as chlorosis and necrosis, stunting, leaf discoloration and inhibition of root growth with damage evident at external concentrations of 0.2μM[23]. At the cellular level, toxicity may result from i) binding to sulfhydryl groups in proteins, thereby inhibiting enzyme activity or protein function; ii) induction of a deficiency of other essential ions; iii) impaired cell transport processes; iv) oxidative damage. Cu concentrations in cells need to be maintained at low levels (as the apparent LC50 for Cu^{2+} was 0.22 mM) [21] since this element is extremely toxic in view of its high redox properties [21]. The average content of Cu in plant tissue is 10 $\mu g.g^{-1}$ dry weight [22].

Copper is a significant micronutrient required for the catalytic center of the enzyme as a redox cofactor. However, due to its high chemical reactivity, free copper is potentially dangerous. Thus, the organism exerts strict control over Cu + transport (import and export) and flow through different compartments to ensure the in vivo balance and prophylactic effects of copper protein synthesis. Recent studies based on biochemistry, bioinformatics and metal proteomics have revealed a highly regulated system of transcriptional regulators, soluble molecular chaperones, membrane transporters, and target proteins distributed in various bacterial compartments[24]. The accumulation of copper as a resistance mechanism is clearly not uncommon because it has been observed that several copper-tolerant *Pseudomonas* and copper-resistant *rhizobia loti* have accumulated copper[25]. In addition, some species of the strain did not have a known copper to select the history of accumulated copper and had resistance. In these bacteria, copper accumulation may have a beneficial effect, rather than resisting high levels of copper. The resistance of these strains may be only a secondary effect of the more efficient evolution of copper transport and storage systems[25].

Zinc. Zinc is a substantial micronutrient that plays different roles in the plant

physiology. The normal range for zinc in plant tissue is 15-60 ppm and in the growing medium between 0.10-2.0 ppm [26]. Zinc deficiency or toxicity does not often occur; however, they both negatively impact crop growth and quality. Any deficiency or toxicity has to be addressed before crop damage is irreversible. Plants are taking up zinc typically as a divalent cation which is redox-stable under physiological conditions. [27] Zinc has a strong tendency to form the covalent bonds with N-, O and S-ligands that causes this element to be an essential component of thousands of proteins and enzymes in plants. In enzymes zinc has catalytic (e.g., carbonic anhydrase and carboxypeptidase), co-catalytic or structural (e.g., alcohol dehydrogenase) function[27]. It is also responsible for gene regulation and stabilization of the protein structure including Zn fingers, Zn clusters and RING finger domains[28]. Zinc is plays important role in ribosomes structure where it is required for maintaining their structural integrity [29]. It might be bound by phospholipid and sulfhydryl groups of membrane components and thereby maintain the integrity of biomembranes [29]. Zinc is also involved in the processes such as photosynthesis and CO_2 fixation. Excess and deficiency of zinc in plants lead to high plant mortality, reduced and stunted growth, chlorosis, necrosis, small leaves and delay in flowering[26].

Zinc ions play an indispensable role in bacteria biochemistry. However, the bacteria have an impressive ability to obtain Zn^{2+} from the environment, making it particularly difficult to achieve a lack of Zn^{2+}, so a comprehensive understanding of the importance of Zn^{2+} has not yet been achieved[30]. Like the reports said the Zn^{2+} content of Escherichia coli growth medium was reduced to below 60 nM, without resorting to a specific chelating agent. The growth rate of cells in Zn^{2+} deficient medium decreased and the intracellular Zn^{2+} content was up to 5 times. However, as for all metals, if accumulated too much, Zn^{2+} may be toxic. It is surprising that this conclusion comes from experiments where the Zn^{2+} level in the culture medium is reduced only by reducing its amount [31], Making the depleted Zn^{2+} of this bacteria is very difficult. Add Zn^{2+} , no metal extraction or chelate.

Trace metals deficiency results in pathological damage or alterations in plants or bacteria. This damage is reversible when metal levels come back to normal levels. However, when the concentrations of these essential metals increase to a threshold value, their presence become suppressed then toxic and even lethal for the organism. In this moment previous essential metals act like toxic metals. The only difference is that toxic metals have a direct toxic or lethal effect at very low concentration values, even in different stage of the life process requirement of metals are different. For example, Cu and Zn, in low concentrations, are essential to the life processes acting as constituents of various proteins, enzymes and cofactors in many living organism. But, depending on the tolerance of the organism, copper may induce mortality or sub lethal stress that reduces the ability of the organism to compete effectively in its habitat. Dose-response curves for essential trace metals illustrate that metal deficiency or accumulation outside a specific concentration range are poisonous for the cells. Generally speaking the toxicity of a metal depends on the amount of metal presence in the organism.

1.2. *S*trategies of metal mobilization, uptake, transport and storage/elimination

Many proteins and enzymes contain metals and it is well established that their biological activity will depend on the presence of the metal so strategies of metal mobilization, uptake, and transport are of utmost importance.

Iron: The ability of plants to respond to Fe availability ultimately affects human nutrition, both in terms of crop yield and the Fe concentration of edible tissues. Thus, elucidating the mechanisms of Fe uptake and transport is essential for the breeding of crops that are more nutrient rich and more tolerant of Fe-limited soils[7]. Although Fe is one of the most abundant metals in the earth's crust, its availability to plant roots is very low. Fe availability is dictated by the soil redox potential and pH. In soils that are aerobic or of higher pH, Fe is readily oxidized, and present predominately in the form of insoluble ferric oxides. At lower pH, the ferric Fe is freed from the oxide, and becomes more available for uptake by roots[7].

The strategies developed by plants include: (i) reduction-based strategy: in response to Fe deficiency, protons are released into the rhizosphere lowering the soil pH and making Fe more soluble, the ferric chelate reductase reduces Fe (III) to Fe (II), which can then be transported into the root epidermis by the divalent metal transporters, (ii) chelation-based strategy the uptake of Fe chelated by soluble plant siderophores (PS) with a high affinity for Fe^{3+} synthesized from L-methionine and released from the root epidermis in response to Fe deficiency; the resulting Fe (III)-PS complexes are readily transported into the root epidermis via a high-affinity uptake system [3].

Plants have developed complex mechanisms to absorb Fe from the soil and transport it from roots to shoots and grains. In order to obtain Fe from the soil, gramineous plants secrete small molecules called papaya acid plant cells (MAs), and their dissolved Fe, Fe (III) -MA complexes are easily absorbed by specific transporters on the root surface. In recent years, significant advances have been made in elucidating the MA biosynthetic pathway, identifying proteins that transport Fe in various forms, and reveal transcription factors that control Fe homeostasis[32].

Several strategies of iron scavenging have been identified in pathogenic bacteria, including the reduction of iron into ferrous iron, the presence of intracellular niche, the use of host iron compounds and the formation of iron carriers. Although direct evidence suggests that only a few cases have provided a high affinity mechanism for iron function, many of these systems are likely to play a central role in the pathogenesis of infection [7]. In order to combat invasive bacteria, animals enter the iron metabolism pattern; some invasive bacteria may react by producing a specific iron chelator-iron carrier, which removes iron from the host source. Other bacteria rely on direct contact with the host ferritin, or extract iron on its surface, or absorb it into the cytoplasm like heme[33].

Recently (**Fig. 1.1**) siderophore production by different *Pseudomonas* species has been widely studied and is found to be dependent on iron content present in soil. Meanwhile this suggests a high amount of siderophore produced by RSP5 solubilized

more iron from soil and transported iron more efficiently to various plant parts of Maize (dietary food) than RSP8. The increased iron content in the stem, leaf, and the seed of Maize will be beneficial for the supplementation of dietary iron (non-heme) in human food and animal and feed[34].

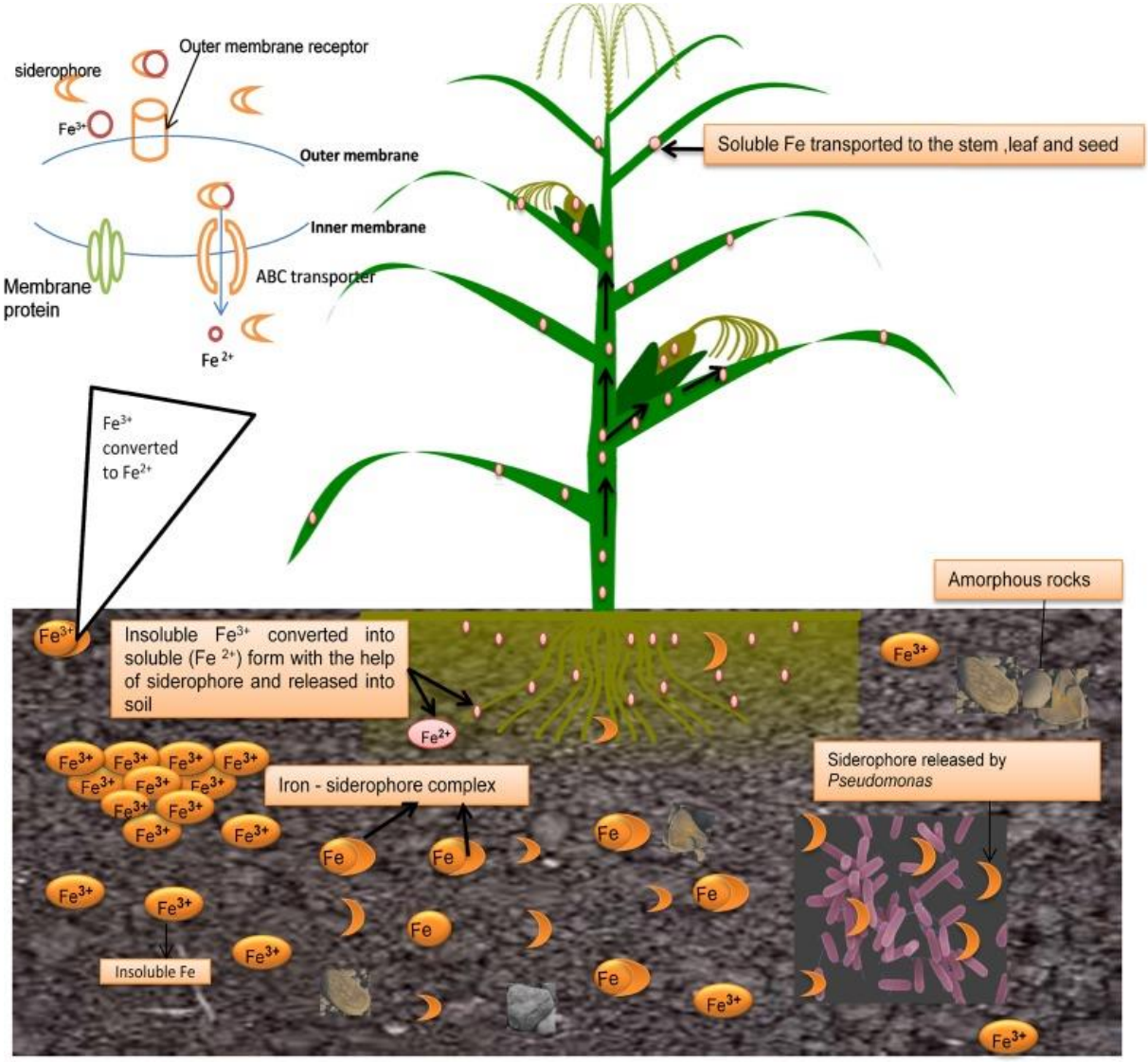

Fig. 1.1 Schematic representation of iron transportation to stem, leaf, and seed with the help of siderophore released by *Pseudomonas* [34].

Cobalt, nickel and copper. Two types of uptake mechanisms, ABC transporters and Ni-specific permeation enzymes have been identified in many microbes, but many of the molecular details about these systems remain to be elucidated. The total concentration of cobalt and nickel was found to be close to the detection limit of

ICP-MS in aerobic growth of E. coli, as low as sub-μM. This is consistent with the expression of low-nickel metallases under these growth conditions, and their presence in only a few metallases relative to enzymes containing Fe, Zn and Mn. Nickel has been identified as a necessary cofactor for nine different enzymes, including NiFe-hydrogenase, Ni-superoxide dismutase and urease[35].

Zinc There is no subcellular layer deposition of excess metals, bacteria in the Zn^{2+} in vivo balance depends mainly on strict import and export mechanism[36]. The predominantly high - affinity Zn^{2+} uptake system is the ABC transporter ZnuABC. Escherichia coli has an impressive ability to obtain and concentrate Zn [37]

The available literature presents three types of systems able to mediate metal ion transport through membranes (**Fig. 1.2**). Channel proteins utilize the chemical or electrical potential of the membrane to drive the transport of the substrate [S] through a pore in the membrane.

Carrier proteins undergo a conformational change to facilitate movement of ions across membranes using the concentration gradient of [S] or the gradient of a cosubstrate [S']. The co-substrate can be transported in the same direction as the substrate (symport) or in the opposite direction (antiport).Pumps utilize energy, usually provided by adenosine triphosphate (ATP) hydrolysis (directly) to drive the transport of substrate[38, 39]

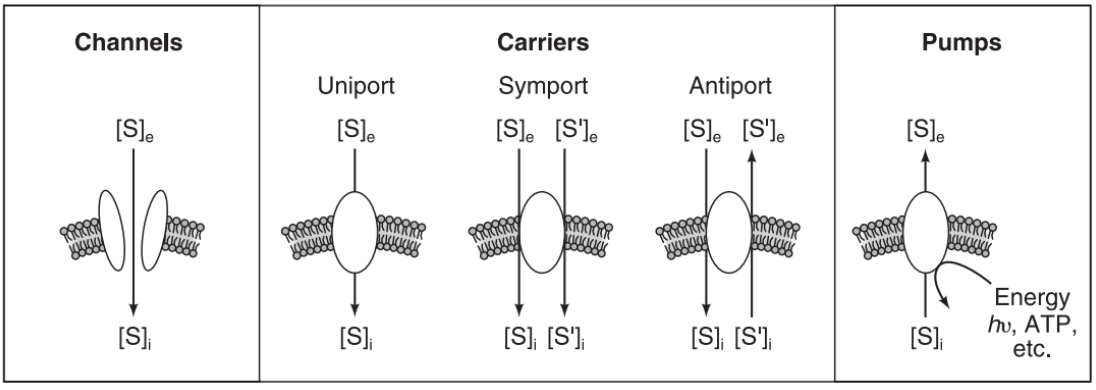

Fig. 1.2 Types of transport proteins: The substrate denoted by $[S]_e$ on the external side of the membrane and $[S]_i$ denotes substrate on the internal side of the membrane, S'– co-substrate, h_μ- energy [38, 39]

The transfer of metals across the plasma membrane of the cell most likely occurs via facilitated diffusion or by energy dependent processes: (a) transport by a membrane-protein of relatively wide specificity; (b) transport by intrinsic proteins of the plasma membrane through which metal ions pass selectively; or (c) endocytosis [40]

Once within the cell, the metal binds to a variety of existing ligands that maintain an inwardly directed diffusion gradient and prevent efflux of the metal. In this way, the electrochemical gradient is always maintained. The rates of intracellular accumulation of metals are determined by the number and binding characteristics of the available metal ligands and their accessibility. Metal uptake can be enhanced and detoxified by the synthesis of small (6-7 kDa) cysteine-rich metal-binding proteins named metallothioneins (MT) or by increased formation of mineralised granules (including phosphate and carbonate granules and excretory concretions)[40].

1.3. Low molecular weight metal complexes in plant and bacteria

Functional metalloproteins are a small proportion of the total trace-metal content in living organisms. Typically, the majority of a trace metal is distributed among low molecular weight complexes, storage metalloproteins, and insoluble forms associated with cell wall and other cell surfaces and structures. Of these, low molecular weight complexes are frequently the most abundant and of considerable importance both for the plant's metabolism and for animal and human nutrition. Electrophoretic and chromatographic experiments have demonstrated the presence of trace-metal complexes of low molecular weight in many plants (Table 1) and bacteria species (**Table 2**). Studies over the past five years have progressed in the identification and Characterization of these transporters and have provided the role of many metal ion ligands in metal homeostasis. The focus of the recent advances in elucidating the role of small organic molecules as metal-binding ligands and the nature of the proteins involved in their transport. Particularly the effect of mugineic acid (MA), nicotianamine (NA), organic acids, histidine and phytate (**Fig. 1.3**) to metal homeostasis.

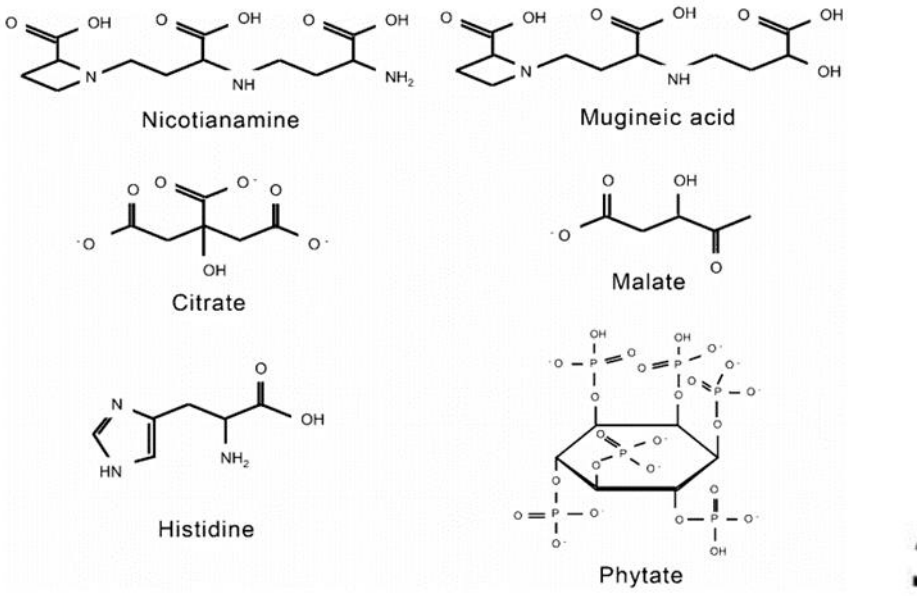

Fig. 1.3 Metal ion ligands for iron (Fe), zinc (Zn), copper (Cu), manganese (Mn) and nickel (Ni) in plants [41].

Table 1.1 Examples of low molecular weight metal complexes in plants

Metal	Species name	Plant	Experimental method (total content)	Ref.
Fe^{2+}	NA	*A. thaliana*	in vitro speciation studies	[42]
Fe^{2+}	mugineic acids	maize	HPLC–PAD HPLC–AAS	[43]
Fe^{2+}	IP6	Grains of field grown barley	SEC-ICP-MS IP-ICP-MS (40–80 ppm)	[44]
Fe^{3+}	Fe_3Cit_3 Fe_2Cit_2	xylem sap of tomato	HILIC-MS both ICP-MS and ESI-MS(TOF), the use of stable isotope (54Fe) labeling	[45]
Fe	Fe(III)-acetate	xylem sap of tomato	XANES on a highly brilliant synchrotron	[46]
Zn^{2+}	Zn-His	*T. caerulescens*	EXAFS	[47]
Zn^{2+}	Zn-NA	*T.caerulescens*	EXAFS	[47]
	Zn-phytate	*T.caerulescens*	(SEC)-ICP-MS combined with off-line ESI-MS of the Zn-containing LC fractions	[48]
Cu	Cu(II)-DMA	xylem sap of *O. sativa*	SEC with both off-line GFAAS Cu determination and off-line ESI-MS molecular detection based on exact molecular mass and isotopic signature (5-34 μM)	[49]
Cu	Cu-Cit, Mal, NA and amino acids (e.g., His)	*S. acuminata*	combination of MS and NMR	[50]
Ni	Ni-NA	*T.caerulescens* *S. acuminata*	SEC-ESI-MS/MS or SEC -ICP-MS off-line ESI-MS/MS	[51]
Ni	Ni-carboxylate malate, aconitate, erythronate, galacturonate, tartarate, aconitate, saccharate	*S. acuminata*	advanced MS and NMR techniques	[50]

For more than 60 years, the study of bioinorganic chemistry of these metal binding molecules, including basic coordination chemistry, has provided insight into the key role of metal carriers in the balance of bacteria and ions. In view of the emergence of antibiotic-resistant bacteria and the need to prevent the global growth of these superfamilies, the importance of basic chemistry to understand the biological basis of bacteria has been highlighted in recent years. Selected sidephores are listed in **Table 1.2**, out of those Enterobactin is the strongest one (Kf~10^{50}) having the capacity to chelate iron ions even from the environment with iron concentrations as low as 10^{-27}mol/L), and some of the structures are given in **Fig. 1.4** and **Fig. 1.5.**

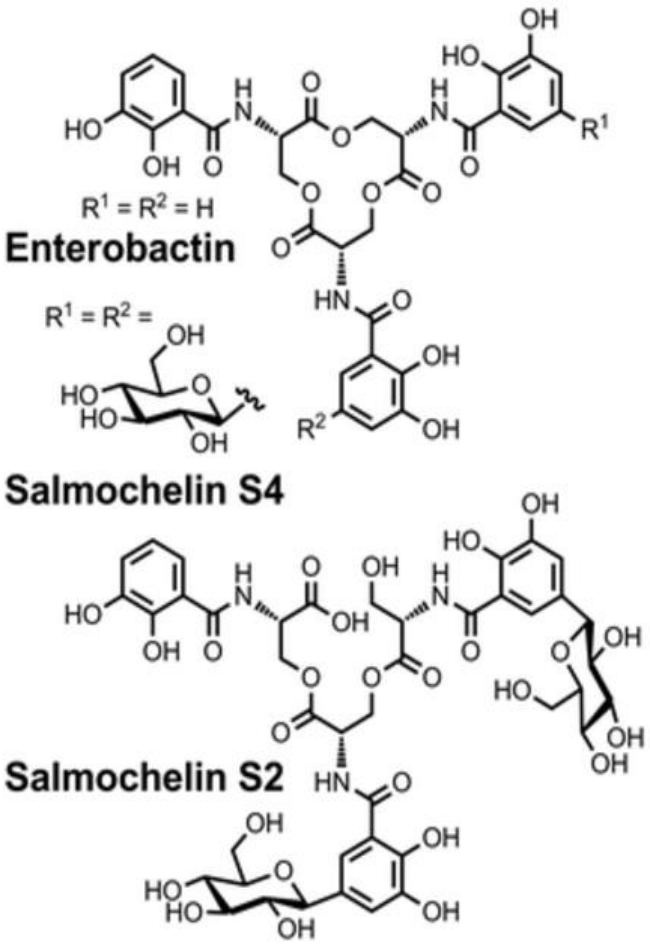

Fig. 1.4. Chemical structures of the siderophores listed in the **Table 1.2**

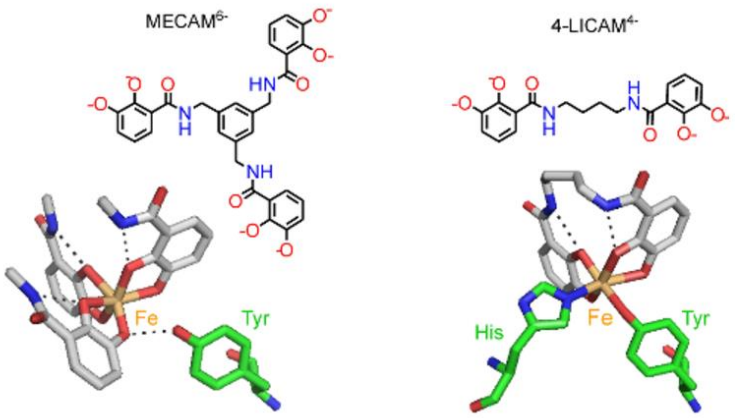

Fig. 1.5. Fe(III) (orange) coordinated to the siderophore mimics MECAM^{6-} and 4-LICAM^{4-} (coloured by atom type) with key amino acid residues in the binding pocket of CeuE shown (green cylinders as carbon atoms) [52].

Table 1.2. Examples of low molecular weight iron complexes found in bacteria (identification by FT ICR MS)

Species name	bacteria	Ref.
Ferrioxamine E and *G1*	*Streptomyces*	[53]
Sabichelin		
Ferrioxamine Et2 and *Et3*	*Campylobacter jejuni*	[52]
MECAM^{6-} *4-LICAM*$^{4-}$		
S Synechobactin C, B, etc	*Synechococcus*	[54]
Amphibactin B,C, D etc	*Vibrio*	[55]
Moanachelins Gly-C, Ala-B		
and *Gly-D*		
Enterobactin (enterochelin)	*Enterobacteriaceae family e.g.*	[56]
	Salmonella sp. and Escherichia coli	
Salmochelin (diglucosyl of	*Salmonella sp. Escherichia sp.*	[57]
enterobactin)	*Klebsiella sp.*	
Vibriobactin	*Vibrio cholerae*	[58]

Griseobactin	*Streptomyces sp. ATCC 700974 Streptomyces griseusStreptomyces lilacinus NRRL B-1968*	[59]
Alcaligin	*Alcaligenes denitrificans*	[60]
Ferrichrome	*Shigella flexneri Pseudomonas aeruginosa*	[61]
Exochelin	*Mycobacterium tuberculosis*	[62]
Amphibactin(amphiphilic siderophore)	*Vibrio sp. Alcanivorax borkumensis SK2*	[63]
α-Hydroxycarboxylate type Vibrioferrin	*Vibrio parahaemolyticus*	[64]
Legiobactin (rhizoferrin from L. pneumophila	*Legionella pneumophila*	[65]
Achromobactin	*Acinetobacter baumannii*	[66]
Pseudomonine	*Alcanivorax borkumensis SK2*	[63]
Acinetobactin	*Acinetobacter baumannii*	[67]
Gobichelin A and B	*Streptomyces sp. NRRL F-4415*	[68]
Fimsbactins A-F	*Acinetobacter baumannii, Acinetobacter baylyi*	[68]
Baumannoferrin A-B	*Acinetobacter baumannii*	[69]
Aerobactin	*Salmonella spYersinia spShigella spKlebsiella pneumoniae; Escherichia coli*	[70]
Mycobactin (amphiphilic siderophores)	*Mycobacterium tuberculosis*	[71]
Amphi-enterobactins	*Vibrio harveyi BAA-1116 (reclassified as Vibrio campbellii)*	[72]
Carboxymycobactins (amphiphilic siderophores)	*Mycobacterium tuberculosis*	[73]

Cupriachelins (amphiphilic siderophores)	*Cupriavidus sp.*	[74]
Pyoverdines	*Pseudomonas sp. e.g. P. aeruginosa.*	[74]
Pyochelin	*Pseudomonas aeruginosa*	[75]
Yersiniabactin	*Yersinia sp.Escherichia sp.*	[76] [57]

1.4. Incorporation of metals into high molecular weight species

In the newly established field of metallomics focuses on identification of biomolecules bound to metal ions and the elucidation of their physiological and biological roles to living organisms [77, 78].

Most metal ions are bound to specific proteins or enzymes and act as inherent parts of the active or structural center of the proteins, responsible for many metabolic processes, such as energy conversion in photosynthesis and respiration, gene regulation and expression, and catalytic processes[79]. It is estimated that metalloproteins are made up about a third of all the proteins of the organism [80]. **Tables 1.3** and **1.4** give examples of high molecular weight metal species identified in plants and bacteria, respectively. **Table 1.3** shows the proteins associated to metals in the oat, wheat and soybean samples[81]. In general, these proteins have a molecular weight between 7 and 72 kDa, respectively[81]. Ferritin is a subfamily of iron-binding proteins that form a multi-subunit nanoscale iron storage structure and prevent oxidative stress-induced apoptosis. The protein of the ferritin subfamily is one of the largest groups of iron-binding proteins. The members of the 12 subfamilies contain structures and evolution-related iron-binding domains that are present in a variety of different functional proteins. The ferritin subfamily consists of three different members, including ferritin, which can bind iron, and they can also act as storage molecules. These proteins are capable of achieving this function by forming a multi-subunit nanoscale cage structure that can store up to 4000 iron atoms in a large multi-subunit structure formed by ferritin. In addition, ferritin can protect cells from

iron toxicity and other free radicals, such as hydrogen peroxide [82].

Table 3. Examples of the incorporation of metals into high molecular weight species in plants [73].

Metal	protein	Plant
Cu Zn	Glycinin chain A2B1a (precursor), Glycinin A1bB2-784	oat
Mn	Nonspecific lipid-transfer protein 2G (LTP2G)	Wheat
Cu	Trypsin (EC 3.4.21.4) (precursor)	Wheat
Cu Fe Mn Zn	5a2 protein (Fragment)	Wheat
Fe Mn	Globulin Beg1 (precursor)	Soybean
Cu Mn	Putative dehydrin (Fragment)	Soybean
Cu	Proteinase inhibitor (Bowman-Birk), Dehydrin Glycinin, G5 (precursor) D-II, Glycinin A3B4 (G4) subunit, Glycinin chain A5A4B3 (precursor), Trypsin inhibitor A (Kunitz) (precursor) Glycinin chain A1aBx (precursor)	Soybean
Cu Fe Mn Zn	Glycinin chain A1aBx (precursor), Trypsin inhibitor A (Kunitz) (precursor)	Soybean

The discussion of metal uptake regulator proteins in bacteria should be more general. They include those active for ferric ions (Fur), nickel (Nur), zinc (Zur) and control metal uptake and homeostasis, are responsible for controlling the intracellular concentrations of metals[60, 83, 84].

Table 4 Selected examples of the incorporation of metals into high molecular weight species in bacteria

Metal	Species name	bacteria	Identification method, conc. level, role etc...	Ref.
Fe	ferritin, transferrin, haemoglobin and myoglobin.	E.coli strains	up to 200 mg/L	[85]
Co(II) Cu(I).	apo-CopZ	Enterococcus hirae	Q-TOF MS	[86]
Iron	Fur	Escherichia coli	Ferric iron uptake regulator	[87]
		E. coli	Ferrichrome transport	
		E. coli	Alternative sigma factor for transcription of the ferric citrate transport operon	
		E. coli	Biosynthesis of aerobactin	
		E. coli	Iron-dependent superoxide dismutase	
		E. coli	Aconitase A	
		E. coli	Shiga-like toxin	
Zinc	Zur	E. coli	Zinc uptake regulator	[88]
		E. coli	High-affinity zinc uptake system	
		B. subtilis	Zinc uptake regulator	
		B. subtilis	ABC zinc transporter	
Iron	Irr	Bradyrhizobium japonicum	Iron response regulator of haem biosynthesis	[89]
		B. japonicum	Aminolevulinic acid dehydratase	

Chapter 2. Current challenges in research of metal related physiology of plants and bacteria

Transition metals ions such as iron (Fe^{3+} Fe^{2+}), zinc (Zn^{2+}), and copper (Cu^{2+}) play vital roles in the metabolism of all living organisms. Research on the metals metabolism, transportation, storage and incorporation as cofactors in cells or organisms need a systematic approach to detect the metal concentration, identify the metal-binding complex, and investigate the existence of metal–ligand complexes in life processes. The metal speciation studies in biological samples are often confronted with analytical challenges. All those challenges are due to the relatively low contents and poor stability of the metal complexes during sample pretreatment and the subsequent steps of the analytical procedure [90].

The most critical issues include discovery and structural characterization of metal species and as well as of their quantification and comprehensive studies of the global distribution of metal among species.

2.1. Discovery and identification of new ligands

Despite many studies the list of ligands able to complex metal in plant and bacteria is not exhaustive and reports on new species appear [91]. The complexes composition depends on metal to ligands stoichiometries and metal oxidation states [92, 93]. For instance, in a solution with a 1:2 Fe:Cit ratio at pH 4, up to thirteen different Fe-Cit species were detected by ESI-MS, whereas only two species occurred in a solution prepared at 1:100 Fe:Cit ratio at the same pH [93]. As more and more ligands enter the screening process, ligand discovery initiatives are facing interesting challenges. Especially new ligand discovery, without standards available, it is extremely difficult for reliable identification of the formula, stereochemical structure and binding affinities. Both direct infusion (without prior chromatographic separation) and HPLC-electrospray ionization mass spectrometry (ESI MS) are used as a tools for the identification of novel metabolites in bacterial cultures and are widely applied in metabolomics[94]. High resolution MS instrumentation such as time-of-flight MS

[95], Orbitrap Fourier transform (FT) MS and FT ion cyclotron resonance MS (FT-ICR-MS [96]) are used due to the specificity provided by resolution of isobaric ions and highly accurate determination of mass-to-charge (*m/z*) ratios.

2.2. Quantification of species involved in metal complexation

A large majority of studies published are focused on the identification of ligands, either in confirmatory or exploratory investigations. However, reliable qualification of natural metal ligands, such as the phytosiderophores, their precursor nicotianamine and their metal complexes, in plant samples is of a particular interest. Based on the isotopic signatures of the complexed metals in molecular mass spectrometry, metal–PSs and metal–NA complexes have been found in many plant and bacteria species but almost no quantitative data have been provided. In fact, even for stable metal species, ligand exchange (altering the actual composition of the sample) reactions may occur at any step previous to detection, due to the presence of competing ligands and/or redox mediators. Ligand exchanges have already been reported in the cases of Fe(III)-NA and Fe(III)-DMA [97]. These phenomena are especially critical in separation-based methods (e.g., HPLC, CE), because the separation of the free ligand does change the metal-to-ligand ratio, and also because the pH may change considerably when organic solvent modifiers are used [45] and make the quantification particularly difficult. The column recoveries are typically at the 60-70% level [98].

Quantification on the basis of an external calibration curve is hardly feasible. The method of standard addition of iron complexes to samples is not possible either – it leads to disturbance of complexation equilibria. Post-column unspecific isotopic dilution quantification was carried out by continuously adding ^{57}Fe in EDTA between the exit of the column and the ICP MS nebulizer. The HILIC-ICP-MS intensity chromatograms were converted into Fe molar flow chromatograms using the isotope pattern deconvolution (IPD) equations. Accurate isotope abundances of the isotopically enriched solutions were determined by direct ICP-MS injections and used

for the calculations of eluted Fe-citrate complex in tomato plant xylem [99]. A broad iron peak, tentatively assigned to Fe-oxyhydroxide, was observed at unusually long retention time and considered as a possible artefact [99]. The availability of isotopic enriched materials and improved ICP-MS equipments has broadened the application fields of online ID [100].

2.3. Comprehensive studies of the distribution of metals among different species

The distribution of a metal among its various species has a major effect on its behavior and is of a particular interest in such diverse fields as toxicology, clinical chemistry, geochemistry, and environmental chemistry. It is especially important in the context of the bioavailability of essential elements, such as Fe, Zn, from plant food stuffs.

The use of a dedicated measurement approach and state-of-the-art methodologies are necessary to obtain such information [100]. However, in view of the discussion in section 2.2., it is evident that fully quantitative information is almost impossible to obtain. The recent approach in terms of element speciation, called metallomics, addresses the totality of metal species in a studied system and covers the inorganic element content and the totality of its complexes with biomolecules, particularly proteins, participating in the organism's response to beneficial or harmful conditions [101]. Compared to the conventional elemental speciation analysis, this approach is challenging, particularly given the difficulties in identification/characterization of the organic (e.g. protein) moieties of species. The complexity of the task often leads to approximate evaluation based on fractionation of the species without their full identification. As a result, the presence of individual – usually operationally defined classes of species – is reported. Eagling, T., et al reported identification by SEC-ICP-MS Fe speciation varied between milling fractions with a low molecular weight (LMW) complex likely to be Fe−deoxymugenic acid/nicotianamine being the predominant extractable Fe species in white flour, accounting for approximately 85% of the extractable Fe. Bran fractions had a lower amount of LMW-Fe form but more

as soluble Fe−phytate and an unidentified high molecular weight peak [102].

Chapter 3. Analytical methodology for metal speciation analysis in plant and bacteria

3.1. Sampling, storage and pretreatment

Sample preparation is an important, time-consuming and labor-intensive part of the analytical procedure. Sampling and sample preparation is necessary in order to limit the results bias and enable the following steps such as qualification and quantification and as such it is the significant part of the project. Errors made during the initial steps may conduct to important bias in the whole measurement process.

Sampling and storage procedures (temperature, light, etc.), can be considered as key aspects to preserve the metal species occurring in samples during the whole analytical process[103]. Temperature needs to be as low as possible to reduce metal species transformation. For this purpose, lyophilization and shock-freezing in liquid N_2 are the most common procedures used to preserve metal species in fluids. The latter is considered the safest technique to prevent metal species changes because it can be performed immediately at the sampling site and also because the sample is stored in an inert gas atmosphere. Light can cause changes in metal speciation because it can induce electron transfer reactions affecting the stability of the metal complexes and also the structural integrity of the ligands. For instance, photochemical reduction of Fe(III) complexes with ligands such as di- and tri-carboxylic acids is well known [104], and is accompanied by oxidative decarboxylation of the ligand. This issue could limit the use of irradiation with high intensity synchrotron X-rays for metal speciation [46].

Changes in the composition may occur during sample storage. This may be due to evaporation, diffusion, surface adsorption, photochemical reactions, oxidation, precipitation, biodegradation and enzymatic reactions. The plant sample may be a liquid or a solid. Fresh liquid samples are usually filtered or centrifuged and then stored in the dark at a temperature of -4°C for a short period of time and a longer period at of -20 °C. The alternative is freezing and storage as frozen samples or

lyophilization and storage of dry material. The solid samples (such as leaves, roots, etc.) after harvest are rinsed with water [89], dried or lyophilized and ground to a fine powder.

Biological processes which may occur during sample storage include biodegradation and enzymatic reactions. Again, sample degradation becomes more problematic at low analyte concentration and trace analysis. The collected samples are exposed to conditions other than the original source. For example, an analyte in a sample that is not exposed to light undergoes a significant photochemical reaction when exposed to sunlight. The completeness of any sample cannot be retained indefinitely. A practical way is to run a test to check if the sample can last for a long time without degradation and then complete the analysis within that time [105].

Changes of the metal complexes present in the plant liquid during sampling and/or storage, and especially during sample preparation brings on the challenge in separation and determination. That is because[106]: (i) the dynamic metal ligand system (such as the metal-ligand system in the plant solution) inevitably includes unstable or transient metal species materials; (ii) biochemical processes such as enzymatic activity may result in degradation of the metal complex, (iii) the metals are present at very low concentrations in the plant liquid, (iv)the distribution of complexes depends not only on pH but also on the proportion of metal to ligands [51, 107]. The latter is particularly important in plant liquids because of the many metal ligands are present in the xylem and phloem (e.g., amino acids and carboxylates) can act as tridentate ligands [108].

3.2. Direct speciation methods

In biological systems metals are involved in complex networks of biomolecular interactions, and in many cases their analysis requires sample preparation which can result in complex degradation, ligands and metal disassociation or free metal binding to the ligands present in the sample thus leading to false results. X-ray absorption spectroscopy (XAS) can be used for direct analysis of the metal species in samples,

with the surrounding metal-coordination environment, without a sample extraction step. However, the requirement for a high metal concentration in the samples limits the general use of this method. Synchrotron-based technology provides researchers with the ability to image and quantify specific chemical functional groups and trace metals directly at cell or subcellular level, making it a powerful tool for understanding the chemical processes of complex biological systems with minimal sample modification. This has made it possible to identify and quantify the seed mineral content and anti-nutrient compounds in the fields of agriculture and horticulture, as well as on the effects of nutrient on nutrient starvation, accumulation and toxic metal morphology of algae [109].

X-ray spectroscopy (XAS) provides information on the oxidation state and immediate coordination environment of iron present in the sample. The X-ray absorption near-edge structure (XANES) region of XAS spectra is sensitive to the oxidation state and coordination environment whereas the EXAFS (Extended X-ray Absorption Fine Structure) region is characteristic (coordination number and interatomic distances) of the local atomic structure surrounding an iron atom.

The XAS spectra are analyzed by linear combination fitting (LCF) using the spectra of standard compounds. This implies the need for prediction of the existence of some species and the availability of the corresponding standards. Even though XANES can be used to determine the local structure of atoms in the molecule and many features. XANES also has its shortcomings. X radiation may be destructive to the sample, causing damage to the sample during the measurement. The evolution of XAS goes towards the use of high brilliance sources which, on one hand, decreases the detection limits down to sub-ppm levels, but, on the other hand, increases the risk of radiation damage to the analyte [110-112]. An analyses of xylem sap samples revealed Fe(III) to be complexed by citrate and acetate; the presence of Fe(0) in one of the samples was considered to be an artifact created by sample irradiation with high intensity synchrotron X-rays [110-112].

3.3. Hyphenated techniques

3.3.1. Chromatographic techniques

Chromatography is the collective term for a set of separation techniques that operate based on the differential partitioning of mixture components between a mobile and a stationary phase. The mobile phase (a liquid or a gas) travels through the stationary phase (a liquid or a solid) in a defined direction. The distribution of components between the two phases depends on adsorption, ionic interactions, diffusion, solubility or, in the case of affinity chromatography, specific interactions. Depending on the experimental design, the separation in a liquid mobile phase may be carried out via column or planar chromatography, on analytical or preparative scales[113]

The importance of chromatography lies primarily in its use as an analytical separations tool although preparative applications have gained prominence during the last two decades. It serves as a means of resolution of mixtures and for the isolation and partial description of the components whose presence may be known or suspected. After a period of time they will be distributed in space over the stationary phase and subsequently emerge out of the stationary phase as single components. Several techniques, depending upon the choice of stationary and mobile phases, are used [98]. They include paper chromatography, thin layer chromatography (TLC), gas chromatography (GC), liquid chromatography and (LC); high performance liquid chromatography (HPLC)

Chromatographic methods are important in the analytical and preparative separation of biological samples. In the next sections chromatographic methods used in this work including size exclusion chromatography (SEC) and hydrophilic interaction liquid chromatography (HILIC) will be discussed [114, 115].

3.3.1.1. Size exclusion chromatography (SEC)

Size exclusion (or gel permeation) chromatography separates compounds on the

basis of their molecular size as illustrated in **Fig. 3.1**. SEC is used in a variety of chemical applications including polymer synthesis, natural product isolation, and purification of biomolecules. This technique has become a standard in the field of chromatography for the separation of analytes in life science due to its robustness. Many biochemistry and polymer laboratory experiments include experiments that rely on at least one purification step involving SEC [115].

SEC separates molecules according to differences in size without binding to the chromatography medium so the buffer composition does not directly affect resolution. Consequently, a significant advantage of SEC is that conditions can be varied to suit the type of sample or the requirements for further purification, analysis, or storage without altering the separation. SEC is well-suited for separaton of biomolecules that are sensitive to changes in pH, concentration of metal ions, or cofactors and harsh environmental conditions. Separations can be performed in the presence of essential ions, cofactors, detergents, urea, or guanidine hydrochloride at high or low ionic strength; at 37°C or in the cold room according to the requirements of the experiment [100]. A Superdex Peptide HR 10/30 (300 mm x 10 mm i.d) was chosen for the analysis of plant samples and extracts in our study because of its high tolerance to biological matrices that allows injection of complex samples without prior extensive sample preparation steps.

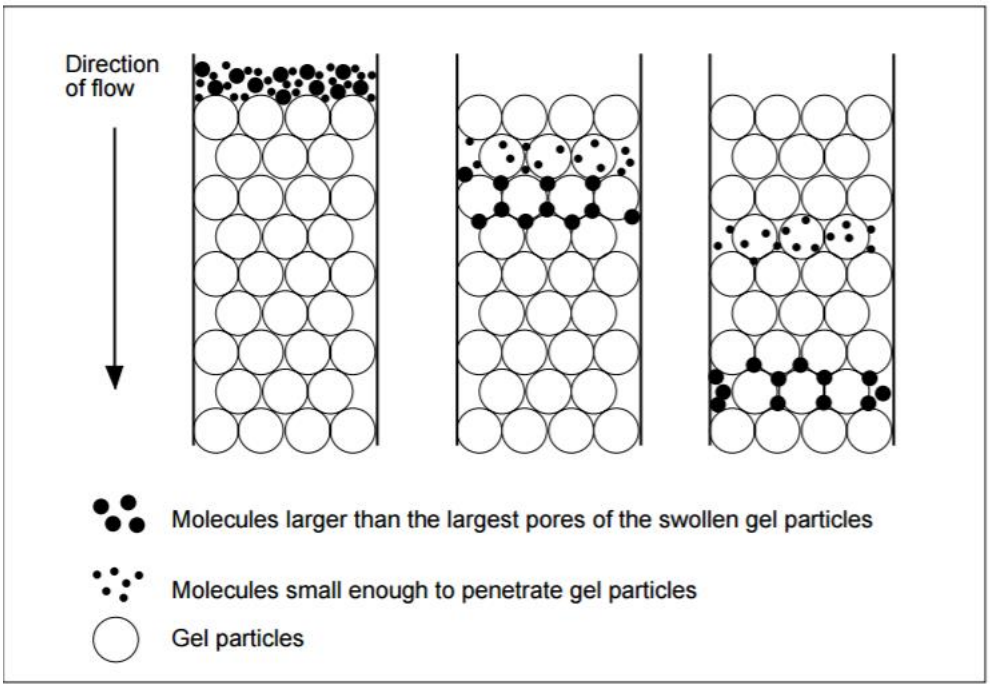

Fig. 3.1. The principle of size-exclusion chromatography [115].

3.3.1.2. Hydrophilic interaction liquid chromatography (HILIC)

Hydrophilic interaction liquid chromatography (HILIC) provides an approach to effectively separate small polar compounds on polar stationary phases. The more polar compound the more strongly it will be retained in HILIC; typically 70-90 %(v/v) acetonitrile and a volatile buffer salt is used in the mobile phase. This feature makes HILIC highly suitable for ESI MS detection and it often improves the MS sensitivity compared to alternative techniques for polar compounds[116]. It is believed that the surface of HILIC stationary phase is covered by a water rich layer formed by the mobile phase. The analyte retention is a result of its partitioning between a water-rich layer on the surface of the stationary phase and hydrophobic eluent as it is shown in **Fig. 3.2**.

In theory, if a compound is not retained on a reversed phase column then it will be retained on HILIC. As a rule, samples should not be dissolved in water since this is the strong solvent. It may therefore also be necessary to change and optimize the sample pre-treatment. This can offer an extra advantage when sample proteins are precipitated in acetonitrile and the sample can then be directly injected after

centrifugation, without the need for evaporation to dryness and re-dissolving in mobile phase (necessary for RP) [116]..

An interesting option may also be to use HILIC for a polar analyte that is not retained, on a reversed phase column. In particular, some peptides may show retention on both reversed phase and HILIC columns, enabling orthogonal and two-dimensional separations [117].

The characteristics of the hydrophilic stationary phase may affect, and in some cases limit, the freedom of choice when deciding on mobile phase composition, ion-strength, or buffer pH value, since mechanisms other than hydrophilic partitioning could take place.

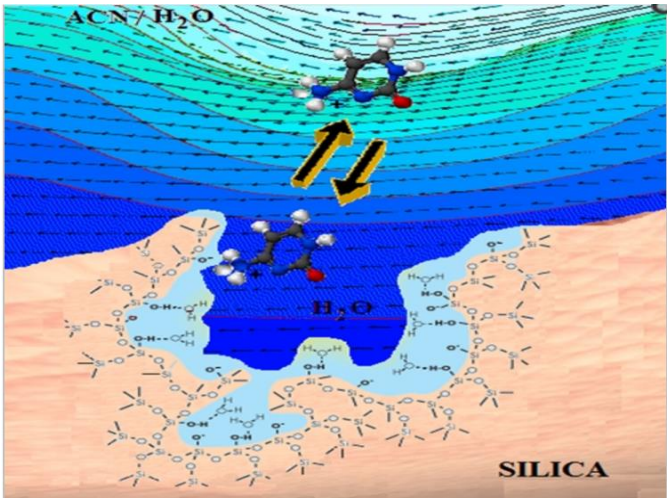

Fig. 3.2. Scheme of the separation mechanism in HILIC system [116]

3.3.1.3. Other LC separation mechanisms

Reversed phase liquid chromatography is a powerful technique for separation of hydrophobic organic species present complex matrices including those of plant extracts and saps or bacteria cultures. The separation mechanism of RP LC is based on the compounds partitioning between nonpolar stationary phase and a polar mobile phase [118]. More hydrophobic compounds are retained on the column longer that hydrophilic molecules. The RP separation can be performed in isocratic mode with

the constant concentration of organic solvent in mobile phase or using gradient elution where the content of organic solvent is continuously increasing during the analysis. The organic solvents used in RP HPLC are acetonitrile, methanol and 2-propanol that can contain ionic modifiers, such as trifluoroacetic acid. The ionic modifier, the organic solvent composition, the gradient slope or the operating temperature are the parameters that can be optimized in order to retain and resolve the analytes. The stationary phases usually employed by RP HPLC are based on micro particulate porous silica that is modified commonly with alkyl group C18 and less often with n-butyl (C4) and n-octyl (C8. [119]. In the context of this work the RP HPLC is important for the analysis of ligands involved in metal binding but cannot be used fo the complexes which usually are hydrophilic.

Ion exchange chromatography allows the separation of ions and polar molecules depending on their charge and therefor is used for separation of charged compounds. The IEC mechanism is based on coulombic (ionic) interactions where analyte ions in the mobile phase interact with the covalently bound charged ionic functional groups of the stationary phase (cations or/and anions) [120]. When the mobile phase is introduced, the electrostatically bound ions can be exchanged for stoichiometrically equivalent amount of other ions of same sign. The separation using IEC requires drastic elution condition where acids, bases and high salt concentrations are used. This harsh conditions are generally unsuitable for the studies carried out in the frame of this project.

3.3.2. ICP MS as an element specific detector for Fe, Co, Cu, Zn and Ni

Inductively coupled plasma mass spectrometry (ICPMS) is an analytical technique that performs isotopic-specific elemental analysis with excellent sensitivity. The ICP-MS instrument employs argon plasma (ICP) as the ionization source and a mass spectrometer (MS), usually with a quadrupole mass filter, to separate the ions produced [107]. The scheme of ICP-MS shows like **Fig. 3.3**

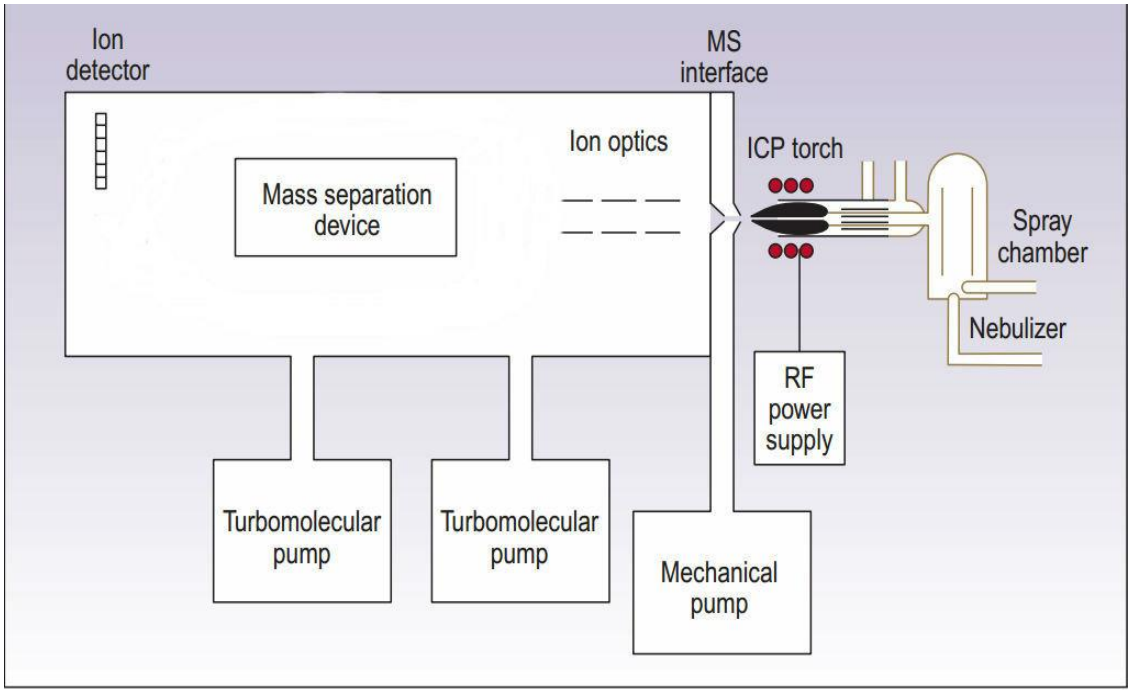

Fig. 3.3. Scheme of an ICP-MS system [121].

It can simultaneously measure most elements in the periodic table and determine analyte concentrations down to the sub nanogram per litre or parts per trillion (ppt), level performing qualitative, semi quantitative, and quantitative analysis, and compute isotopic ratios. In a standard ICP-MS configuration, liquid samples are introduced by a peristaltic pump to a nebulizer where a sample aerosol is formed [122]. A spray chamber ensures that a consistent aerosol is introduced to the plasma. Several models of nebulizers and spray chambers exist.

Argon gas is introduced through a series of concentric quartz tubes, known as the ICP torch. The torch is located in the centre of a RF coil. A Tesla coil ionizes the argon gas and free electrons are accelerated by a 27 MHz radio frequency field. Collisions between the accelerated electrons and the argon gas generate high temperature plasma. The sample aerosol is instantaneously decomposed in the plasma to form analyte atoms, some of which are ionized; the degree of ionization depends on the element [123].

The ions produced are extracted from the plasma into the mass spectrometer region, which is maintained at a high vacuum (typically 10-6torr) using differential

pumping. Placing a plasma, operating at 6000 °C, near an ion focusing device operating near room temperature gives a large temperature difference. Thus, the operating pressure of the plasma is much higher than the vacuum required for the ion lens and allows the mass spectrometer part of the instrument. The interface between the plasma and the ion lens system ensures that the ions generated by the plasma enter the ion lens region. The analyte ions are extracted through a pair of orifices known as the sampling cone and the skimmer cone. The analyte ions are then focused by a series of lenses into a (usually) quadrupole mass analyzer which separates the ions based on their mass-tocharge ratio (*m/z*). Finally, ions are detected using an electron multiplier, and data at all masses are collected and stored through a computer interface. The mass spectrum generated is extremely simple [123].as shown in **Fig. 3.4**.

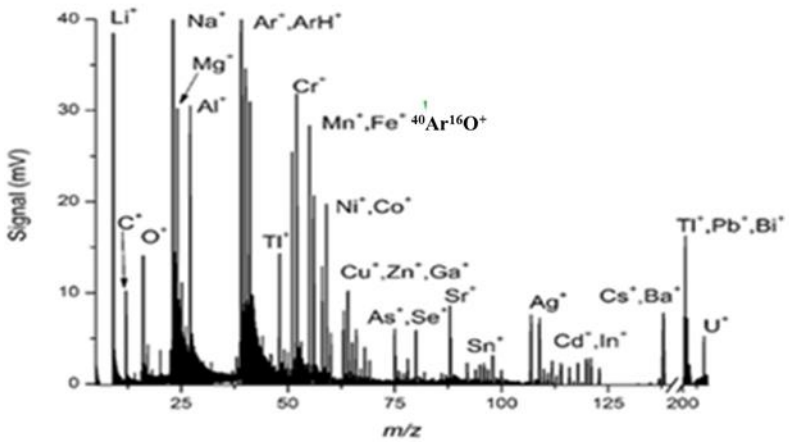

Fig. 3.4. An example of an ICP MS mass spectrum.

A relatively novel module introduced to the ICP MS instrument is a collision cell used to remove the polyatomic ions formed in the plasma and causing interferences in the analysis (cf. section 3.4.2.2.). Their operation is presented in the **Fig. 3.5** and involves the introduction an additional gas meant to collide and/or react with undesirable species.

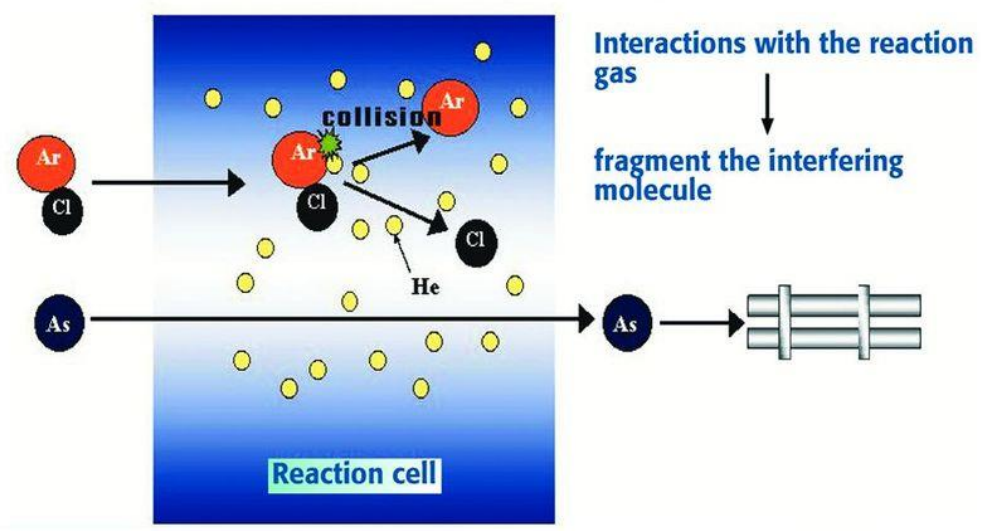

Fig. 3.5. Scheme of an collision cell in ICP-MS system [121].

3.3.2.1. Technical aspects of HPLC-ICP MS coupling

Hyphenated techniques based on coupling chromatographic separation techniques with ICP-MS detection are now established as the standard analytical tool available for real-life speciation analysis.. ICP-MS is usually coupled to size exclusion (SEC), ion exchange (IE), reverse phase chromatography (RP) and capillary electrophoresis (CE) (**Fig. 3.6**). The hyphenation requires that the connecting interface (transfer line) transmits the fractionated sample quantitatively from the separation system to the plasma of the ICP-MS in a form that the plasma can tolerate[124]. The parameters to be taken into account include the eluent flow rate and its composition.

The key to a succesful HPLC and ICP-MS coupling is the interface. Matching the best column flow with the optimum nebulizer flow is critical to achieving effective separation. Since the ICP-MS can tolerate flows from nLs to more than 1 mL/min, the nebulizer is typically selected to match the column flow to assure the presence of the highest proportion of fine droplets in the aerosol. This is critical because small droplets are more efficiently transported through the spray chamber and atomized and ionized in the plasma. For typical HPLC flows of 100 μL/min to 1 mL/min, conventional concentric sprayers (glass, quartz or fluoropolymer) are used

[125].

For some chromatographic separations, organic solvents must be used resulting in a compatibility problem. The plasma will burn the solvent resulting in the deposition carbon is inside the instrument leading to its pollution and reduced performance. A small addition of oxygen mixed in the argon stream of the atomizer alleviates this problem. It will react with carbon in organic matter forming carbon dioxide, which will be expelled with the exhaust gas. Another precaution is cooling of the spray the chamber to reduce the amount of organic matter reaching the plasma[122].

As ICP-MS is a specific detector for metals (or semimetals) at extremely low levels, its synergic use with a previous high-resolution separation of the elemental species offers an extremely efficient analytical tool. Mass spectrometry-based techniques play an increasingly major role in speciation analysis and metallomics providing identification and determination of individual metal forms after a high-resolution separation [126, 127].

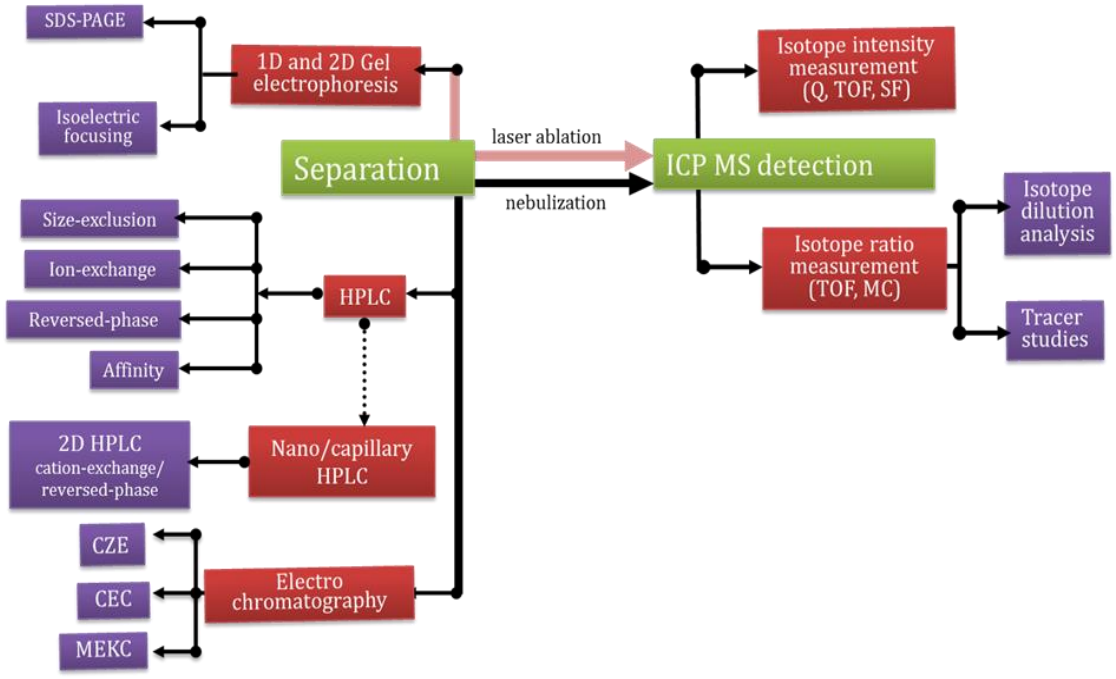

Fig. 3.5. ICP MS based hyphenated techniques used in speciation analysis [128]

3.3.2.2. Interferences and sources of error

Although interferences do occur in ICP-MS, they are relatively few in number (when compared to many other analytical techniques such as for example inductively coupled plasma atomic emission spectrometry, ICP-AES), generally predictable and can often be corrected for or may be minimized by optimizing instrument operating conditions. The three types of interferences that occur are isobaric, molecular (or polyatomic) and doubly-charged ion interferences which are discussed below with a focus on metal studied in the frame of this project.

Isobaric interferences. Occur for equal mass isotopes of different elements. Examples include the following: ^{58}Fe on ^{58}Ni, ^{64}Ni on ^{64}Zn. They are best avoided by choosing alternative, non interfered analyte isotopes, if available. Given acknowledge of the natural abundances of the isotopes of all elements, isobaric interferences are easily corrected by measuring the intensity of another isotope of the interfering element and subtracting the appropriate correction factor from the intensity of the interfered isotope.

Molecular interferences. They are due to the recombination of sample and matrix ions with Ar or other matrix components (e.g. O, N, Cl, etc.) in the cooler regions of the plasma. Examples include the following:^{40}Ar^{16}O on ^{56}Fe. Most molecular ions formed by matrix components are predictable and may be corrected for by applying correction factors determined by analyzing interference solutions (**Table 3.1)**. Molecular interferences may also be avoided by using alternative, non-interfered analyte isotopes. In some cases they can be reduced in severity or even eliminated completely by using more appropriate sample introduction systems or optimizing instrument operating conditions[129]. For example, in this project iron had to be monitored, so it was analyzed by using collision cell (described in section 3.4.2) with hydrogen and monitoring isotopes ^{54}Fe and ^{57}Fe.

Table 3.1 A Table of Polyatomic Interferences in ICP-MS [130] for the elements of interest for this project [106].

Isotope	Abundance	Interference	Reference
^{54}Fe	5.82	$^{37}Cl^{16}O^{1}H^{+}$, $^{40}Ar^{14}N$, $^{38}Ar^{15}N^{1}H^{+}$, $^{36}Ar^{18}O^{+}$, $^{38}Ar^{16}O^{+}$, $^{36}Ar^{17}O^{1}H^{+}$, $^{36}S^{18}O^{+}$, $^{35}Cl^{18}O^{1}H^{+}$, $^{37}Cl^{17}O$	(15)(18)(22)(29)(36)
^{56}Fe	91.66	$^{40}Ar^{16}O^{+}$, $^{40}Ca^{16}O^{+}$, $^{40}Ar^{15}N^{1}H^{+}$, $^{38}Ar^{18}O^{+}$, $^{38}Ar^{17}O^{1}H^{+}$ $^{37}Cl^{18}O^{1}H^{+}$	(3)(22)(29)
^{57}Fe	2.19	$^{40}Ar^{16}O^{1}H^{+}$, $^{40}Ca^{16}O^{1}H^{+}$, $^{40}Ar^{17}O^{+}$, $^{38}Ar^{18}O^{1}H^{+}$, $^{38}Ar^{19}F^{+}$	(8)(9)(21)(22)(29)(34)
^{58}Fe	0.33	$^{40}Ar^{18}O^{+}$, $^{40}Ar^{17}O^{1}H^{+}$	(22)
^{59}Co	100.	$^{43}Ca^{16}O^{+}$, $^{42}Ca^{16}O^{1}H^{+}$, $^{24}Mg^{35}Cl^{+}$, $^{36}Ar^{23}Na^{+}$, $^{40}Ar^{18}O^{1}H^{+}$, $^{40}Ar^{19}F^{+}$	(5)(8)(9)(13)(19)(22)(29)(34)
^{60}Ni	26.16	$^{44}Ca^{16}O^{+}$, $^{23}Na^{37}Cl^{+}$, $^{43}Ca^{16}O^{1}H^{+}$	(3)(13)(26)(29)
^{61}Ni	1.25	$^{44}Ca^{16}O^{1}H^{+}$, $^{45}Sc^{16}O^{+}$	(1)(25)
^{62}Ni	3.66	$^{46}Ti^{16}O^{+}$, $^{23}Na^{39}K^{+}$, $^{46}Ca^{16}O^{+}$	(1)(9)(25)
^{64}Ni	1.16	$^{32}S^{16}O_2{}^{+}$, $^{32}S_2{}^{+}$	(22)(29)
^{63}Cu	69.1	$^{31}P^{16}O_2{}^{+}$, $^{40}Ar^{23}Na^{+}$, $^{47}Ti^{16}O^{+}$, $^{23}Na^{40}Ca^{+}$, $^{46}Ca^{16}O^{1}H^{+}$, $^{36}Ar^{12}C^{14}N^{1}H^{+}$, $^{14}N^{12}C^{37}Cl^{+}$, $^{16}O^{12}C^{35}Cl^{+}$	(2)(9)(19)(28)(29)
65Cu	30.9	$^{49}Ti^{16}O^{+}$, $^{32}S^{16}O_2{}^{1}H^{+}$, $^{40}Ar^{25}Mg^{+}$, $^{40}Ca^{16}O^{1}H^{+}$, $^{36}Ar^{14}N_2{}^{1}H^{+}$, $^{32}S^{33}S^{+}$, $^{32}S^{16}O^{17}O^{+}$, $^{33}S^{16}O_2{}^{+}$, $^{12}C^{16}O^{37}Cl^{+}$, $^{12}C^{18}O^{35}Cl^{+}$,	(5)(15)(17)(21)(22)(29)(34)
^{64}Zn	48.89	$^{32}S^{16}O_2{}^{+}$, $^{48}Ti^{16}O^{+}$, $^{31}P^{16}O_2{}^{1}H^{+}$, $^{48}Ca^{16}O^{+}$, $^{32}S_2{}^{+}$, $^{31}P^{16}O^{17}O^{+}$ $^{34}S^{16}O_2{}^{+}$, $^{36}Ar^{14}N_2{}^{+}$	(2)(9)(11)(15)(19)(22)(34) (35)
^{66}Zn	27.81	$^{50}Ti^{16}O^{+}$, $^{34}S^{16}O_2{}^{+}$, $^{33}S^{16}O_2{}^{1}H^{+}$, $^{32}S^{16}O^{18}O^{+}$, $^{32}S^{17}O_2{}^{+}$, $^{33}S^{16}O^{17}O^{+}$, $^{32}S^{34}S^{+}$, $^{33}S_2{}^{+}$	(9)(11)(15)(22)
^{67}Zn	4.11	$^{35}Cl^{16}O_2{}^{+}$, $^{33}S^{34}S^{+}$, $^{34}S^{16}O_2{}^{1}H^{+}$, $^{32}S^{16}O^{18}O^{1}H^{+}$, $^{33}S^{34}S^{+}$, $^{34}S^{16}O^{17}O^{+}$, $^{33}S^{16}O^{18}O^{+}$, $^{32}S^{17}O^{18}O^{+}$, $^{33}S^{17}O_2{}^{+}$, $^{35}Cl^{16}O_2{}^{+}$	(1)(9)(11)(15)(22) (35)
^{68}Zn	18.57	$^{36}S^{16}O_2{}^{+}$, $^{34}S^{16}O^{18}O^{+}$, $^{40}Ar^{14}N_2{}^{+}$, $^{35}Cl^{16}O^{17}O^{+}$, $^{34}S_2{}^{+}$, $^{36}Ar^{32}S^{+}$, $^{34}S^{17}O_2{}^{+}$, $^{33}S^{17}O^{18}O^{+}$, $^{32}S^{18}O_2{}^{+}$, $^{32}S^{36}S^{+}$	(11)(15)(22) (35)
^{70}Zn	0.62	$^{35}Cl^{35}Cl^{+}$, $^{40}Ar^{14}N^{16}O^{+}$, $^{35}Cl^{17}O^{18}O^{+}$, $^{37}Cl^{16}O^{17}O^{+}$, $^{34}S^{18}O_2{}^{+}$, $^{36}S^{16}O^{18}O^{+}$, $^{36}S^{17}O_2{}^{+}$, $^{34}S^{36}S^{+}$, $^{36}Ar^{34}S^{+}$, $^{38}Ar^{32}S^{+}$	(9)(22)

Doubly-charged ion interferences. They are due to relatively rare doubly-charged matrix or sample ions with twice the mass of the analyte and hence the same mass/charge ratio, E.G., $90Zr^{+}$ on 45Sc.The formation of doubly-charged species can generally be minimized by optimizing the instrument operating conditions. Luckily, the first ionisation potential of Ar, although high enough to efficiently ionise most elements once, is not high enough to produce doubly-charged ions of most elements,

thus limiting their numbers in Ar plasma [120].

Matrix effects. Clogging of the orifices in either or both of the interface cones may be a problem when samples with high total dissolved solid (above 0.1 wt %.) contents are analysed. The presence of abundant, easily ionised matrix components such as Na in seawater may lead to a suppression in the ionisation efficiency of analytes. Once again, this effect may be reduced by sample dilution or by removal of the easily ionised matrix component[131].

In this project state-of-the-art ICP MS Agilent 7500 and 7700 instruments were used in order to eliminate or minimize the interference mentioned above. The analyses were carried out by using platinum cone and lens to avoid nickel interference from the normal nickel parts and a collision cell was used (H_2 and He can be used as reaction gas).

3.3.3. Electrospray Orbitrap mass spectrometry identification of metal species

The elemental detection by ICP MS does not give the information about the species identity which can be obtained by molecular mass spectrometry (**Fig. 3.7**).

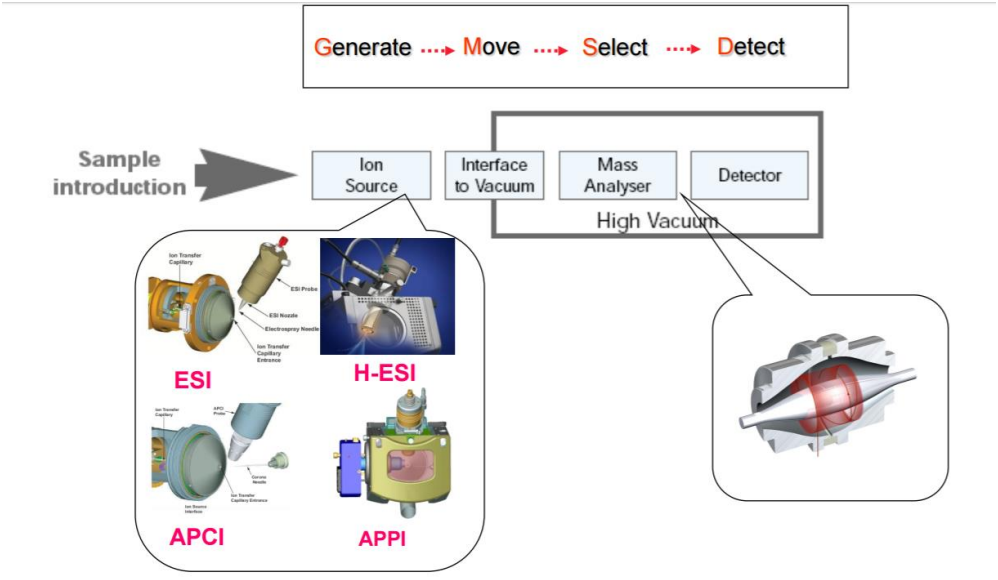

Fig. 3.7. Simplified scheme of a molecular mass spectrometer [123]

Among many types of ionization methods, the most widely used in modern

molecular mass spectrometry are electrospray ionization (ESI), atmospheric pressure chemical ionization (APCI) and matrix assisted laser desorption ionization (MALDI). ESI has an advantage in terms of LC compatibility[132]. The principle of ESI is shown in **Fig. 3.8.** ESI uses energy to help ions transfer from the solution to the gas phase prior to mass spectrometry. The transfer of the ionic material from the solution to the gas phase by ESI involves three steps involving: (1) dispersing the charged droplets, then (2) solvent evaporation, and (3) ion formation from highly charged droplets, The continuous sample solution stream is passed through a stainless steel or quartz silica capillary, which is maintained at a high voltage (e.g., 2.5-6.0 kV) relative to the walls of the surrounding chamber. It produce a highly charged droplets having the same polarity as the capillary voltage. The application of atomized gas (e.g., nitrogen) that is cut around the eluted sample solution enhances the higher sample flow rate. The charged droplets generated at the exit of the electrospray head pass the pressure gradient and the potential gradient to the analyzer area of the mass spectrometer. By increasing the ESI-source temperature and/or another nitrogen dry gas stream, the size of the charged droplets is continuously reduced by evaporation of the solvent, resulting in an increase in surface charge density and a decrease in droplet radius. Finally, the intensity of the electric field within the charged droplet reaches a critical point at which the ions of the droplet surface will be dynamically injected into the gas phase. The emitted ions are sampled by the sampling separator cone and then accelerated to the mass analyzer for subsequent analysis of the molecular weight and the measured ionic strength[133].

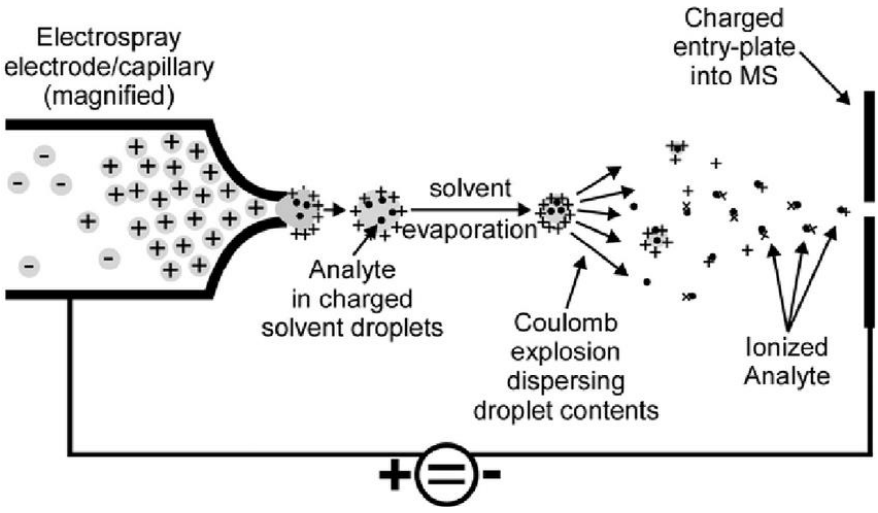

Fig.. 3.8. Principle of electrospray ionization

In plant and bacteria metallometabolomics ESI-MS is generally used to generate singly charged metal-ligand spectra allowing the identification of the species of interest using relative abundance of isotopic spectra corresponding to the occurring metals (isotopic patterns [97]). Furthermore, ESI-MS instruments allow for optimization of efficient detection conditions (e.g., positive and negative ionization mode) for the metal complexes of interest across a range of solvents and pH conditions. This approach can be extended with prior separation steps such as coupled liquid chromatography-MS (LC-MS) and capillary electrophoresis-MS (CE-MS), which further increase the detection sensitivity of different metal–ligand complexes[97].

Mass analyzers can be grouped into classes on the basis of their properties, including ion beam versus ion-trapping types, continuous versus pulsed analysis, operation using low versus high translational energy ions, and on the basis of the time scale of the analysis. Mass-to-charge ratio analysis can be based on the measurements of momentum in magnetic sector and kinetic energy in electrostatic sector instruments, path stability in linear quadrupoles, orbital frequency in both ion cyclotron resonance mass spectrometers and quadrupole ion traps, and velocity in time-of-flight instruments. Each method has its own strengths and weaknesses. The Orbitrap, a relatively new type of mass analyzer invented by Makarov [134] and used in this

work, bears a similarity to an earlier ion storage device, the Kingdon trap. It consists of a thin-wire central electrode, an electrically isolated coaxial outer cylindrical electrode, and two endcap electrodes [135]. The Orbitrap operates by radially trapping ions around a central spindle electrode. An outer barrel-like electrode is coaxial with the inner spindle-like electrode and mass/charge values of the orbitally trapped ions.are measured from the frequency of harmonic ion oscillations, along the axis of the electric field. This axial frequency is independent of the energy and spatial spread of the ions. Ion frequencies are measured nondestructively by acquisition of time-domain image current transients, with subsequent fast Fourier transforms (FT) being used to obtain the mass spectra. The Orbitrap is frequently used in research applications to elucidate low-abundance, high complexity, or otherwise difficult samples due to ts high resolving power and high mass accuracy.

In the system used (**Fig. 3.9**), the ions are produced by the electrospray ion source at the extreme left. Ions then proceed through the source, collision quadrupole, selection quadrupole and then pass into the storage quadrupole. The storage quadrupole serves as an ion accumulator and buncher, allowing a pulsed mass analyzer such as the Orbitrap to be coupled to a continuous source like an electrospray ionization source. After accumulation and bunching in the storage quadrupole, the exit lens is pulsed low, the ion bunches traverse the ion transfer lens system and are injected into the Orbitrap mass analyzer[135].

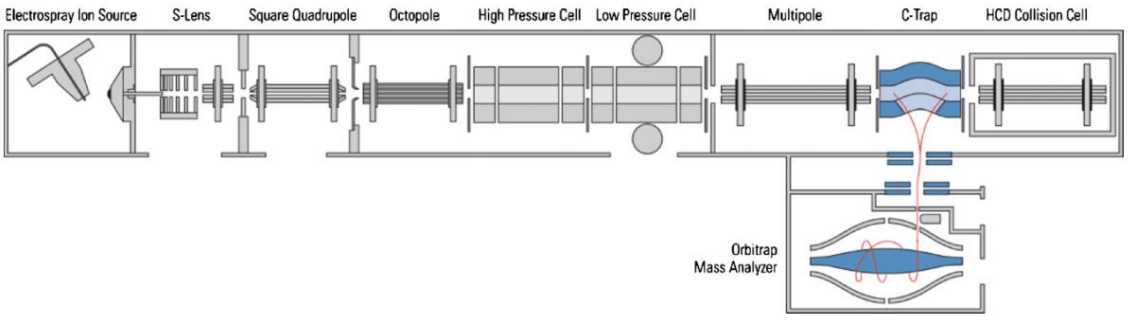

Fig. 3.9. The scheme of the Orbitrap mass spectrometer used[135].

In mass spectrometry, four terms: (i) mass resolving power, (ii) mass resolution, (iii) mass accuracy and (iv) mass precision are used to characterize the performance of high-resolution, accurate-mass mass spectrometers. Features of the Orbitrap at its present stage of development include high mass resolution (up to 500 000 now), large space charge capacity, high mass accuracy (2–5 ppm), a mass/charge range of at least 6000, and dynamic range greater than 10^3. The resolution of Orbitrap instruments for different *m/z* compared to commercially available time-of-flight mass spectrometers are shown in **Fig. 3.10.**

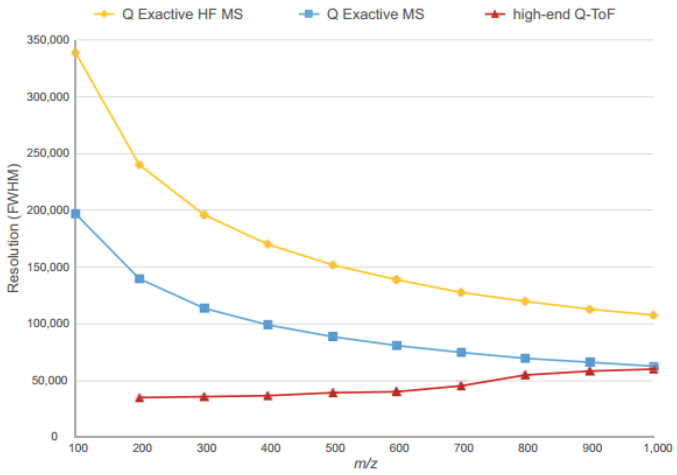

Fig. 3.10. Resolution vs. *m/z* for small molecule mass range[136].

The accurate mass measurement, coupled with sufficient resolution, makes it possible to greatly restrict the number of possible molecular formulas that might be represented by a particular molecular mass. Mass measurement accuracy of 10 ppm allows useful measurements of molecular formulas, although 1 to 2 ppm is preferable (**Fig. 3.11**).

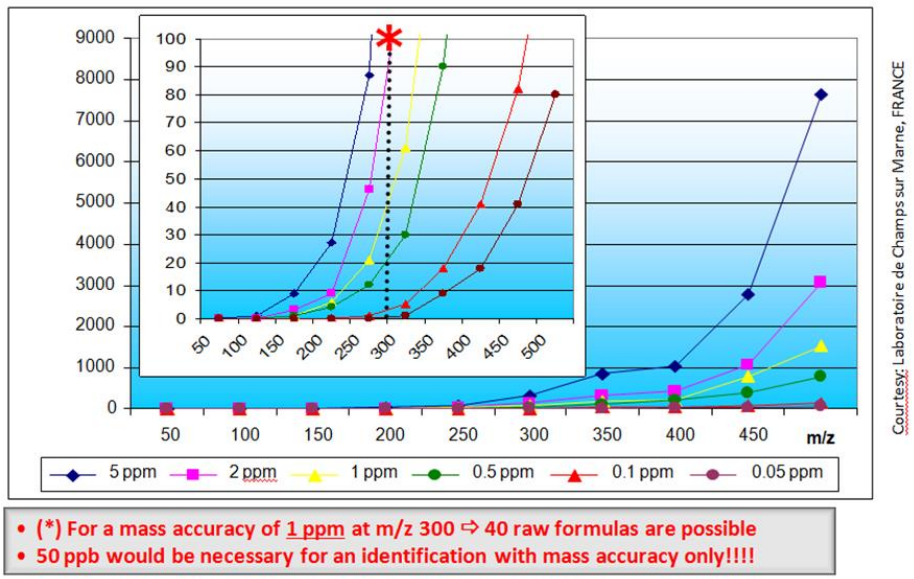

Fig. 3.11. The number of possible formulas generated for MS data obtained at different mass accuracy (courtesy of the Laboratory of Champs-sur-Marne, France).

Likewise for the fast improvement of metabolomics, techniques for the simultaneous analysis of sets of small biomolecules or metal complexes(metalphores) are constatntly being developed and improved, providing more details about the metabolism of metals in complex biological systems[94]. Comprehensive and unbiased metabolite analysis is an indispensable tool for systems biology together with transcriptomics and proteomics.

Metabolomic studies increasingly require the analysis of extremely complex mixtures, such as whole-cell lysates, and detection of analytes of a wide variety of types over a wide range of concentrations[135]. They are also stimulating the introduction of new analytical criteria involving multiplexing, differential measurements, data-dependent data acquisition, and automation. Direct-infusion ESI MS using an ion trap MS (DI MSn) was used to determine metabolic differences between endophyte-infected and endophyte-free perennial ryegrass (*Lolium perenne*) seed samples[137].

Mass spectrometric analysis of complex mixtures for particular analytes is often facilitated by tandem or multiple stage mass spectrometry (MSn) as well as by high

resolution/high-mass accuracy measurements. The value of multiple-stage mass spectrometry is well established, both for characterization of particular compounds using product ion scans and for recognizing members of classes of compounds using neutral loss1 or gain scans, and precursor ion scans.

MS / MS instruments are recommended for continuous chromatographic techniques using MS detection (eg, LC-MS), where the major molecular species are slightly fragmented (soft ionization). Tandem MS was used to determine the protein structure. MS/MS CID processing is performed in LTQ-FT-MS. The method produces satisfactory results that can be used as a quantitative tool for proteomics. However, the key to the creation and application of quantification is to strengthen the clarification of the structure.

3.3.3.1. The HPLC - ESI MS coupling

The coupling of mass spectrometry to LC allows the separation of sample components and reduces matrix complexity thus facilitating the analysis. The Orbitrap MS is most frequently coupled to reversed-phase chromatography; the use of ultrahigh pressure LC (UPLC), both for peptide and small molecule analyses, is of a particular interest. Additionally, combinations of several chromatographic mechanisms, such as cation-exchange and reversed phase, form the basis of multi-dimensional LC separation strategies used for metal complex analyses[138].

Reversed-phase LC. Out of the many LC techniques coupled to MS, the reversed phase LC is undoubtedly encountered most frequently, in both proteomics and small molecule applications. In many applications a limited amount of starting biological material stimulates the use of capillary columns with low flow rates (in the order of several hundreds of nanolitres per minute). In the present work, the interest of RP HPLC lies in the analysis of organic ligands potentially involved in metal complexation [42]. For metabolomic profiling studies, the focus is on the development of efficient and robust LC–MS methods for the identification of a large number of metabolites in biological samples using both positive and negative

electrospray modes. For example, a detailed study performed with the LTQ Orbitrap compared various LC stationary phases in conjunction with multiple mobile-phase systems. It benchmarked the selection of the best mobile and stationary phase based on the separation efficiency of a 45-component metabolite mixture. A material with small pore size (e.g., <100 Å) and large surface area (e.g., >400 m^2/g) provided the greatest retention of small, polar analytes. The optimized gradient elution with a mobile phase containing 10 mM ammonium acetate in water and in 90% acetonitrile/ which for detection in both positive- and negative-ESI mode [36]. The method was extended for monitoring at least one product ion simultaneously detected in the linear ion trap. Although the product MS spectrum is being acquired at low resolution, the information serves for the confirmation of compound identity. The method allowed the quantification of the analyte down to the detection limits of 0.01 g/L [42].

Hydrophilic interaction chromatography (HILIC) is being mentioned in the context of bioanalysis. (e.g., phosphopeptide analysis) and - in particular - metabolomics. Global metabolite extracts can be quite complex and generally include small organic acids and amino acids, nucleotides, carbohydrates, vitamins, and lipids. The highly volatile organic mobile phases such as methanol and ACN used in HILIC provide low column backpressure as well as an increased ionization efficiency [63]. The utility of HILIC in retaining hydrophilic compounds while allowing hydrophobic species to flow through rapidly is a significant advantage for metabolomic profiling experiments. In the context of this project, the most interesting is the possibility of the separation of intact metal-ligand complexes.

The coupling of HILIC with ESI - TOF MS (canonical in metabolomics [139, 140] allowed the detection of whole range of carboxylates in the plant tissue extracts and fluids including oxalic, 2-oxoglutaric, cis-aconitic, malic, quinic, shikimic, fumaric, formic, and metaphosphoric (MPA), succinic citric and ascorbic acids) [141]. The analysis for metal complexes is more challenging as it requires a careful

optimization of the ionization mode and the separation of the metal-ligand complex from the excess of the free ligand which could interfere in the ESI process [99]. HILIC ESI MS has largely contributed to the understanding of the role of citrate [142] and citrate-malate complexes in iron transport and metabolism. Both citrate and Fe–citrate complexes, important in iron transport in plants, are highly polar and there is a consensus on the choice of a zwitterionic hydrophilic interaction stationary phase (ZIC-HILIC) for their separation [51, 140, 143]. An important restriction in the optimization of the separation conditions is the need to maintain the original pH of the sample during chromatography in order to preserve the metal-ligand equilibria.

Bajad et al. [144] used HILIC to identify metabolite profiling of *Escherichia coli* extracts following a triple quadrupole MS. After optimizing the HILIC conditions (Luna NH_2 column, 250×2 mm, 5 μm), they were able to effectively separate and determine many highly soluble metabolites that were not eluted by RP chromatography，which enable the identification and quantification of some 69 compounds. And another research the hydrophilic interaction chromatography (HILIC) coupled with tandem MS was used to detect neomycin by Oertel,R et al [145].

3.3.3.2. Data mining strategies

The identification of metabolites from raw signals detected by mass spectrometers is a challenging task in metabolomics that still demands considerable effort [146]. Two types of MS technologies are in general use for high-throughput metabolomics analyses. High-accuracy MS using ICR-FT MS or time-of-flight MS [94] as well as Orbitrap FT MS are used. Highly accurate *m/z* measurements narrow down the search space by providing a short list of chemical formulae (elemental compositions, cf. **Fig. 1.12**), although without additional isotope abundance data this list may remain extensive [147].

The search for metal-containing species is facilitated by the characteristic isotopic patterns allowing their recognition among other compounds. The ability of the Orbitrap mass analyzer to clearly observe an isotopic pattern can be used to trigger

data-dependent product ion scans. The method has a broader detection capability compared to classical approaches utilizing product ion or neutral loss scans, since it is independent of the collision-induced dissociation behavior of the compounds. This feature has been used for the analysis of metal-containing compounds. Identification of natural metal speciation such as plant phytosiderophores (PSs) and their precursor nicotianamine (NA) and their metal complexes in plant samples is significant, because they are critical to the availability and translocation of different nutrients in crops. The metal-PS and metal-NNA complexes have been identified in several plant species by ESI-time-of-flight (TOF) -MS and LC-ESI-TOF-MS based on the isotopic patterns of the containing metal[97].

Another characteristic feature of metal containing species is the characteristic mass defect. It can serve as a means of species recognition and/or confirmation of the presence of the metal in molecule structure.

The presence of a metal atom in the metabolite of interest offers an exciting possibility to combine the results from the LTQ Orbitrap MS with those from inductively coupled plasma mass spectrometry (ICP-MS). The LTQ Orbitrap data proved to be highly complementary with its ability to fully structurally characterize molecules based on their MSn spectra. A two-pronged approach using ICP-MS and the Orbitrap MS was applied to the speciation of arsenic and, in particular, arsenite phytochelatin complexes. Both of these MS techniques were necessary to identify and quantify the arsenic species in plant root extracts [148]. The unique capability to provide multiple levels of fragmentation (MSn) with accurate mass reading has been utilized to elucidate the structure of a sulphated pentasaccharide impurity seen in Fondaparinux preparation. Valuable structural information was generated through sequential MS fragmentation by isolating specific adducts and assessing their fragmentation pathways [140].

The integrated ICP MS and ESI MS approach is illustrated below for the speciation of Fe in plant fluid [149]. First, the HPLC-ICP-MS analysis provided information on the retention time, the number and quantity of iron species in the

sample (**Fig. 3.12a**). Then, the ESI MS spectrum was searched at the retention time of the Fe peak for the characteristic iron isotopic pattern (shown in the inset to **Fig. 3.12a**) using MetWorks' software. In order to find the low abundant species the spectra were searched for partial isotopic pattern and the searching parameters of *MetWorks*, such as tolerance on inter-isotopic mass difference were taken into account. In this literature example, Flis et al. found the Fe-containing species at the *m/z* 811.8420. The generated XIC (**Fig. 3.12b**) matched the retention type and peak shape in parallel HPLC-ICP MS chromatogram [149].

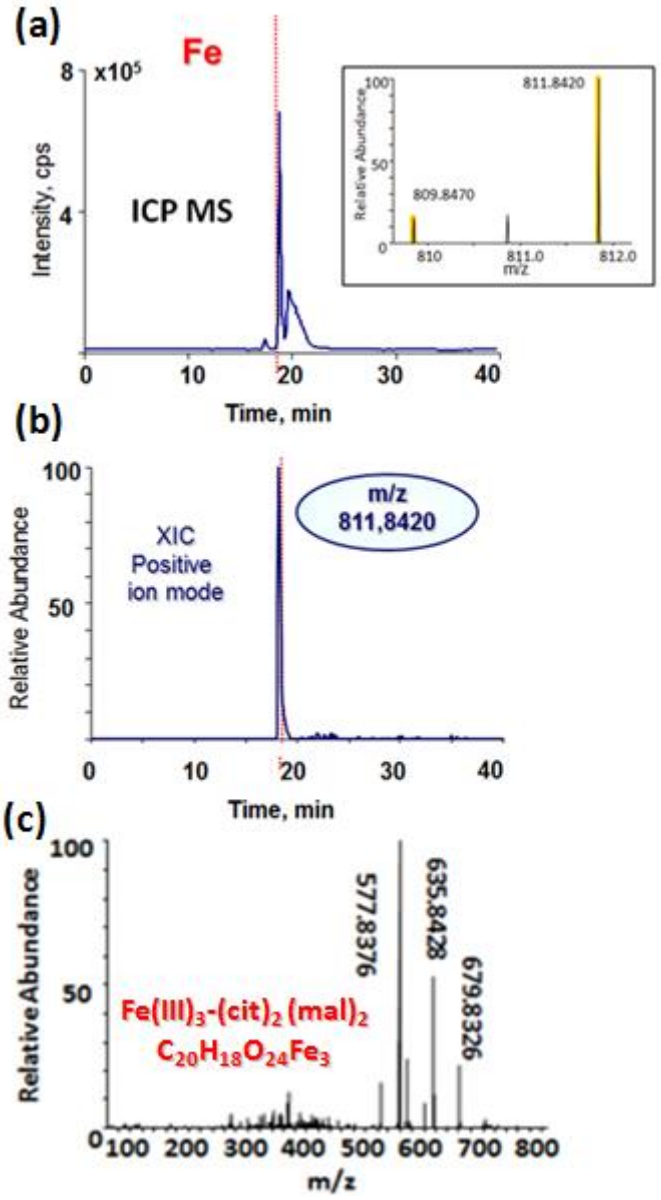

Fig. 3.12. Integrated HPLC- ICP MS/ESI MS approach for metallometabolomics. (a) HILIC-ICP MS (Fe isotopic pattern shown in the inset) (b) XIC chromatogram of *m/z* 811.8420, (c) ESI MS/MS spectrum of *m/z* 811.8420 ion [149].

The next step was the generation of experimental formulas using Xcalibur; the number of possible formulas was limited due to the high mass accuracy of the spectrometer used [131]. The structural characterization was carried out by tandem MS (**Fig. 3.12c**) leading to the identification of a mixed citrate-malate iron complex[149]. Once all the potential formulas of a metal species had been identified, the next chromatographic analysis of the same sample was carried out. In order to confirm that the sample contains a metal in the structure, an isolation width is established to maintain the isotopic characteristics of the target metal complex. The analysis in the MS/MS mode allows the characterization of the metal compound structure. In the case of a compound having an unidentified identity, the mass spectrum obtained by the sample was compared with the mass spectrum obtained by the standard to confirm the identification. If it is unidentified there is no standard the fragmentation of the compound will be recommended by the software and then these fraction information are used to profiling the structure of the molecular.

Additional steps were made to confirm the identity of the species $C_{20}H_{18}O_{24}Fe_3$. For metal complexes, more specific information based on mass spectrometry detection of demetaled ligand can be obtained. Thus, the mass spectrum was searched for the ions containing the metal and the corresponding free ligands. The mass differences between the metal complex and the demetallated ligand can be used to confirm the correctness of the formula. Mass defects, isotope patterns, as well as studies using different separation mechanisms and different ionization modes serve for the identification and characterization of metal/metalloid species, even at low concentrations.

All of these steps are combined to provide a systematic approach in this study that allows for the identification of metal compounds present in samples.

The other approach exploited in high throughput metabolomics is tandem MS (MS/MS or MSn) using an ion trap that can provide fragmentation data on the initial MS1 ions, although in practice this capacity is often foregone. These fragmentation data obtained by HR-MS are useful for the elucidation and classification of chemical structures. Technologies combining these two features, e.g. ion trap with FT-ICR-MS, are also available to provide high mass resolution MS1 profiles and information on fragmentation patterns. However, applying this combination to obtain high resolution data on both MS1and MS2 ions for large numbers of samples is impractical due to the slow scan speeds required by the FTvICR-MS. All of these technologies generate complex data sets and there are many steps in translating raw signals into chemical entities. With access to the raw data now readily available in standard formats such as mzXML[150], new or improved algorithms can be employed in many steps of data analysis, such as data preprocessing (including baseline detection and removal, peak detection, peak, or retention time alignment, etc.) and inference of the identity of components; for a recent review of LC-MS data processing for metabolomics and currently available software. Recently direct-infusion ESI MS using DIMSn was used to determine metabolic differences between endophyte-infected and endophyte-free ryegrass seed samples[151].

3.3.3.3. Quantitative analysis of organic ligands involved in metal complexation

The identification of ligands forming metal complexes in a wide range of samples has mainly involved electrospray ionization-mass spectrometry (ESI-MS) because of its high selectivity and sensitivity along with gentle transition from the solution to gas phase. The ligands can be identified and characterized by ESI MS/MS. However, the demonstration of the presence of the metal-ligand link requires the use of another complementary to ESI MS/MS technique[152].The determination of precise molecular mass by ESI MS is sufficient to determine the empiric formula and elucidate the metal-ligand stoichiometry.

In ESI-MS, the ion signal is proportional to analyte concentration and largely

independent of flow rate and injection volume used for sample introduction. The signal is linear from the limit of detection (usually pmol/L) to around 10 μmol/L of analyte concentration. For quantitative measurement, it is important to incorporate an internal standard in the procedure to compensate for losses during sample preparation and variable detection sensitivity of the MS system. The internal standard should have a structure similar to that of the analyte and the ideal practice is to synthesise an internal standard by incorporating stable isotopes on the molecules of interest. For example, for the quantification of free carnitine (mz 162), an internal standard containing 3 deuterium atoms to replace 3 hydrogen atoms was used (*m/z* 165) [153]. When an ideal internal standard is not available, molecules with similar structure can also be used. For example, nicotinamine has been used as an internal standard for ESI-MS/MS analysis of the staphylopine [154]. Another critical issue in quantitative ESI-MS is suppression of ionisation due to matrix interference. A biological sample would give significantly lower ionisation signals compared to pure standard solutions with similar analyte concentrations. This phenomenon is the result of high concentrations of non-volatile materials from the biological sample being present in the spray with the analyte. Possible non-volatile interfering solutes are salts and lipids in the biological samples. To overcome the matrix interference, extensive sample purification processes are required; for example, liquid-liquid extraction and solid phase extraction by disposable columns. However, these procedures are time-consuming and can cause poor recovery. A recent development is to use short LC columns (or guard columns) and apply a fast HPLC purification prior to MS analysis. The HPLC serves to separate the non-volatile compounds from the analyte. For HPLC systems with column-switching capability, the analyte in the biological sample can be purified and concentrated on separate columns before MS analysis.

Liquid chromatography-tandem mass spectrometry (LC-MS/MS) has been recognized as a primary methodology for the accurate bioanalysis. Multiple reaction monitoring (MRM) using mass spectrometry is a highly sensitive and selective method for the targeted quantification of small organic molecules in biological

samples. During an analysis in MRM mode, the first analyzer (Q1) is set to transmit the parent ions corresponding to the species of interest. Selected ions are fragmented in the second analyzer (Q2), and the third analyzer (Q3) is set to transmit a specific fragment of the anayte. An extracted ion chromatogram specific to the selected transition serves for the quantification (**Fig. 3.13**).

They tested the applied fragmentation energies that are required for releasing the free metals from the corresponding metal complex ions by using six different dilutions of Cu(II)–NA and Ni(II)–NA complex standard solutions. Results in MS_2 spectra further showed the requirement for increased fragmentation energy for the released free Cu and Ni isotopes with decreased abundance of the Cu(II)–NA and Ni(II)–NA complexes in the series of diluted samples. In the same sample, the intensity of free Cu/Ni isotopes was increased under high collision energies, HCD: 80–90%, as compared with lower collision energies, HCD: 40–50%. The fragmentation energies also differed for different metal complexes because the Cu (II)–NA complex required lower percentages of collision dissociation energies than the Ni(II)–NA complexes

Tsednee et al. used ESI-MS/MS to identify Fe–DMA/NA complexes in Japonica rice shoots by Multiple Reaction Monitoring (MRM). They selected the parent ion of three isotopic Fe(III)–DMA complex spectra, *m/z* 356.051, 358.046 and 359.046, and three Fe(II)-NA complex spectra, *m/z* 356.074, 358.070 and 359.072, and then generated, in a collision cell, product ions by fragmenting with different collision energies. In this way, product ion spectra corresponding to three Fe isotopes: *m/z* 53.939, 55.934 and 56.942 were acquired. Apparently, the identification of the Fe(III)–NA complex in the vicinity of the Fe(II)-NA complex was possible from the release of ^{56}Fe with *m/z* 55.934 from its precursor Fe(III)-NA, *m/z* 357[155].

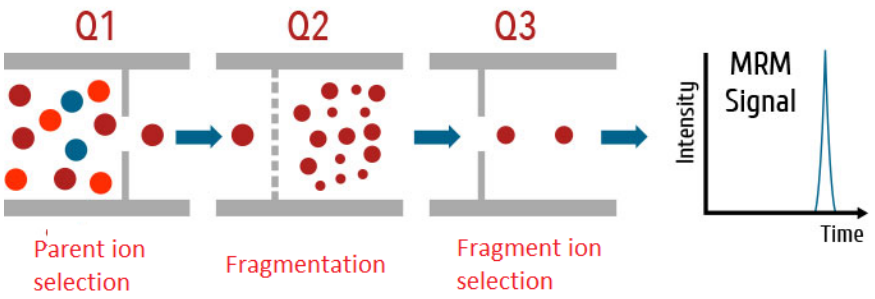

Fig. 3.13. Principle of LC MS/MS MRM quantification (http://www.anaquant.com/mrm-srm).

3.4. Fractionation approaches for bioavailability studies of essential metals from food

Due to the fact that elements are distributed among different classes of species (proteins, polysaccharide, lipids etc), the use of fractionation approaches methods as a sample preparation is an efficient tool in metal speciation identification concerning the process of analysis of quality, traceability, safety, and nutritional evaluation[156]. Many experiments involve enzymatic hydrolysis of speciation from food resources such as milk, meat, fish, eggs, or plants to produce a variety of species. The study of food bioavailability at any given time is very complex and diverse. The main limitations of bioavailability studies are associated with heterogeneity in the differences in physicochemical properties of the essential element species present. Fractionation can be a compromise giving insight into metal-binding and allowing to predict bioavailability. So dedicated methods based on the chemical character of species in the samples need to be developed. They usually also include simulated digestion conditions which can get an approximate idea about bioaccessible fraction. Each of the fractions may be analyzed in more detail by coupled techniques. Several fractionation methods were described as follows[157].

Organic solvents and aqueous solutions. Extraction parameters can play a significant role in determining the detection and quantification of low molecular weight species. It have shown that temperature (between −80°C and 4°C) does not change metabolite quantification while other parameters such as addition of acid to

methanol extraction solvent and washing of samples before extraction play a big role in increasing or reducing the metabolite signals detected by mass spectrometry. As a general metabolomics extraction protocol, extraction with cold methanol without any washing is satisfactory, even though for few targeted metabolites or special application where intra and extra metabolites should be distinguished, an optimized extraction protocol should be chosen. This insights will allow us to improve our current extraction methods and provide a more robust and optimized method for metabolomics studies[158]..

Concerning metabolite intracellular concentration, researches detected ligands in lower amounts in leaves were harvested from five different plants by developed extraction procedure (**Fig. 3.14.**) coupling DI-FTICR-MS. Like *V. vinifera* malate (*m/z* 133.01403, $[M-H^-]$), citrate (*m/z* 191.01990, $[M-H]^-$), acetylsalicylic acid (*m/z* 179.03516, $[M-H]^-$), abscisic acid (*m/z* 265.14381, $[M+H]^+$), the gibberellins A20 (*m/z* 355.15096, $[M+Na]^+$). These results demonstrate that the proposed extraction method was able to extract a wide range of compounds, even those present in low amounts[159].

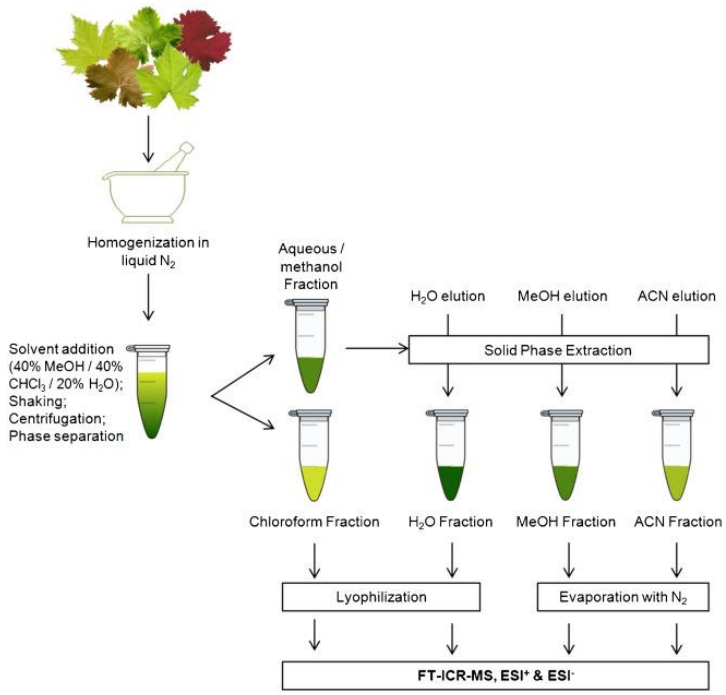

Fig. 3.14. Experimental procedure for metabolite extraction from grapevine leaves

compatible with FTICR[159].

Aqueous Enzymatic Extraction. An alternative approach combining aqueous and enzymatic extraction is attracting attention. Enzymes can aid in the extraction of proteins in several ways. Carbohydrases, which can attack the cell wall components, may increase protein yield by liberating more protein from the matrix source. A combination of cell wall-hydrolyzing enzymes has been used to cleave linkages within the polysaccharide matrix effectively and hence, liberate more intracellular species from oat bran[160]. In the last few years, different proteases, alone or in combination, have been used to partially hydrolyze proteins to peptides, increasing their solubility and making them more easily extractable. Recently, De Moura and co-workers (2011)[161] developed a two-step countercurrent aqueous enzymatic extraction process for soybean, significantly reducing the amount of water used. They achieved slightly higher oil and protein extraction yields than those from standard single-stage aqueous enzymatic extraction[162].

In view of the high cost of quantifying the bioavailability of Fe through human and animal studies, in vitro screening of food samples represents the most viable system for screening large numbers of samples to identify factors and interactions that affect the bioavailability of Fe [5]. Current techniques for in vitro screening include food simulating gastrointestinal and intestinal digestion, as well as human intestinal epithelial cells, particularly Caco-2 cell lines to measure Fe uptake. The cell line exhibits the characteristics of small intestinal epithelial cells, which is considered to be the main site of Fe absorption in the human gastrointestinal tract. Caco-2 cells have been shown to exhibit extensive intestinal epithelial morphology and functional characteristics in the absorption of Fe and other nutrients, which makes Caco-2 cells an excellent model system. These features include [6]: (i) Caco-2 cells reduce Fe^{3+} to Fe^{2+}, (ii) The transport of Fe in the Caco-2 cell line responds to the Fe state of the cells

In fact, Fe is less available from vegetarians rather than vegetarian diets for

human absorption. The effect of biochemical factors on Fe availability depends on the form of Fe. Iron in plants is mainly present in non-heme iron. The compounds in food affect the bioavailability of non-heme Fe by limiting the solubility or inhibiting the availability of iron transporters on the surface of the intestinal tract; thus increasing the Fe concentration alone may not solve the problem of Fe deficiency in the diet [3]. Ascorbic acid, cysteine and "meat factor" are all compounds known to enhance the absorption of non-heme Fe in human gut [4]. The main characterization of Fe bioavailability in plant foods is phytates and polyphenols, although other compounds may also be present [4]. In view of the high cost of quantifying the bioavailability of Fe through human and animal studies, in vitro screening of food samples represents the most viable system for screening large numbers of samples to identify factors and interactions that affect the bioavailability of Fe [5]. Current techniques for in vitro screening include food simulating gastrointestinal and intestinal digestion, as well as human intestinal epithelial cells, particularly Caco-2 cell lines to measure Fe uptake. The cell line exhibits the characteristics of small intestinal epithelial cells, which is considered to be the main site of Fe absorption in the human gastrointestinal tract. Caco-2 cells have been shown to exhibit extensive intestinal epithelial morphology and functional characteristics in the absorption of Fe and other nutrients, which makes Caco-2 cells an excellent model system. These features include [6]: (i) Caco-2 cells reduce Fe^{3+} to Fe^{2+}, (ii) the transport of Fe in the Caco-2 cell line responds to the Fe state of the cells, and (iii) a comparative study using human subjects and the Caco-2 cell system concluded that Caco-2 cells predicted quite well the bioavailability of Fe.

References

1. Valko, M., H. Morris, and M.T.D. Cronin, *Metals, Toxicity and Oxidative Stress.* Current Medicinal Chemistry, 2005. **12**(10): p. 1161-1208.
2. Jaishankar, M., et al., *Toxicity, mechanism and health effects of some heavy metals.* Interdiscip Toxicol, 2014. **7**(2): p. 60-72.
3. Morrissey, J. and M.L. Guerinot, *Iron uptake and transport in plants: the good, the bad, and the ionome.* Chemical reviews, 2009. **109**(10): p. 4553-4567.
4. Colombo, C., et al., *Review on iron availability in soil: interaction of Fe minerals,*

plants, and microbes. Journal of Soils and Sediments, 2014. **14**(3): p. 538-548.

5. Colombo, C., et al., *Review on iron availability in soil: interaction of Fe minerals, plants, and microbes.* Journal of Soils and Sediments, 2014. **14**(3): p. 538.
6. Karakaseva, E., S. Jovanova, and B. Boev, *Accumulation and distribution of heavy metal in perennials parts of vine in five local varieties (Rizling, Smederevka, Hamburg, Kratošia and Afus ali) from Ovče pole (r. Macedonia).* Geologica Macedonica, 2013. **26**(2): p. 1-11.
7. Morrissey, J. and M.L. Guerinot, *Iron uptake and transport in plants: the good, the bad, and the ionome.* Chem Rev, 2009. **109**(10): p. 4553-67.
8. Ratledge, C. and L.G. Dover, *Iron metabolism in pathogenic bacteria.* Annual reviews in microbiology, 2000. **54**(1): p. 881-941.
9. Valko, M., H. Morris, and M. Cronin, *Metals, toxicity and oxidative stress.* Current medicinal chemistry, 2005. **12**(10): p. 1161-1208.
10. Weisany, W., Y. Raei, and K.H. Allahverdipoor, *Role of some of mineral nutrients in biological nitrogen fixation.* Bull. Env. Pharmacol. Life Sci, 2013. **2**(4): p. 77-84.
11. Pilon-Smits, E.A.H., et al., *Physiological functions of beneficial elements.* Current Opinion in Plant Biology, 2009. **12**(3): p. 267-274.
12. Morrissey, J., et al., *The ferroportin metal efflux proteins function in iron and cobalt homeostasis in Arabidopsis.* Plant Cell, 2009. **21**(10): p. 3326-38.
13. Lange, B., et al., *Copper and cobalt accumulation in plants: a critical assessment of the current state of knowledge.* New Phytologist, 2017. **213**(2): p. 537-551.
14. Cheng, J., et al., *An ABC-Type Cobalt Transport System Is Essential for Growth of Sinorhizobium melilotiat Trace Metal Concentrations.* Journal of Bacteriology, 2011. **193**(17): p. 4405-4416.
15. Watson, R.J., et al., *Sinorhizobium meliloti Cells Require Biotin and either Cobalt or Methionine for Growth.* Applied and Environmental Microbiology, 2001. **67**(8): p. 3767-3770.
16. Brown, P.H., R.M. Welch, and E.E. Cary, *Nickel: A Micronutrient Essential for Higher Plants.* Plant Physiology, 1987. **85**(3): p. 801-803.
17. Mobley, H. and R. Hausinger, *Microbial ureases: significance, regulation, and molecular characterization.* Microbiological reviews, 1989. **53**(1): p. 85-108.
18. *<Plant Physiol.-1987-Brown-801-3.pdf>*.
19. Mulrooney, S.B. and R.P. Hausinger, *Nickel uptake and utilization by microorganisms.* FEMS Microbiology Reviews, 2003. **27**(2-3): p. 239-261.
20. Sawers, R.G., *Nickel in Bacteria and Archaea*, in *Encyclopedia of Metalloproteins*,

R.H. Kretsinger, V.N. Uversky, and E.A. Permyakov, Editors. 2013, Springer New York: New York, NY. p. 1490-1496.

21. Yruela, I., *Copper in plants.* Brazilian Journal of Plant Physiology, 2005. **17**: p. 145-156.
22. Yruela, I., *Copper in plants.* Brazilian Journal of Plant Physiology, 2005. **17**(1): p. 145-156.
23. Yruela, I., *Copper in plants: acquisition, transport and interactions.* Functional Plant Biology, 2009. **36**(5): p. 409-430.
24. Argüello, J.M., D. Raimunda, and T. Padilla-Benavides, *Mechanisms of copper homeostasis in bacteria.* Frontiers in Cellular and Infection Microbiology, 2013. **3**: p. 73.
25. Hao, X., et al., *Copper tolerance mechanisms of Mesorhizobium amorphae and its role in aiding phytostabilization by Robinia pseudoacacia in copper contaminated soil.* Environmental science & technology, 2015. **49**(4): p. 2328-2340.
26. Hafeez, B., Y. Khanif, and M. Saleem, *Role of zinc in plant nutrition—a review.* American journal of experimental Agriculture, 2013. **3**(2): p. 374-391.
27. Broadley, M.R., et al., *Zinc in plants.* New Phytologist, 2007. **173**(4): p. 677-702.
28. Ravasi, T., et al., *Systematic Characterization of the Zinc-Finger-Containing Proteins in the Mouse Transcriptome.* Genome Research, 2003. **13**(6b): p. 1430-1442.
29. Cakmak, I., *Tansley Review No. 111 Possible roles of zinc in protecting plant cells from damage by reactive oxygen species.* New Phytologist, 2000. **146**(2): p. 185-205.
30. Graham, A.I., et al., *Severe Zinc Depletion of Escherichia coli: ROLES FOR HIGH AFFINITY ZINC BINDING BY ZinT, ZINC TRANSPORT AND ZINC-INDEPENDENT PROTEINS.* Journal of Biological Chemistry, 2009. **284**(27): p. 18377-18389.
31. Da Silva, J.F. and R.J.P. Williams, *The biological chemistry of the elements: the inorganic chemistry of life*. 2001: Oxford University Press.
32. Bashir, K., Y. Ishimaru, and N.K. Nishizawa, *Iron Uptake and Loading into Rice Grains.* Rice, 2010. **3**(2): p. 122-130.
33. Beasley, F.C., *Serum iron uptake and virulence in Staphylococcus aureus.* 2011.
34. Sah, S., N. Singh, and R. Singh, *Iron acquisition in maize (Zea mays L.) using Pseudomonas siderophore.* 3 Biotech, 2017. **7**(2): p. 121.
35. Boer, J.L., S.B. Mulrooney, and R.P. Hausinger, *Nickel-Dependent Metalloenzymes.* Archives of biochemistry and biophysics, 2014. **0**: p. 142-152.
36. Blencowe, D.K. and A.P. Morby, *Zn (II) metabolism in prokaryotes.* FEMS

microbiology reviews, 2003. **27**(2-3): p. 291-311.

37. Kershaw, C.J., N.L. Brown, and J.L. Hobman, *Zinc dependence of zinT (yodA) mutants and binding of zinc, cadmium and mercury by ZinT.* Biochemical and biophysical research communications, 2007. **364**(1): p. 66-71.
38. Stillman, M., *Biological Inorganic Chemistry. Structure and Reactivity. Edited by Ivano Bertini, Harry B. Gray, Edward I. Stiefel and Joan S. Valentine.* Angewandte Chemie International Edition, 2007. **46**(46): p. 8741-8742.
39. *<Transport and Storage of Metal Ions in Biology.pdf>*.
40. Mason, A.Z., K.D. Jenkins, and P.A. Sullivan, *Mechanisms of trace metal accumulation in the polychaete Neanthes arenaceodentata*. Journal of the Marine Biological Association of the United Kingdom, 2009. **68**(1): p. 61-80.
41. Haydon, M.J. and C.S. Cobbett, *Transporters of ligands for essential metal ions in plants.* New Phytologist, 2007. **174**(3): p. 499-506.
42. Klatte, M., et al., *The Analysis of Arabidopsis Nicotianamine Synthase Mutants Reveals Functions for Nicotianamine in Seed Iron Loading and Iron Deficiency Responses.* Plant Physiology, 2009. **150**(1): p. 257-271.
43. Weber, G., G. Neumann, and V. Römheld, *Speciation of iron coordinated by phytosiderophores by use of HPLC with pulsed amperometric detection and AAS.* Analytical and Bioanalytical Chemistry, 2002. **373**(8): p. 767-771.
44. Arruda, M.A.Z. and R.A. Azevedo, *Metallomics and chemical speciation: towards a better understanding of metal-induced stress in plants.* Annals of Applied Biology, 2009. **155**(3): p. 301-307.
45. Rellán-Álvarez, R., et al., *Identification of a Tri-Iron(III), Tri-Citrate Complex in the Xylem Sap of Iron-Deficient Tomato Resupplied with Iron: New Insights into Plant Iron Long-Distance Transport.* Plant and Cell Physiology, 2010. **51**(1): p. 91-102.
46. Terzano, R., et al., *Iron (Fe) speciation in xylem sap by XANES at a high brilliant synchrotron X-ray source: opportunities and limitations.* Analytical and Bioanalytical Chemistry, 2013. **405**(16): p. 5411-5419.
47. Trampczynska, A., et al., *Nicotianamine forms complexes with Zn(ii)in vivo.* Metallomics, 2010. **2**(1): p. 57-66.
48. Deinlein, U., et al., *Elevated Nicotianamine Levels in Arabidopsis halleri Roots Play a Key Role in Zinc Hyperaccumulation.* The Plant Cell, 2012. **24**(2): p. 708-723.
49. Ando, Y., et al., *Copper in xylem and phloem saps from rice (Oryza sativa): the effect of moderate copper concentrations in the growth medium on the accumulation of five essential metals and a speciation analysis of copper-containing*

compounds. Functional Plant Biology, 2012. **40**(1): p. 89-100.

50. Callahan, D.L., et al., *LC–MS and GC–MS metabolite profiling of nickel(II) complexes in the latex of the nickel-hyperaccumulating tree Sebertia acuminata and identification of methylated aldaric acid as a new nickel(II) ligand.* Phytochemistry, 2008. **69**(1): p. 240-251.
51. Xuan, Y., et al., *Separation and identification of phytosiderophores and their metal complexes in plants by zwitterionic hydrophilic interaction liquid chromatography coupled to electrospray ionization mass spectrometry.* Journal of Chromatography A, 2006. **1136**(1): p. 73-81.
52. Raines, D.J., et al., *Bacteria in an intense competition for iron: Key component of the Campylobacter jejuni iron uptake system scavenges enterobactin hydrolysis product.* Proceedings of the National Academy of Sciences of the United States of America, 2016. **113**(21): p. 5850-5855.
53. Walker, L.R., et al., *Unambiguous identification and discovery of bacterial siderophores by direct injection 21 Tesla Fourier transform ion cyclotron resonance mass spectrometry.* Metallomics, 2017. **9**(1): p. 82-92.
54. Boiteau, R.M. and D.J. Repeta, *An extended siderophore suite from Synechococcus sp. PCC 7002 revealed by LC-ICPMS-ESIMS.* Metallomics, 2015. **7**(5): p. 877-884.
55. Mansson, M., L. Gram, and T.O. Larsen, *Production of Bioactive Secondary Metabolites by Marine Vibrionaceae.* Marine Drugs, 2011. **9**(9): p. 1440-1468.
56. Caza, M. and J. Kronstad, *Shared and distinct mechanisms of iron acquisition by bacterial and fungal pathogens of humans.* Frontiers in Cellular and Infection Microbiology, 2013. **3**(80).
57. Hider, R.C. and X. Kong, *Chemistry and biology of siderophores.* Natural Product Reports, 2010. **27**(5): p. 637-657.
58. Li, N., et al., *Unique Iron Coordination in Iron-chelating Molecule Vibriobactin Helps Vibrio cholerae Evade Mammalian Siderocalin-mediated Immune Response.* Journal of Biological Chemistry, 2012. **287**(12): p. 8912-8919.
59. Patzer, S.I. and V. Braun, *Gene Cluster Involved in the Biosynthesis of Griseobactin, a Catechol-Peptide Siderophore of Streptomyces sp. ATCC 700974.* Journal of Bacteriology, 2010. **192**(2): p. 426-435.
60. Saha, R., et al., *Microbial siderophores: a mini review.* Journal of Basic Microbiology, 2013. **53**(4): p. 303-317.
61. Hannauer, M., et al., *The Ferrichrome Uptake Pathway in Pseudomonas aeruginosa Involves an Iron Release Mechanism with Acylation of the Siderophore and Recycling*

of the Modified Desferrichrome. Journal of Bacteriology, 2010. **192**(5): p. 1212-1220.

62. Li, W., et al., *Comparative Genomic Insights Into the Biosynthesis and Regulation of Mycobacterial Siderophores.* Cellular Physiology and Biochemistry, 2013. **31**(1): p. 1-13.
63. Denaro, R., et al., *Alcanivorax borkumensis produces an extracellular siderophore in iron-limitation condition maintaining the hydrocarbon-degradation efficiency.* Marine Genomics, 2014. **17**: p. 43-52.
64. Tanabe, T., et al., *The Vibrio parahaemolyticus Small RNA RyhB Promotes Production of the Siderophore Vibrioferrin by Stabilizing the Polycistronic mRNA.* Journal of Bacteriology, 2013. **195**(16): p. 3692-3703.
65. Burnside, D.M., et al., *The Legionella pneumophila Siderophore Legiobactin Is a Polycarboxylate That Is Identical in Structure to Rhizoferrin.* Infection and Immunity, 2015. **83**(10): p. 3937-3945.
66. Méndez, J.A., et al., *Quantitative proteomic analysis of host—pathogen interactions: a study of Acinetobacter baumannii responses to host airways.* BMC Genomics, 2015. **16**(1): p. 422.
67. Penwell, W.F., B.A. Arivett, and L.A. Actis, *The Acinetobacter baumannii entA Gene Located Outside the Acinetobactin Cluster Is Critical for Siderophore Production, Iron Acquisition and Virulence.* PLOS ONE, 2012. **7**(5): p. e36493.
68. Chen, Y., et al., *Gobichelin A and B: mixed-ligand siderophores discovered using proteomics.* MedChemComm, 2013. **4**(1): p. 233-238.
69. Proschak, A., et al., *Structure and Biosynthesis of Fimsbactins A–F, Siderophores from Acinetobacter baumannii and Acinetobacter baylyi.* ChemBioChem, 2013. **14**(5): p. 633-638.
70. Penwell, W.F., et al., *Discovery and Characterization of New Hydroxamate Siderophores, Baumannoferrin A and B, produced by Acinetobacter baumannii.* ChemBioChem, 2015. **16**(13): p. 1896-1904.
71. Sah, S. and R. Singh, *Siderophore: Structural And Functional Characterisation – A Comprehensive Review*, in *Agriculture (Polnohospodárstvo)*. 2015. p. 97.
72. McMahon, M.D., J.S. Rush, and M.G. Thomas, *Analyses of MbtB, MbtE, and MbtF Suggest Revisions to the Mycobactin Biosynthesis Pathway in Mycobacterium tuberculosis.* Journal of Bacteriology, 2012. **194**(11): p. 2809-2818.
73. Zane, H.K., et al., *Biosynthesis of Amphi-enterobactin Siderophores by Vibrio harveyi BAA-1116: Identification of a Bifunctional Nonribosomal Peptide Synthetase Condensation Domain.* Journal of the American Chemical Society, 2014. **136**(15): p.

5615-5618.

74. Kem, M.P. and A. Butler, *Acyl peptidic siderophores: structures, biosyntheses and post-assembly modifications.* BioMetals, 2015. **28**(3): p. 445-459.
75. Schalk, I.J. and L. Guillon, *Pyoverdine biosynthesis and secretion in Pseudomonas aeruginosa: implications for metal homeostasis.* Environmental Microbiology, 2013. **15**(6): p. 1661-1673.
76. Brandel, J., et al., *Pyochelin, a siderophore of Pseudomonas aeruginosa: Physicochemical characterization of the iron(iii), copper(ii) and zinc(ii) complexes.* Dalton Transactions, 2012. **41**(9): p. 2820-2834.
77. Haraguchi, H., *Metallomics as integrated biometal science.* Journal of Analytical Atomic Spectrometry, 2004. **19**(1): p. 5-14.
78. Lobinski, R., et al., *Metallomics: guidelines for terminology and critical evaluation of analytical chemistry approaches (IUPAC Technical Report).* Pure and Applied Chemistry, 2010. **82**(2): p. 493-504.
79. Bittencourt, L.M., et al., *Determination of metal associated with proteins of wheat seed samples after sequential extraction procedure.* Journal of the Brazilian Chemical Society, 2014. **25**(2): p. 264-270.
80. Susanne Becker, J., R. Lobinski, and J. Sabine Becker, *Metal imaging in non-denaturating 2D electrophoresis gels by laser ablation inductively coupled plasma mass spectrometry (LA-ICP-MS) for the detection of metalloproteins.* Metallomics, 2009. **1**(4): p. 312-316.
81. Rigueira, L.M.B., et al., *Identification of metal-binding to proteins in seed samples using RF-HPLC-UV, GFAAS and MALDI-TOF-MS.* Food Chemistry, 2016. **211**: p. 910-915.
82. Eid, R., et al., *Identification of human ferritin, heavy polypeptide 1 (FTH1) and yeast RGI1 (YER067W) as pro-survival sequences that counteract the effects of Bax and copper in Saccharomyces cerevisiae.* Experimental Cell Research, 2016. **342**(1): p. 52-61.
83. Peppers, D. and N. Grossoehme, *Purification and Characterization of Nickel Uptake Regulator (NUR) and Single NUR Mutants from Streptomyces coelicolor.* The Winthrop McNair Research Bulletin, 2016. **1**(1): p. 12.
84. Khacheryan, L., et al., *Biochemical Analysis of the Zinc Uptake Regulator (Zur) from Klebsiella oxytoca.* The FASEB Journal, 2017. **31**(1 Supplement): p. 756.1-756.1.
85. Andrews, S.C., A.K. Robinson, and F. Rodríguez-Quiñones, *Bacterial iron homeostasis.* FEMS Microbiology Reviews, 2003. **27**(2-3): p. 215-237.

86. Urvoas, A., et al., *Analysis of the metal-binding selectivity of the metallochaperone CopZ from Enterococcus hirae by electrospray ionization mass spectrometry.* Rapid Communications in Mass Spectrometry, 2003. **17**(16): p. 1889-1896.

87. Escolar, L., J. Pérez-Martín, and V. De Lorenzo, *Opening the iron box: transcriptional metalloregulation by the Fur protein.* Journal of bacteriology, 1999. **181**(20): p. 6223-6229.

88. Gaballa, A. and J.D. Helmann, *Identification of a Zinc-Specific Metalloregulatory Protein, Zur, Controlling Zinc Transport Operons inBacillus subtilis.* Journal of bacteriology, 1998. **180**(22): p. 5815-5821.

89. Qi, Z., I. Hamza, and M.R. O'Brian, *Heme is an effector molecule for iron-dependent degradation of the bacterial iron response regulator (Irr) protein.* Proceedings of the National Academy of Sciences of the United States of America, 1999. **96**(23): p. 13056-13061.

90. Porcheron, G., et al., *Iron, copper, zinc, and manganese transport and regulation in pathogenic Enterobacteria: correlations between strains, site of infection and the relative importance of the different metal transport systems for virulence.* Frontiers in Cellular and Infection Microbiology, 2013. **3**: p. 90.

91. Santos, A.F., et al., *Study of the antimicrobial activity of metal complexes and their ligands through bioassays applied to plant extracts.* Revista Brasileira de Farmacognosia, 2014. **24**(3): p. 309-315.

92. Rellán-Álvarez, R., et al., *Changes in the proteomic and metabolic profiles of Beta vulgaris root tips in response to iron deficiency and resupply.* BMC Plant Biology, 2010. **10**(1): p. 120.

93. Silva, A.M.N., et al., *Iron(iii) citrate speciation in aqueous solution.* Dalton Transactions, 2009(40): p. 8616-8625.

94. Dettmer, K., P.A. Aronov, and B.D. Hammock, *Mass spectrometry‐based metabolomics.* Mass spectrometry reviews, 2007. **26**(1): p. 51-78.

95. Dunn, W.B., N.J.C. Bailey, and H.E. Johnson, *Measuring the metabolome: current analytical technologies.* Analyst, 2005. **130**(5): p. 606-625.

96. Aharoni, A., et al., *Nontargeted metabolome analysis by use of Fourier transform ion cyclotron mass spectrometry.* Omics: a journal of integrative biology, 2002. **6**(3): p. 217-234.

97. Tsednee, M., et al., *Identification of metal species by ESI-MS/MS through release of free metals from the corresponding metal-ligand complexes.* Scientific Reports, 2016. **6**: p. 26785.

98. Wooldridge, K.G. and P.H. Williams, *Iron uptake mechanisms of pathogenic bacteria.* FEMS Microbiology Reviews, 1993. **12**(4): p. 325-348.

99. Flis, P., et al., *Inventory of metal complexes circulating in plant fluids: a reliable method based on HPLC coupled with dual elemental and high‐resolution molecular mass spectrometric detection.* New Phytologist, 2016. **211**(3): p. 1129-1141.

100. Jitaru, P. and C. Barbante, *Elemental speciation analysis, from environmental to biochemical challenge.* J. Phys. IV France, 2006. **139**: p. 269-294.

101. Kot, A. and J. Namieśnik, *The role of speciation in analytical chemistry.* TrAC Trends in Analytical Chemistry, 2000. **19**(2–3): p. 69-79.

102. Eagling, T., et al., *Distribution and Speciation of Iron and Zinc in Grain of Two Wheat Genotypes.* Journal of Agricultural and Food Chemistry, 2014. **62**(3): p. 708-716.

103. Mesko, M.F., et al., *Sample preparation strategies for bioinorganic analysis by inductively coupled plasma mass spectrometry.* International Journal of Mass Spectrometry, 2011. **307**(1): p. 123-136.

104. Bennett, J.H., et al., *Photochemical reduction of iron. II. Plant related factors.* Journal of Plant Nutrition, 1982. **5**(4-7): p. 335-344.

105. Mitra, S., *Sample preparation techniques in analytical chemistry*. Vol. 237. 2004: John Wiley & Sons.

106. Husted, S., et al., *Review: the role of atomic spectrometry in plant science.* Journal of Analytical Atomic Spectrometry, 2011. **26**(1): p. 52-79.

107. Rellán-Álvarez, R., J. Abadía, and A. Álvarez-Fernández, *Formation of metal-nicotianamine complexes as affected by pH, ligand exchange with citrate and metal exchange. A study by electrospray ionization time-of-flight mass spectrometry.* Rapid Commun Mass Spectrom, 2008. **22**.

108. Cuypers, A., K. Smeets, and J. Vangronsveld, *Heavy metal stress in plants.* Plant Stress Biology: From genomics to systems biology, 2009: p. 161-178.

109. Vijayan, P., et al., *Synchrotron radiation sheds fresh light on plant research: The use of powerful techniques to probe structure and composition of plants.* Plant and Cell Physiology, 2015: p. pcv080.

110. Terzano, R., et al., *Iron (Fe) speciation in xylem sap by XANES at a high brilliant synchrotron X-ray source: opportunities and limitations.* Analytical and bioanalytical chemistry, 2013. **405**(16): p. 5411.

111. Singh, S.P., et al., *Pattern of iron distribution in maternal and filial tissues in wheat grains with contrasting levels of iron.* Journal of experimental botany, 2013. **64**(11): p.

3249-3260.

112. De Brier, N., et al., *Element distribution and iron speciation in mature wheat grains (Triticum aestivum L.) using synchrotron X‐ray fluorescence microscopy mapping and X‐ray absorption near‐edge structure (XANES) imaging.* Plant, cell & environment, 2016. **39**(8): p. 1835-1847.

113. Robards, K., P.R. Haddad, and P.E. Jackson, *Principles and practice of modern chromatographic methods*. 1994: Academic Press.

114. Guiochon, G., *Basic Principles of Chromatography*, in *Handbook of Analytical Techniques*. 2008, Wiley-VCH Verlag GmbH. p. 173-198.

115. *<Size exclusion chromatography handbook.pdf>*.

116. Buszewski, B. and S. Noga, *Hydrophilic interaction liquid chromatography (HILIC)—a powerful separation technique.* Analytical and Bioanalytical Chemistry, 2012. **402**(1): p. 231-247.

117. Boersema, P.J., S. Mohammed, and A.J. Heck, *Hydrophilic interaction liquid chromatography (HILIC) in proteomics.* Analytical and bioanalytical chemistry, 2008. **391**(1): p. 151-159.

118. Aguilar, M.-I., *Reversed-phase high-performance liquid chromatography*. 2004: Springer.

119. Campanella, B. and E. Bramanti, *Detection of proteins by hyphenated techniques with endogenous metal tags and metal chemical labelling.* Analyst, 2014. **139**(17): p. 4124-4153.

120. Barth, H.G., et al., *Column liquid chromatography.* Analytical Chemistry, 1988. **60**(12): p. 387-435.

121. Part, X., *A Beginner's Guide to ICP-MS.* SPECTROSCOPY, 2001. **16**: p. 10.

122. Batsala, M., et al., *Inductively coupled plasma mass spectrometry (ICP-MS).* Int J Res Pharm Chem, 2012. **2**(3): p. 671-680.

123. Ramyalakshmi, G. and P. Venkatesh, *7. A Review on Inductively Coupled Plasma Mass Spectroscopy.* International Journal of Drug Development and Research, 2012.

124. Sanz-Medel, A., M. Montes-Bayón, and M. Luisa Fernández Sánchez, *Trace element speciation by ICP-MS in large biomolecules and its potential for proteomics.* Analytical and Bioanalytical Chemistry, 2003. **377**(2): p. 236-247.

125. Wang, T., *Liquid Chromatography–Inductively Coupled Plasma Mass Spectrometry (LC–ICP–MS).* Journal of Liquid Chromatography & Related Technologies, 2007. **30**(5-7): p. 807-831.

126. Pröfrock, D. and A. Prange, *Inductively Coupled Plasma–Mass Spectrometry*

(ICP-MS) for Quantitative Analysis in Environmental and Life Sciences: A Review of Challenges, Solutions, and Trends. Applied Spectroscopy, 2012. **66**(8): p. 843-868.

127. Michalski, R., *Application of IC-MS and IC-ICP-MS in environmental research*. 2016: John Wiley & Sons.
128. Łobiński, R., D. Schaumlöffel, and J. Szpunar, *Mass spectrometry in bioinorganic analytical chemistry.* Mass Spectrometry Reviews, 2006. **25**(2): p. 255-289.
129. Acikara, O.z.B., *Ion-exchange chromatography and its applications*, in *Column chromatography*. 2013, InTech.
130. May, T.W. and R.H. Wiedmeyer, *A table of polyatomic interferences in ICP-MS.* ATOMIC SPECTROSCOPY-NORWALK CONNECTICUT-, 1998. **19**: p. 150-155.
131. Makishima, A. and E. Nakamura, *Suppression of Matrix Effects in ICP‐MS by High Power Operation of ICP: Application to Precise Determination of Rb, Sr, Y, Cs, Ba, REE, Pb, Th and U at ng g‐1 Levels in Milligram Silicate Samples.* Geostandards and Geoanalytical Research, 1997. **21**(2): p. 307-319.
132. *Mass Spectrometry, Review of the Basics: Ionization.* Applied Spectroscopy Reviews, 2015. **50**(2): p. 158-175.
133. Kebarle, P. and U.H. Verkerk, *Electrospray: from ions in solution to ions in the gas phase, what we know now.* Mass spectrometry reviews, 2009. **28**(6): p. 898-917.
134. Sutton, K.L. and J.A. Caruso, *Liquid chromatography–inductively coupled plasma mass spectrometry.* Journal of Chromatography A, 1999. **856**(1): p. 243-258.
135. Hu, Q., et al., *The Orbitrap: a new mass spectrometer.* Journal of Mass Spectrometry, 2005. **40**(4): p. 430-443.
136. Strupat, K., O. Scheibner, and M. Bromirski, *High-Resolution, Accurate-Mass Orbitrap Mass Spectrometry–Definitions, Opportunities, and Advantages.*
137. Scalbert, A., et al., *Mass-spectrometry-based metabolomics: limitations and recommendations for future progress with particular focus on nutrition research.* Metabolomics, 2009. **5**(4): p. 435-458.
138. Roth, M.J., et al., *Sensitive and Reproducible Intact Mass Analysis of Complex Protein Mixtures with Superficially Porous Capillary Reversed-Phase Liquid Chromatography Mass Spectrometry.* Analytical Chemistry, 2011. **83**(24): p. 9586-9592.
139. Nováková, L., L. Havlíková, and H. Vlčková, *Hydrophilic interaction chromatography of polar and ionizable compounds by UHPLC.* TrAC Trends in Analytical Chemistry, 2014. **63**: p. 55-64.
140. Spagou, K., et al., *Hydrophilic interaction chromatography coupled to MS for*

metabonomic/metabolomic studies. Journal of separation science, 2010. **33**(6- 7): p. 716-727.

141. Rellán-Álvarez, R., et al., *Development of a new high-performance liquid chromatography–electrospray ionization time-of-flight mass spectrometry method for the determination of low molecular mass organic acids in plant tissue extracts.* Journal of agricultural and food chemistry, 2011. **59**(13): p. 6864-6870.
142. Rellán-Álvarez, R., et al., *Identification of a tri-iron (III), tri-citrate complex in the xylem sap of iron-deficient tomato resupplied with iron: new insights into plant iron long-distance transport.* Plant and Cell Physiology, 2009. **51**(1): p. 91-102.
143. Dell'mour, M., et al., *Analysis of iron- phytosiderophore complexes in soil related samples: LC- ESI- MS/MS versus CE- MS.* Electrophoresis, 2012. **33**(4): p. 726-733.
144. Bajad, S.U., et al., *Separation and quantitation of water soluble cellular metabolites by hydrophilic interaction chromatography-tandem mass spectrometry.* Journal of Chromatography A, 2006. **1125**(1): p. 76-88.
145. Oertel, R., U. Renner, and W. Kirch, *Determination of neomycin by LC–tandem mass spectrometry using hydrophilic interaction chromatography.* Journal of Pharmaceutical and Biomedical Analysis, 2004. **35**(3): p. 633-638.
146. Balluff, B., R.J. Carreira, and L.A. McDonnell, *Chapter 7 - Mass Spectrometry Imaging in Proteomics and Metabolomics*, in *Comprehensive Analytical Chemistry*, A.C. Carolina Simó and G.-C. Virginia, Editors. 2014, Elsevier. p. 159-185.
147. Denkert, C., et al., *Mass spectrometry–based metabolic profiling reveals different metabolite patterns in invasive ovarian carcinomas and ovarian borderline tumors.* Cancer research, 2006. **66**(22): p. 10795-10804.
148. Song, W.-Y., et al., *Arsenic tolerance in Arabidopsis is mediated by two ABCC-type phytochelatin transporters.* Proceedings of the National Academy of Sciences, 2010. **107**(49): p. 21187-21192.
149. Flis, P., et al., *Inventory of metal complexes circulating in plant fluids: a reliable method based on HPLC coupled with dual elemental and high-resolution molecular mass spectrometric detection.* New Phytologist, 2016. **211**(3): p. 1129-1141.
150. Li, X.-j., et al., *A tool to visualize and evaluate data obtained by liquid chromatography-electrospray ionization-mass spectrometry.* Analytical chemistry, 2004. **76**(13): p. 3856-3860.
151. Koulman, A., et al., *High- throughput direct- infusion ion trap mass spectrometry: a new method for metabolomics.* Rapid Communications in Mass Spectrometry, 2007. **21**(3): p. 421-428.

152. Tchounwou, P.B., et al., *Heavy Metals Toxicity and the Environment.* EXS, 2012. **101**: p. 133-164.

153. Ho, C.S., et al., *Electrospray Ionisation Mass Spectrometry: Principles and Clinical Applications.* The Clinical Biochemist Reviews, 2003. **24**(1): p. 3-12.

154. Ghssein, G., et al., *Biosynthesis of a broad-spectrum nicotianamine-like metallophore in Staphylococcus aureus.* Science, 2016. **352**(6289): p. 1105-1109.

155. Tsednee, M., et al., *Identification of metal species by ESI-MS/MS through release of free metals from the corresponding metal-ligand complexes.* Scientific reports, 2016. **6**: p. srep26785.

156. Pedreschi, R., et al., *Proteomics for the food industry: opportunities and challenges.* Critical reviews in food science and nutrition, 2010. **50**(7): p. 680-692.

157. Templeton, D.M., et al., *Guidelines for terms related to chemical speciation and fractionation of elements. Definitions, structural aspects, and methodological approaches (IUPAC Recommendations 2000).* Pure and applied chemistry, 2000. **72**(8): p. 1453-1470.

158. Ser, Z., et al., *Extraction parameters for metabolomics from cell extracts.* Analytical biochemistry, 2015. **475**: p. 22-28.

159. Maia, M., et al., *Metabolite extraction for high-throughput FTICR-MS-based metabolomics of grapevine leaves.* EuPA Open Proteomics, 2016. **12**: p. 4-9.

160. Guan, X. and H. Yao, *Optimization of Viscozyme L-assisted extraction of oat bran protein using response surface methodology.* Food chemistry, 2008. **106**(1): p. 345-351.

161. de Moura, J.M., et al., *Protein extraction and membrane recovery in enzyme-assisted aqueous extraction processing of soybeans.* Journal of the American Oil Chemists' Society, 2011. **88**(6): p. 877-889.

162. Leite Nobrega de Moura, J.M.a., et al., *Lunasin and Bowman-Birk protease inhibitor concentrations of protein extracts from enzyme-assisted aqueous extraction of soybeans.* Journal of agricultural and food chemistry, 2011. **59**(13): p. 6940-6946.

PART III.
EXPERIMENTAL

Part III. EXPERIMENTAL

Chapter 4. Instruments, Samples and Procedures

4.1.Instrumentation

4.1.1. Ssample preparation

A Mettler AJ150 (Meettler Toledo AG, Switzerland) scale was used to weight samples and reagents. The samples were incubated at controlled temperature in a combined orbital/linear shaking water bath (OLS200, Grant Instruments, Cambridge, UK) (**Fig. 4.1a**), centrifuged in an Eppendorf MiniSpin centrifuge (Eppendorf AG, German) (**Fig.4.1b**) and digested in a Digi-Prep heated-block digester (SCP Science, Courtaboeuf, France) (**Fig. 4.1c**). A Crios -85°C bench-top freeze dryer (Cryotec, France) was used for lyophilization (**Fig. 4.1d**). An IKA® HS 250 Shaker (KA®-Werke GmbH & Co. KG, Deutschland/Germany) (**Fig. 4.1e)** was used to carry out slow shaking operations during extraction of iron from maize samples. A Milli-Q® Type 1 Ultrapure Water Systems (Millipore, Bedford, Ma) (**Fig. 4.1f)** was used for water purification.

A

B

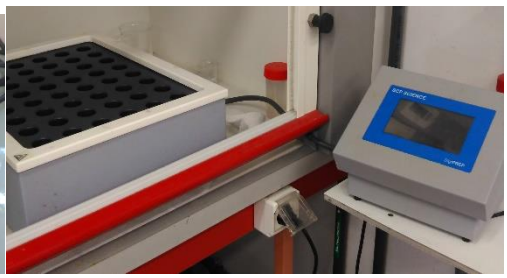

C

D

E

F

Fig. 4.1. Laboratory equipment used in sample preparation: a) shaking water bath, b) centrifuge, c) Digi-Prep digester, d) freeze dryer e) shaker f) water purification system.

4.1.2 Chromatographic equipment

Chromatographic separations were performed using an Agilent 1200 series HPLC pump (Agilent, Tokyo, Japan) (**Fig. 4.2a**) as a delivery system for size exclusion chromatography (SEC), whereas an Agilent 1100 capillary HPLC system equipped with a 100 mL/min splitter module (**Fig. 4.2b**) was used for HILIC experiments.

Fig. 4.2. Agilent 1100 capillary HPLC system (left), Agilent 1200 series HPLC (right)

4.1.3. Inductively coupled plasma mass spectrometers

The ICP MS instruments were Agilent Models 7500 and 7700s (both from Agilent, Tokyo, Japan) equipped with a collision cell with hydrogen as collision gas (**Fig. 4.3**). Operating parameters of ICP MS are listed in Table 2.1.

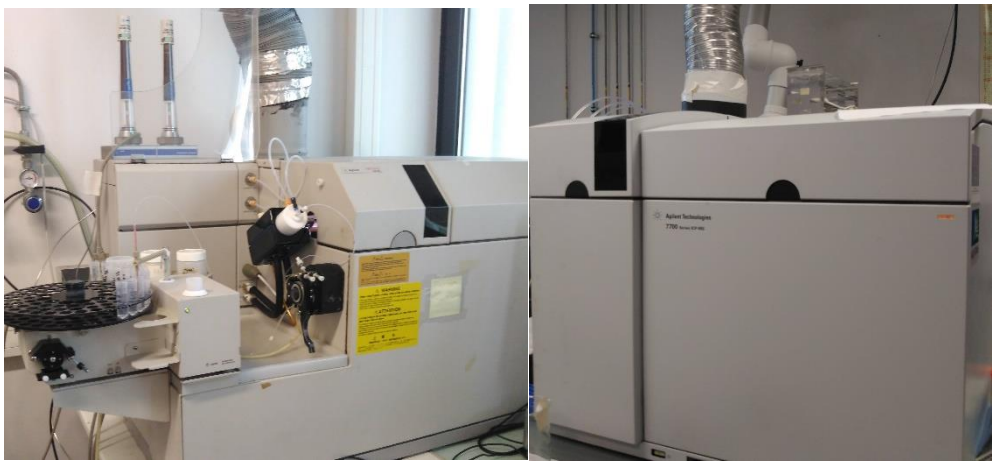

Fig. 4.3. ICP MS instrument used (a) Agilent Model 7500 ICP-MS, (b) Agilent Model 7700s ICP-MS

Table 4.1. ICP MS conditions used

Parameter	
Skimmer/sampler cones	Pt
Operation mode	organic
RF Power	1550 W
RF matching	2 V
Nebulizer pump	0,1 rps
Optional gas*	7 %
Carrier gas	0,67 L/min
Isotopes monitored	^{25}Mg, ^{44}Ca, ^{96}Mo, ^{55}Mn, ^{56}Fe, ^{54}Fe, ^{57}Fe, ^{59}Co, ^{60}Ni, ^{65}Cu, ^{64}Zn, ^{65}Zn, ^{112}Cd, ^{31}P, ^{34}S

*- oxygen used in HILIC-ICP MS coupling

The ICP-MS conditions were optimized daily to obtain the highest intensities and lowest interferences using a standard built-in software procedure using a tune solution containing 1 µg/L each of Li, Mg, Y, Ce, Tl and Co in a matrix of 2% HNO_3.

4.1.3.1. Coupling with HPLC

The exit of the chromatographic column was directly connected by means of polyetheretherketone (PEEK) tubing to a MicroMist nebulizer (Glass Expansion, Romainmotier, Switzerland) for the SEC-ICP MS coupling. The interface between the LC system and the ICP-MS detector consisted of a quartz double pass Scott style spray chamber, a MicroMistEzyFit nebulizer (Glass Expansion, Australia) and a 2.5 mm i.d. injector and a set of platinum cones (Agilent Technologies, USA).

The interface between the LC module and the ICP-MS detector consisted of a glass Cinnabar cyclonic spray chamber (Glass Expansion, Australia), a 50 mL/min Micromist U-series nebulizer (Glass Expansion, Australia), a 1 mm i.d. injector torch (Agilent Technologies, Japan), a T-connector allowing the introduction of 7 % O_2 and a set of platinum cones (Agilent Technologies, USA).

The chromatographic conditions used are given in **Table 4.2.**

Table 4.2. Chromatographic methods used.

HILIC	
column	TSK gel amide 80 (250 x 1 mm id) (Tosoh Bioscience, Germany)
mobile phase	A: ammonium formate 10 mM pH=5.5
	B: ACN
flow rate	50 µL/min
injection volume	7 µL
gradient elution	0-5 min – 90 % B, 5 min - 90 % B, 45 min - 50 % B,
	50 min – 50 % B, 52min – 35 % B, 55 min – 35 % B,
	60 min – 90 % B, 65 min – 90 % B
cleaning of the column	ammonium formate – ACN (50:50) overnight at 50 µl/min
Size – exclusion chromatography	
column	Superdex Peptide HR 10/30 (300 x 10mm i.d.) (GE Healthcare Bio-Science AB, Sweden)
mobile phase	ammonium formate 10 mM at pH=5.5
flow rate	0.7 mL/min
Injection volume	20 µL
elution	isocratic
cleaning of the column	ammonium formate 10 mM overnight at 0.2 mL/min

4.1.4. Electrospray mass spectrometer

An electrospray hybrid linear ion trap-orbital ion trap ESI mass spectrometer (Thermo H-ESI II LTQ Orbitrap Velos, Thermo Fisher Scientific, Waltham, MA, USA) (**Fig. 4.3**) was employed. The instrument was equipped with a heated electrospray ionization source (H-ESI II) (Thermo Fisher Scientific). The operating conditions used are given in **Table 4.3.**

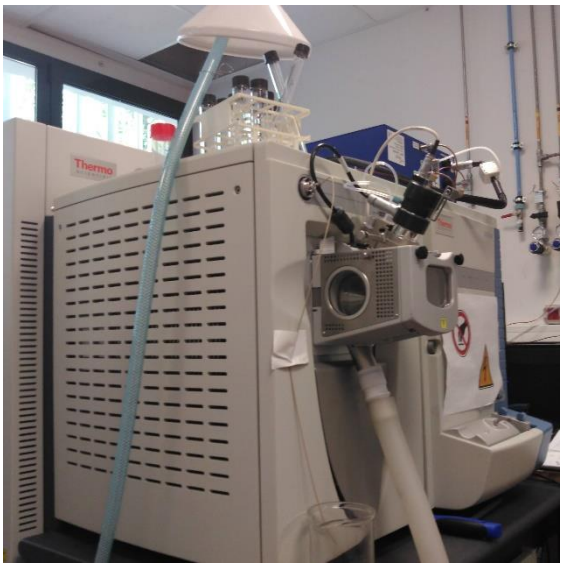

Fig. 4.3. Electrospray hybrid linear ion trap-orbital ion trap mass spectrometer (ThermoFischer Scientific).

Table 4.3. Operating condition of ESI MS.

ESI-Orbitrap- MS	
ionization mode	positive
heater temperature	120 °C
sheath gas flow rate	15 arb
auxiliary gas flow rate	5 arb
sweep gas	1 arb
spray voltage	3.00 kV
capillary temperature	280 °C
lens RF	95%

4.1.4.1. HILIC-ESI-MS/MS and SEC-ESI-MS/MS experiments

The coupling with ESI MS was achieved via a heated electrospray ionization source (H-ESI II) (Thermo Fisher Scientific. Samples were diluted with acetonitrile and water to obtain a 1:2, sample to acetonitrile ratio, and centrifuged. The capillary temperature was 280 ˚C. In full MS mode, the resolution was set at 100 000 (FWHM at *m/z* 400) whereas in MS/MS mode it was set at 30 000. Putative metal species were fragmented during a subsequent chromatographic run with collision induced dissociation (CID) mode at 35% or 45 % energy, respectively.

MS data were processed using Xcalibur 2.1 software and MetWorks 1.2.1 software (Thermo Fischer Scientific) to screen spectra for metal containing molecules. To get accurate masses, MS and MS/MS spectra were recalibrated off-line using precursor/fragment ions with known formulae.

4.2. Reagents

Analytical reagent grade chemicals: acetonitrile, formic acid, acetic acid, nitric acid, ammonium acetate, ammonia, sodium phytate, $NaHCO_3$, nicotianamine，isotope standard solutions 1000ppm of Fe, Co, Ni, Cu, Zn, P, S，ascorbic acid, 70% HNO_3 and 30% H_2O_2 were purchased from Sigma-Aldrich (Saint-Quentin-Fallavier, France). The iron standard solution was from SCP Science (Canada) and citric acid from Acros Organics (Belgium). Ultrapure water (18 MΩ cm) was obtained from a Milli-Q system (Millipore, Bedford, MA). Chelex-100 was obtained from from Sigma-Aldrich.

Bile salts (glycine and taurine conjugates of hyodeoxycholic acid and other bile salts) were purchased from Sigma-Aldrich.

Thermally stable α-amylase (3000 u/mL, 0.1 mL), amyloglucosidase (3260 u/mL), and pepsin (porcine, 10863 u/mg) enzyme solutions for sequential extraction were purchased from Sigma-Aldrich.

Pancreatin from porcine pancreas 8 × USP specifications were purchased from Sigma-Aldrich.

Synthetic staphylopine (N-[3-(N-L-Alanyl)-amino-3-carboxypropyl]-D-histidine) was ordered from Toronto Research Chemical Inc (Toronto, Canada).

4.3 Samples

4.3.1 Genetically modified maize grains

The study on genetically modified maize was carried out in collaboration with two research groups from the US Department of Agriculture:

(i) Owen Hoekenga, Robert W. Holley Center for Agriculture and Health, USDA-ARS, Ithaca, NY,

(ii) Ivan Baxter, Donald Danforth Plant Sciences Center, USDA-ARS Plant Genetics Research Unit, St. Louis, MO)

who provided our group with maize samples already tested in an animal bioavailability study.

The US partners carried out bioavailability studies using 4 maize varieties. The maize was used to feed chicken and the iron level in chicken blood was checked. It was found out that the H maize gave a significant increase compared to L variety. [1, 2].

The samples were divided into four groups depending on the results of the bioavailability study. The groups were coded as: H- presumed high Fe bioavailability, L- presumed low Fe bioavailability. B and M new maize varieties derived from the B73 and Mo17 ones and isolated from sister kernels from the same ears of maize were used[3]. As sister lines were created in both of the parental genetic backgrounds used in the mapping population, nearly isogenic hybrids were made by crossing the parents lines (high with high and low with low) which were named HH and LL types. HB/LB HM/LM and HH/LL varieties are highly similar in terms of their genetics and presumably composition except for iron bioavailability where they have been selected for differences using molecular markers and the Caco2 bioassay.[4, 5]. In preparation for the in analytical trial, maize grains were thoroughly washed in deionized water prior to freeze drying and grounding, they were stored at 4°C until analysis.

4.3.2. Bacterial cells

The samples included *E.coli* cells with expressed operon from *S. aureus* and P. *aeruginosa* devoid of the cntL gene cultivated in chemically defined media (CDM), supplemented with 0.1 µM nickel and *S. aureus* cells cultivated in minimal media culture. The cells were prepared in the partner lab (Romé Voulhoux, CNRS - Aix-Marseille Université, Laboratoire d'Ingénierie des Systèmes Macromoléculaires ; Elise Borezée-Durant, Micalis Institute, INRA, AgroParisTech, Université Paris-Saclay, France) according to the procedure detailed below:

4.4. Procedure

4.4.1. Total metal determination

4.4.1.1. Total metal determination in bacterial cells

Quantification of the total metal content in cell digests was carried out by flow injection analysis – ICP MS using 500 µL injections of sample solutions in to a carrier stream of 2% HNO_3 at 1.00 mL/min.

The 0.1 mL solutions of cell extracts (prepared in the partner laboratory) were lyophilized and the residue was dissolved with a 50 µL mixture of 70% HNO_3 (25 µL) and 30% H_2O_2 (25 µL). The samples were heated at 80°C for 3 h and then diluted with water to reach a final

volume of 500 µL.

4.4.1.2. Total metal determination in maize kernels

50 mg of finely ground maize (HB, LB, HM,LM) was digested with 2.5 mL 70% HNO3 and 2.5 mL 30% H2O2 (3 h at 80° C in DigiPrep), diluted to 50 mL and analyzed by ICP MS using the conditions specified in Table 2.1 Rh was added as internal standard to control the stability of plasma conditions, a standard reference material **(**NIST 8436 Durum Wheat Flour) and a blank were run in parallel, the quantification was carried out by standard addition at 3 levels.

4.4.2. Cell supernatant preparation and measurements for *S. aureus*

WT and mutant strains of S. aureus were grown at 37°C with aeration in either CDM (40, 44) deprived of added metals except magnesium (1 mM; Table S2), demetalated CDM (CDM treated with chelex; dCDM) or LB. For cultures in CDM with metal-NTA resin (rCDM), NTA-treated CDM and metalated resin were prepared as follows: Ni-NTA His-bind resin (EMD Millipore, Billerica) was extensively washed with 100mM EDTA (~15 time the resin volume) to eliminate nickel linked to NTA, and then with double distilled water to remove EDTA. CDM was then incubated overnight with the demetalated NTA resin and further filtrated to obtain NTA-treated CDM. The resin (now metalated by the traces of metals present in CDM) was then placed into Amicon centrifugal filter units (Amicon Ultra-0.5ml 3KDa; Merck Millipore, Tullagreen) inserted into eppendorf tubes. After having cut the bottom of these tubes, they were introduced into 50 ml Falcon tubes containing the NTA-treated CDM. Despite demetalation by EDTA, the total amounts of metal in rCDM treated cells seems to indicate that residual amounts of Mn, Cu and Ni remained trapped by the resin as the uptake of these metals was found higher in rMCD cells than CDM cells. For short time uptake experiments, strains were grown in demetalated CDM until late exponential phase, then supplemented with a metal cocktail (0.3µM Fe(II) and Zn; 0.1µM Ni, Co, Cu, Mn) and incubated for 10 minutes prior to metal level determination by ICP-MS.

Bacteria were recovered after overnight growth by centrifugation at 7,000 g for 15 min. Cells were resuspended in buffer A (20 mM Na,K PO4 (pH 7.5), 500 mM NaCl, 20 mM imidazole) and disrupted using a French press operating at 1000 psi. Cell debris were removed

by centrifugation at 8,000 g for 20 min. The supernatant was centrifuged at 100,000 g for 1 h at 4°C to remove cell wall debris and membrane proteins.

A culture supernatant from a *cntA* mutant of *S. aureus* cultivated in CDM. Nickel was then added to a final concentration of 50 µM to allow the nickel-metallophore complex to form and to bind to CntA. After 2 h of incubation the CntA protein was purified again, exchanged against a buffer containing 10 mM ammonium acetate, and finally analyzed by MS. Cell fraction of an *E. coli* strain expressing the entire *cnt* operon was also analyzed by HILIC/ICP-MS for metal detection and HILIC/ESI-MS for metabolite and metal complex identification.

4.4.3. Cell supernatant preparation and measurements for *P. aeruginosa*

All the *P. aeruginosa* strains derivatives of the parental PA14 strain were grown aerobically with horizontal shaking at 37°C in freshly made Minimal Succinate (MS) medium. All media used in this study were filtered at 0.22 µm with polycarbonate units before used, and stored at 4°C away from light in polycarbonate bottles. Pre-culture of 20mL were inoculated from fresh MS-5% agar plates and grown until late exponential phase in polycarbonate Erlenmeyer flasks. Culture of 25mL were inoculated at OD=0.1 and grown for 8h in freshly made MS or CDM media supplemented or not with EDTA or nickel before inoculation. After 8h, OD_{600} were measured before cells were harvested by centrifugation (2,000*g*, 30min, 4°C). The supernatant was collected, filtered and stored at -80°C. The pellet was washed twice with 1.3mL MS media + 1mM EDTA followed by a wash with 1.3mL MS media. OD_{600} were measured, and cells ruptured by successive sonication cycles. The lysates were then centrifuged at 16,000g for 30min at 4°C and supernatants were collected and stored at -80°C. These cell lysate and supernatant fractions were used for analysis of metal complexes using HILIC/ICP-MS and HILIC/ESI-MS as described below. For metal quantitation, growth of WT and mutant strains was done as described above. After 9h of growth, OD_{600} was measured before cells were harvested by centrifugation (2,000*g*, 30min, 4°C). The pellet was washed 2 times with 1.3mL MS media + 1mM EDTA followed by a wash with 1.3mL MS media. After the OD_{600} was measured, cells were dried overnight at 95°C. The metal quantification was determined by inductively coupled plasma mass spectrometry as described elsewhere[6].

4.4.4. Sample preparation for maize kernels

4.4.4.1. Extraction of iron species

The enzyme solutions were prepared as above following and stored at -20°C before use. The following procedures were used:

a. water extraction: 500 mg water was added to 250 mg maize powder, vortexed for 2 min and centrifuged (3 min, 12600 rpm)**,** the supernatant was kept for analysis

b. hexane extraction: 200 mg of maize samples was weighed in a 10-mL glass screw-top tube and 8 mL of hexane was added; the mixture was vortexed 1 min at medium speed and then shaken horizontally for 1 h at room temperature in a wrist action shaker. Finally, the slurry was left standing for 1 h before the removal of the supernatant to for iron detection in the residue after the evaporation to dryness under N_2[7].

c. saccharification: 0.1 g was maize powder was mixed with 5 mL distilled water to form a slurry containing thermostable α-amylase (0.1mL). The pH of the slurry was adjusted to 6.5 by sulfuric acid (0.1mol/mL) and it was heated to above 90˚C. The liquefaction was continued for 12 mins, and the slurry was then cooled down. Then sulfuric acid (0.1mol/mL) was added to adjust the pH to 4.5 and a Amyloglucosidase, an exo-enzyme (3260 u/mL,0.1mL), was then added to the slurry. This saccharification step continued for 6 hours at 40˚C then the sample was centrifuged and the supernatant kept for analysis[8].

d. protein digestion: 15 mL of pepsin solution [50 μL 840 units/L pepsin in 0.1 M KH_2PO_4 buffer; pH was adjusted to 2.0 not clear] was added to 0.1g maize sample, and the mixture was incubated for 3 h at 37 °C in a shaking water bath; following the centrifugation, the residue was washed by buffer, centrifuged, lyophilized[9].

All the supernatants were dried in DigiPrep at 60°C, except the hexane extracts which were evaporated under nitrogen blowing. The residues remaining after the removal of the supernantants were dried in DigiPrep at 60 °C and digested with 70% HNO_3 and 30% H_2O_2 in 3h at 80 °C

4.4.4.2. Simulated gastrointestinal digestion

The simulated gastrointestinal digestion of maize samples was carried out according to the modified procedure of in vitro digestion in the Caco-2 cell model [3].

Purification of the commercial enzyme preparations. The initial removal of iron traces was necessary for reliable analysis. The enzymes solutions used for simulated gastrointestinal

extraction were prepared as described below:

(i) 0.2 g pepsin (porcine, 10863 u/mg) was dissolved in 5 ml of 0.1 mol/L HCl, mixed with 2.5 g Chelex-100 and shaken for 30 min on a table shaker. The solution was centrifuged to remove Chelex-100 and made up to 10 mL with 0.1 mol/L HCl.

(ii) 0.05 g pancreatin and 0.3 g bile extract were dissolved in 35 ml of 0.1 mol/L $NaHCO_3$ and shaken with 12.5 g of Chelex-100 for 30 min. Chelex-100 was removed by centrifugation.

Both enzyme solutions were stored at-20°C before the use [5].

Enzymatic digestion of maize samples. 0.2 g ground sample was suspended in 4 ml of water containing 0.2 ml pepsin solution, pH was adjusted to 2.0 with 0.1 M HCl. The mixture was shaken for 60 min at 37°C in a water bath and then neutralized with 1M NaOH. 1 ml of pancretin/bile salt solution was added to neutralize pepsin digests and pH was adjusted 7.0 with 1M $NaHCO_3$. The final volume was brought up to 6 ml with 120 mM NaCl /5 mM KCl solution. The mixture was shaken for 2h at 37°C in a water bath, and then the solution was removed with a pipette and centrifuged (10 min, 3000 rpm). The digests were analyzed for the total Fe content and fractionated by SEC-ICP MS.

References

1. Glahn, R.P., et al., *Comparison of Iron Bioavailability from 15 Rice Genotypes: Studies Using an in Vitro Digestion/Caco-2 Cell Culture Model.* Journal of Agricultural and Food Chemistry, 2002. **50**(12): p. 3586-3591.
2. Tako, E., et al., *RETRACTED ARTICLE: High bioavailablilty iron maize (Zea mays L.) developed through molecular breeding provides more absorbable iron in vitro (Caco-2 model) and in vivo (Gallus gallus).* Nutrition Journal, 2013. **12**(1): p. 1-11.
3. Tako, E., et al., *RETRACTED ARTICLE: High bioavailablilty iron maize (Zea mays L.) developed through molecular breeding provides more absorbable iron in vitro (Caco-2 model) and in vivo (Gallus gallus).* Nutrition Journal, 2013. **12**(1): p. 3.
4. Glahn, R.P., et al., *Caco-2 Cell Iron Uptake from Meat and Casein Digests Parallels in Vivo Studies: Use of a Novel in Vitro Method for Rapid Estimation of Iron Bioavailability.* The Journal of Nutrition, 1996. **126**(1): p. 332-339.
5. Glahn, R.P., et al., *Caco-2 Cell Ferritin Formation Predicts Nonradiolabeled Food Iron Availability in an In Vitro Digestion/Caco-2 Cell Culture Model.* The Journal of Nutrition, 1998. **128**(9): p. 1555-1561.

6. Ghssein, G., et al., *Biosynthesis of a broad-spectrum nicotianamine-like metallophore in Staphylococcus aureus.* Science, 2016. **352**(6289): p. 1105-1109.
7. Moreau, R.A., et al., *A Process for the Aqueous Enzymatic Extraction of Corn Oil from Dry Milled Corn Germ and Enzymatic Wet Milled Corn Germ (E-Germ).* Journal of the American Oil Chemists' Society, 2009. **86**(5): p. 469-474.
8. Al-Rabadi, G.J.S., R.G. Gilbert, and M.J. Gidley, *Effect of particle size on kinetics of starch digestion in milled barley and sorghum grains by porcine alpha-amylase.* Journal of Cereal Science, 2009. **50**(2): p. 198-204.
9. Holden, B.A. and G.W. Mertz, *Critical oxygen levels to avoid corneal edema for daily and extended wear contact lenses.* Investigative Ophthalmology & Visual Science, 1984. **25**(10): p. 1161-1167.

PART IV.
RESULTS AND DISCUSSION

PART IV. RESULTS AND DISCUSSION

Chapter 5. High resolution elemental and molecular mass spectrometry for characterization of species involved in metal uptake in bacteria

5.1. Staphylopine – a broad-spectrum metallophore in *Staphylococcus aureus*

The origin of this study goes back to the discovery by our collaborators in frame of an ANR project (Arnoux *et al.*, CNRS Cadarache) using metabolomic exploration, targeted mutagenesis, and biochemical analysis of an operon in *Staphylococcus aureus.* This operon that encodes the different functions required for the biosynthesis and trafficking of a broad-spectrum metallophore related to plant nicotianamine.

The primary goal of the study was the exploration of the intra- and extracellular liquids produced by this study for the presence of metal-containing complexes, correlation of this with the above finding in order to validate it by a chemical approach, and the identification of the biosynthesized complex and ligand in terms of its structure. For this purpose a methodology based on the coupling of hydrophilic interaction chromatography (HILIC) with inductively coupled plasma mass spectrometry (ICP MS) and high resolution electrospray mass spectrometry (HR ESI MS) was developed

At first, HILIC - ICP MS was attempted to evaluate the number of metal complexes (Ni, Co and other metals) present, their amount and their relative level of expression between mutants. This stage was essential to pinpoint the significant complexes and estimate their retention times for a later investigation of their structure by HILIC - ESI MS. For the latter, two complementary approaches were performed: (i) a targeted approach using a triple quadrupole mass spectrometer for sensitive detection and quantification of selected metabolite, and (ii) a global approach (i.e., metabolomics) using an LTQ-Orbitrap mass spectrometers and adequate data mining procedures. The LTQ Orbitrap mass spectrometer provides accurate mass measurements with sub-ppm mass accuracy at high (100,000) mass resolution, which improves metabolite detection and identification in biological media. Coupled with HILIC separation which allows one to keep metal complexes intact, LTQ-Orbitrap MS based detection allows the discovery of these metal complexes based on the mass spectrum pattern that reflect the metal isotopic ratio and the characteristic inter-isotopic mass difference [1]. By these means, it is possible to detect analytical information outside the initial scope of investigation. It is possible within the same analysis to screen for both major and minor complexes, other metals (Zn, Cu,

Fe (II), Fe (III)…) complexing the same ligand or other ligands, eventually producing data sets allowing the description of metal ion equilibria. The data converged to the observation of a unique metallphore for which our collaborators coined the name – staphylopine.

The second objective was a study of the reactivity and affinity for metals of the identified ligand and evaluation of its capacity to intervene in processes involving multiple metals (nickel, cobalt, zinc, copper and iron). This was achieved by testing metal affinity of staphylopine standard by mixing different metals (Fe (II), Fe (III), Cu, Zn, Co, Ni) with this molecule prior to direct analysis by ESI-MS.

5.1.1. Analysis of metal concentrations of different culture media by ICP-MS.

Three kinds of culture media were used to cultivate the bacteria with the objective of finding conditions to support *Staphylococcus aureus* and for *E coli* produce staphylopine. The metal contents determined in the media are reported in **Table 5.1.1.**

Table 5.1.1. Metal concentrations in culture media and in the intracellular fraction of wild-type (WT) cells in different culture conditions.

	Culture media concentration, nM					
	Mn	Fe	Zn	Cu	Ni	Co
LB	116 ± 9	4450 ± 356	5320 ± 426	206 ± 16	25 ± 2	134 ± 11
CDM	17 ± 3	171 ± 14	105 ± 8	7 ± 2	12 ± 2	< 5
dCDM	< 5	20 ± 3	22 ± 3	< 5	< 5	< 5

5.1.2. Detection of staphylopine in the cytoplasm of *E. coli* expressing the enzymes from *S. aureus* by HILIC with dual ICP MS and ESI-MS detection

The existence of a mutant strain (cntABCDF-) of *S. aureus* which produces the metallophore but that is unable to recover it in the form of a metal-complex opens the way to determine the metallophore structure by a combined approach that can be assimilated to a "fishing" procedure. Indeed, in this mutant strain the metallophore is produced and should accumulate in the supernatant. Therefore this supernatants were kept, supplied with nickel at an appropriate concentration and incubated with a purified CntA protein. After re-purification of

CntA, ideally in complex with the metal-metallophore complex, we tried to identify the metallophore by mass spectrometry. Our co-work expressed and purified the SBP (CntA) from *E. coli* and incubated it in a supernatant of a *cntA* mutant of *S. aureus* grown in CDM media. We then supplemented this mix with nickel to force the formation of a nickel-metallophore complex and its binding to CntA. After re-purification of the SBP and further analysis by MS we looked for the characteristic nickel isotopic pattern.

The identification and characterization of the metallophore was performed *in vivo* using *S. aureus* cell culture supernatants. Investigation of these metal complexes by the parallel analysis by HILIC – ICP MS and HILIC - ESI-MS. First, we tracked the relevant molecules by monitoring nickel in HILIC - ICP-MS after adding nickel to the cell extracts.

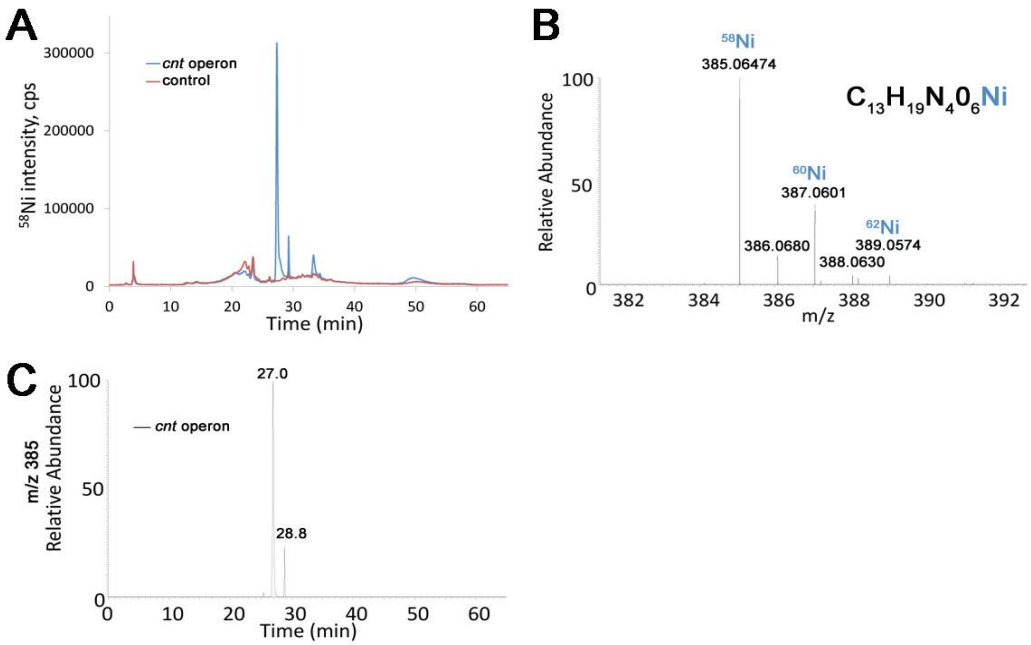

Fig. 5.1.1. Metabolomic study of *E. coli* strains expressing the *cnt* operon or the empty vector. (A) HILIC/ICP-MS chromatograms of intracellular fractions of E. coli strain and expressing the cnt operon from S. aureus (blue line) and comparison with the strain expressing the empty vector (red line). (B) Mass spectra of a chelating compound present in its complexed forms with nickel. Molecular formula was deduced from the exact mass of the 58Ni complex. (C) HILIC/ESI-MS extracted ion.

Fig.5.1.1a shows HILIC –ICP MS chromatograms of the extracellular fraction of S. aureus wild type and its cntL mutant (strain of *S. aureus* devoid of the *cntL* gene) cultivated in chemically defined media (CDM), a media with low metal concentration in which expression of the operon is known [2]. A single intense peak was present at ca. 28 min. for the wild type sample but was absent in the mutant strain chromatogram. The parallel chromatogram obtained

by HILIC – ESI MS (**Fig. 5.1.1**b) allow the identification of nickel isotopic pattern at the same retention time. In brief, we found a candidate molecule with the same mass as found by the metabolomic approaches. Using our set of accurate masses with molecular formula finder software we were able to propose an empiric formula of $C_{13}H_{19}N_4O_6$-Ni.The retention times of this compound in HILIC/ESI-MS matched that of the Ni elution found by HILIC/ICP-MS, therefore indicating that the same Ni complex was observed by the two techniques.

Using Orbitrap, it is possible to detect analytical information outside the initial scope of investigation. We put forward a hypothesis that it should be possible within the same analysis to screen both major and minor complexes, other metals (Zn, Cu, Fe (II), Fe (III)…) complexing the same ligand or other ligands to get an exhaustive idea of metal ion equilibria To this end, LC/MS metabolic fingerprints of supernatant samples of these strains (cultivated in minimal media will be obtained using a LTQ-Orbitrap mass spectrometer fitted with an electrospray source operated in both positive and negative ionization modes. These metabolic fingerprints were then be compared to those obtained using mutants.

The spiking experiment was reproduced with Zn, Cu and Co (**Fig. 5.1.2 a-d**). In each case, a single peak was observed, the retention time depending on the (**Fig. 5.1.1b**). In all the cases these peaks were absent in the *cntL* mutant strain, therefore corroborating the hypothesis of the existence of a direct link between these metal complexes and the central NAS-like enzyme. The chromatograms obtained in the same conditions with ESI MS detection (mass spectra for each metal given in the respective **Fig. 5.1.2**, suggest the presence of the same ligand. Again, the retention times of these compounds in HILIC/ESI-MS match those of the metals elution found by HILIC/ICP-MS, therefore indicating that the same metal complexes were observed by the two techniques.

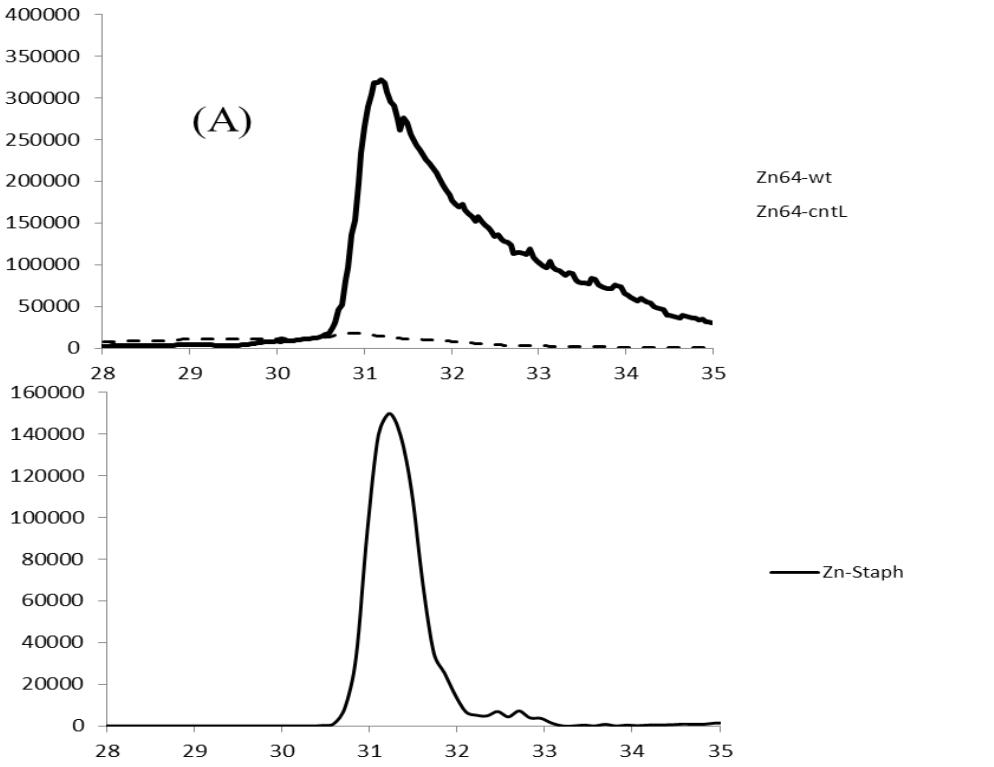
(A)
Zn64-wt
Zn64-cntL
Zn-Staph

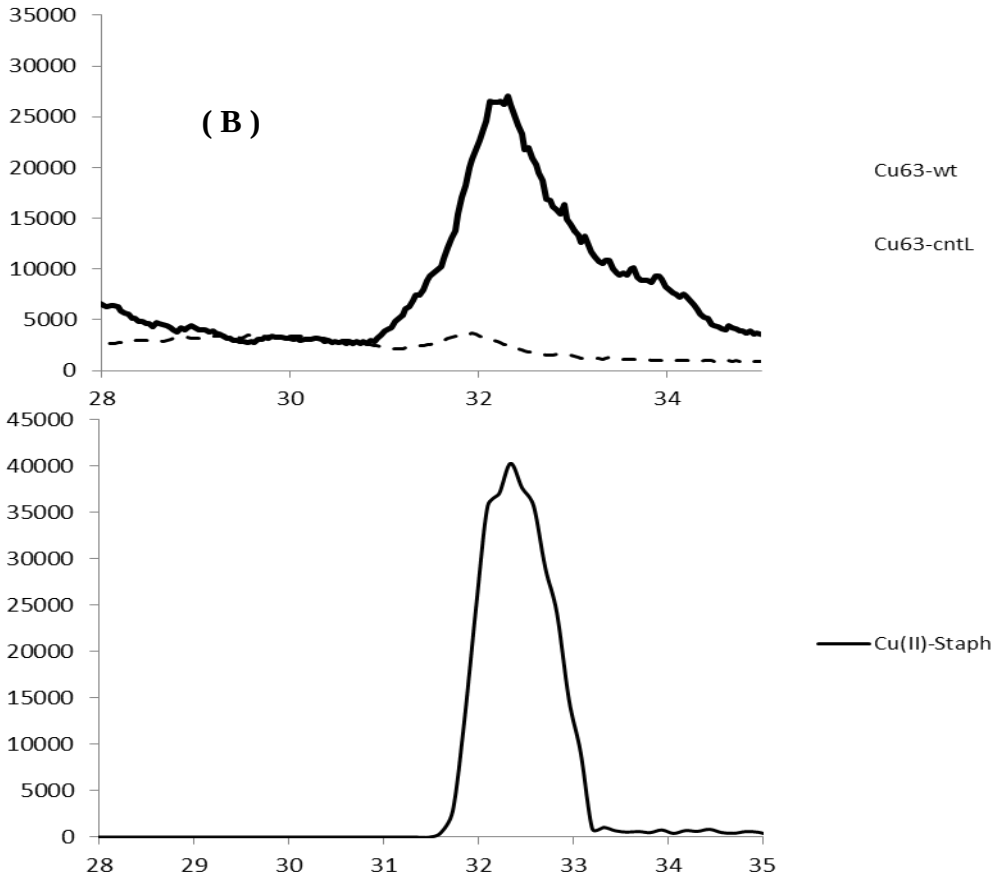
(B)
Cu63-wt
Cu63-cntL
Cu(II)-Staph

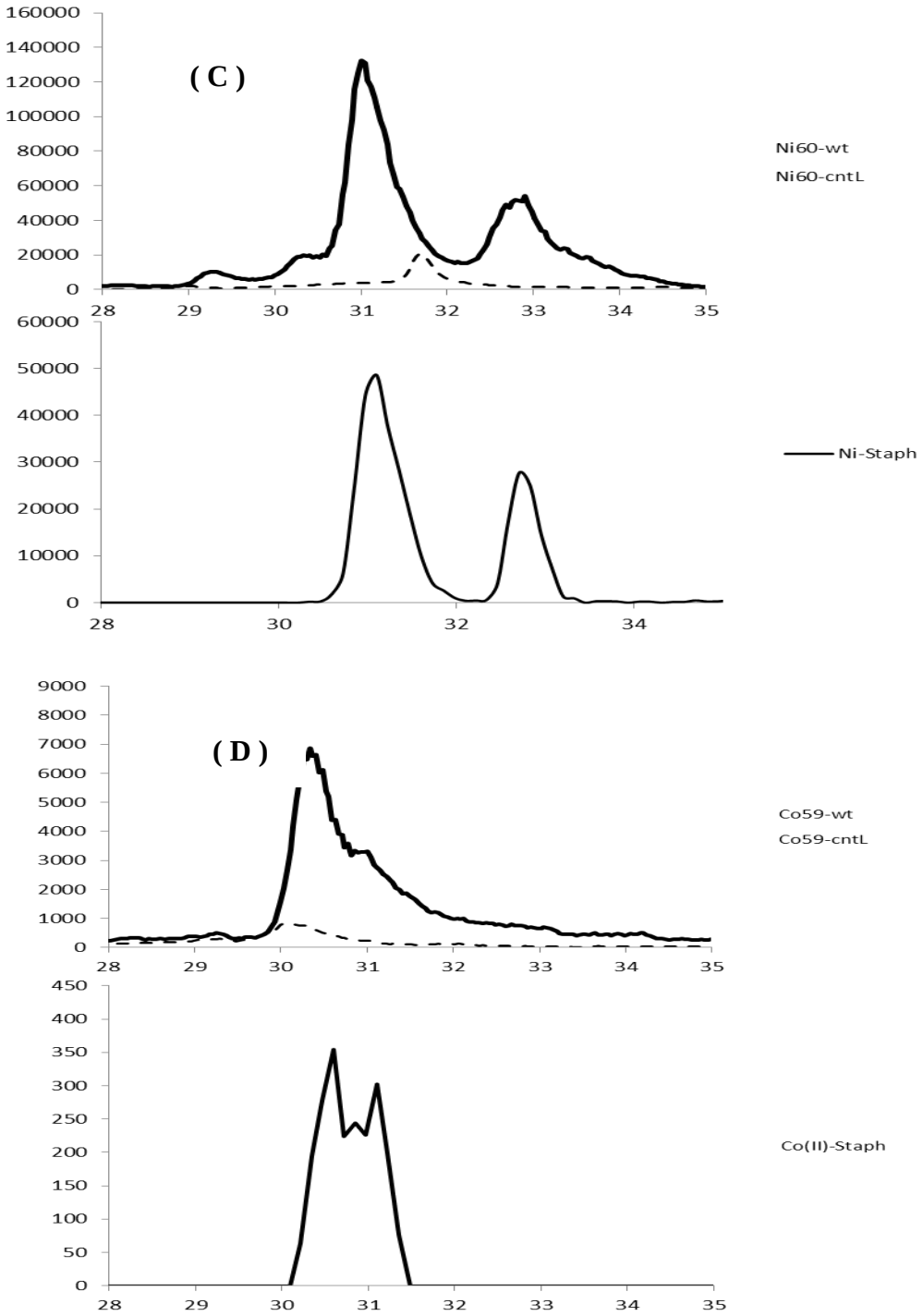

Fig. 5.1.2. (a) HILIC/ICP-MS chromatograms of extracellular fractions of S. aureus and comparison of the WT strain (plain line) with the cntL mutant (dotted lines) (b) mass spectra of a chelating compound present in its free and complexed forms; The empirical molecular formula was deduced from exact masses. c) HILIC/ESI-MS extracted ion chromatograms (XIC) of some metal-ions observed to form a complex with the above-mentioned chelator. Chromatograms were traced using the exact masses (± 3 ppm) of the expected complex and these masses were absent in the extracellular fraction of the cntL mutant.

5.1.3. Identification of the staphylopine structure

The subsequent effort was focused on the identification of the discovered compound with the empiric formula of $C_{13}H_{19}N_4O_6$-Ni.

The preliminary identification was carried out by multiple stage mass spectrometry (**Fig. 5.1.3**). In order to fit the molecular formula that we obtained from accurate masses, we used simple chemical rules as follow: 1/ each time there is a reductive condensation there is a mass loss of 16 Da between the two reactants. 2/ each time there is an α-aminobutyric acid moiety transfer from SAM to an amino acid there is a mass loss of 2 Da between the two reactants. This way, the "simplest" molecule would consist of pyruvate (88Da) reductively condensated with glycine (75 Da) that would be modified by two α-aminobutyric acid moieties (103 Da), which would give a molecular weight of 349 Da, above the 328 Da measured. The only possibility is therefore to use only one α-aminobutyric acid moiety from SAM; and only using histidine (155 Da) and pyruvate we can obtain the expected 328 Da.

Therefore the ligand was identified as (N-[3-(N-L-Alanyl)-amino-3-carboxypropyl]-D-histidine) for which a colloquial name staphylopine was proposed in order to reflect its origin from *S. Aure*us.

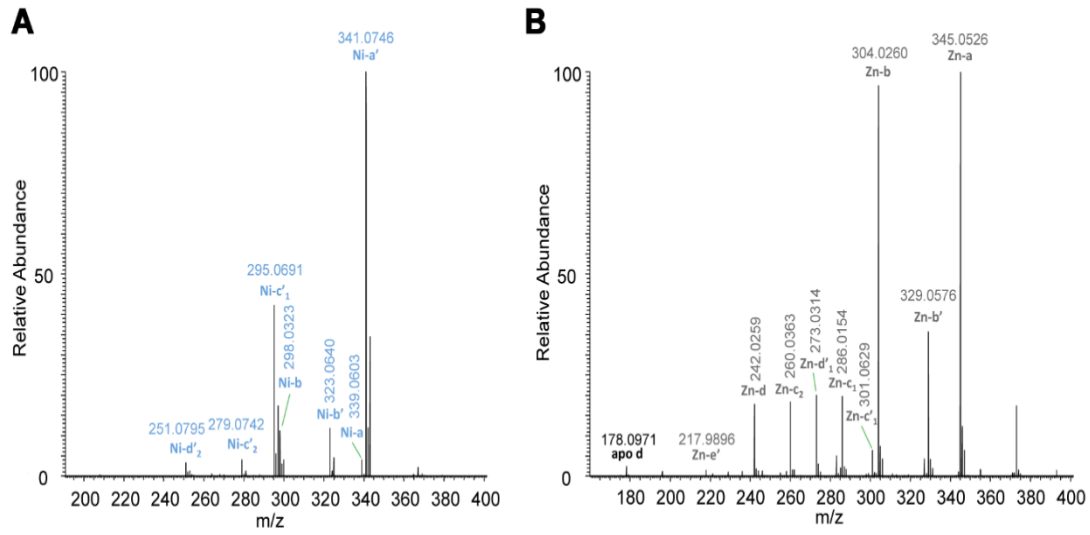

Fig. 5.1.3 MS/MS fragmentation of staphylopine-metal complexes. MS/MS fragmentation of staphylopine-Zn (A) and staphylopine-Ni complexes (B). The mass of the ions are indicated as well as their interpretation with the fragmentation scheme shown in this Figure.

5.1.4. Confirmation of the compound identity using a synthetic standard

In order to confirm the identification hypothesis a synthetic staphylopine Synthetic staphylopine (N-[3-(N-L-Alanyl)-amino-3-carboxypropyl]-D-histidine) was ordered to Toronto Research Chemical Inc (Toronto, Canada) and its NMR spectrum is provided in **Fig. 5.1.4 .** Metal content of the studied elements in staphylopine synthetic standard was measured by ICP MS and was found to be lower than 0.1% of staphylopine mass. Analysis of this synthetic standard by HILIC/ESI-MS showed that it has the same retention time, chromatographic peak shapes, fragmentation behavior in MS instrument and metal affinity than the natural molecule found in culture supernatants. Using this standard we generated MS/MS spectra of nickel and zinc (**Fig. 5.1.5**) and confirmed that the fragmentation pathways were identical for the sample and the standard.

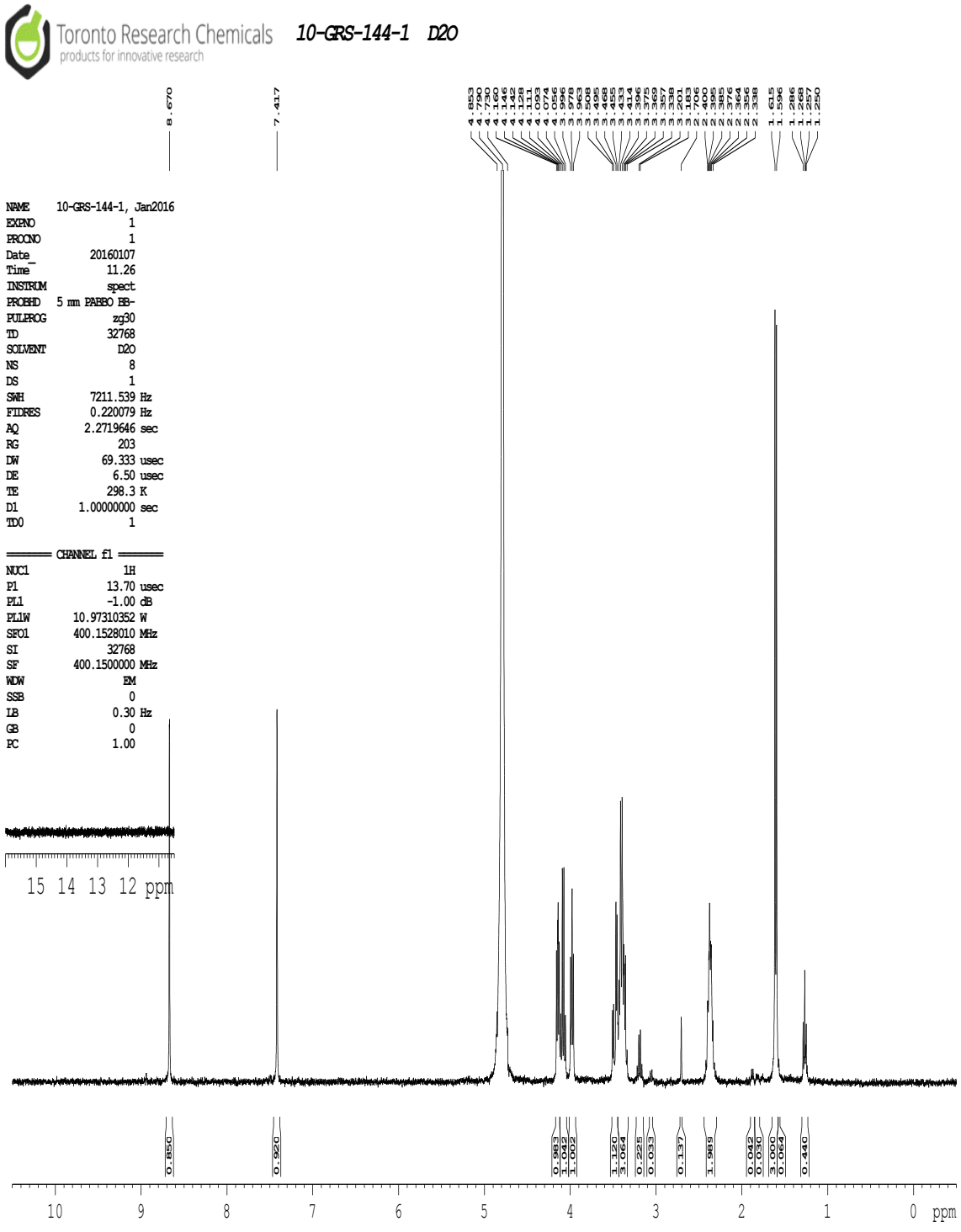

Fig. 5.1.4. NMR spectrum of synthetic staphylopine.

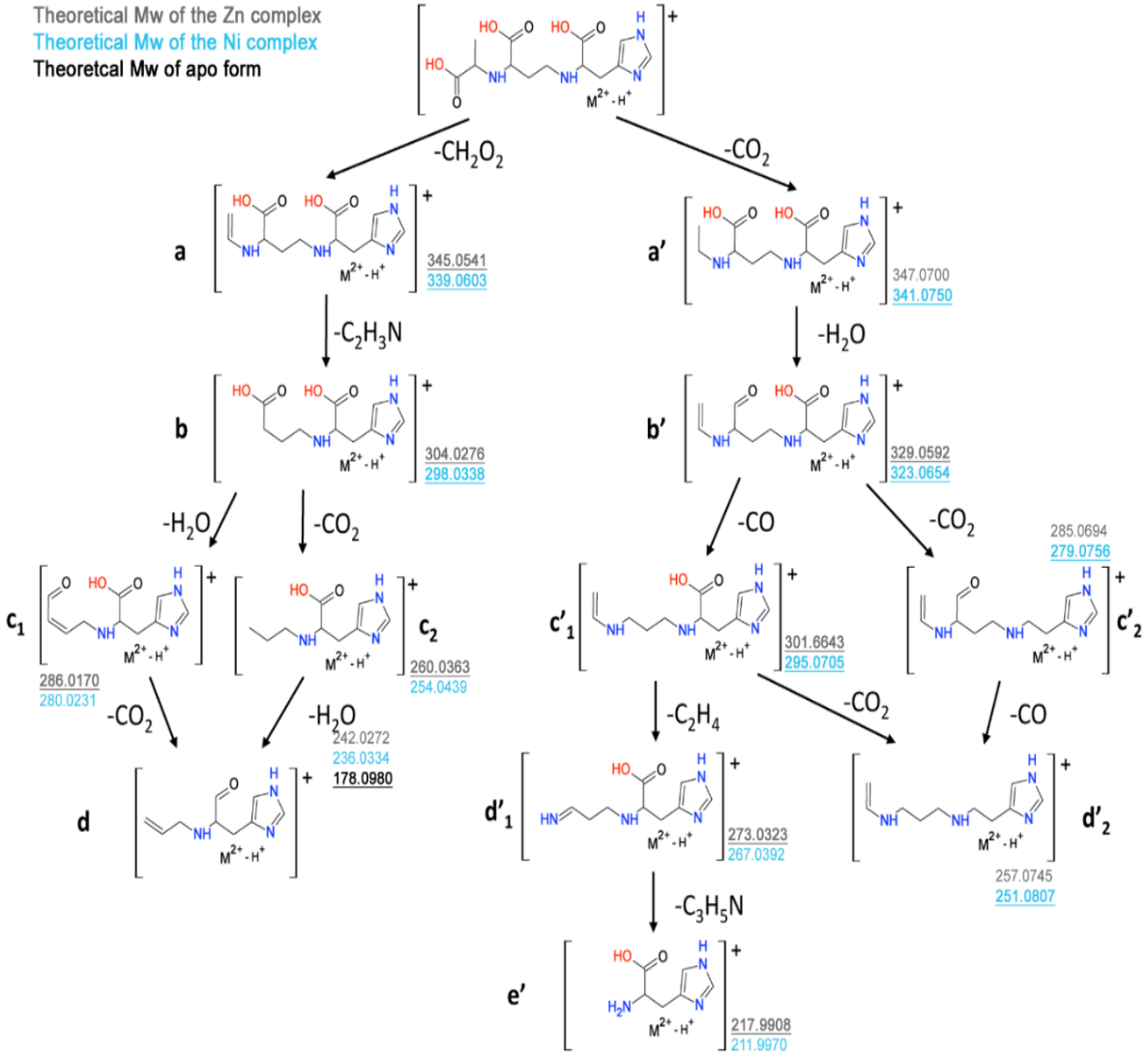

Fig. 5.1.5. Fragmentation pathways of staphylopine-Zn and staphylopine-Ni complexes. The theoretical masses of the ions are indicated on the right of the proposed ion. The underlined masses were detected in the observed fragmentation pattern shown in (A) and (B).

5.1.5. Quantification of staphylopine in bacterial cell extracts

A method for the quantification of staphylopine in spent culture media and extracts was then developed using the method of standard additions. The increase in the staphylopine peak monitored by HILIC/ESI-MS allowed the determination of the staphylopine concentration and confirmed results obtained by HILIC/ICP-MS analysis. Three different level of standard staphylopine 1 mM, 2 mM, 3 mM were added to cells extracts. By following the parent ion and fragmentation ion 385.06/341.07 we found the peek increase at the same retention time by

following the concentration of spiked increasing and we integrated the peeks area to create the calibration curve **(Fig. 5.1.6** and **5.1.7).**.

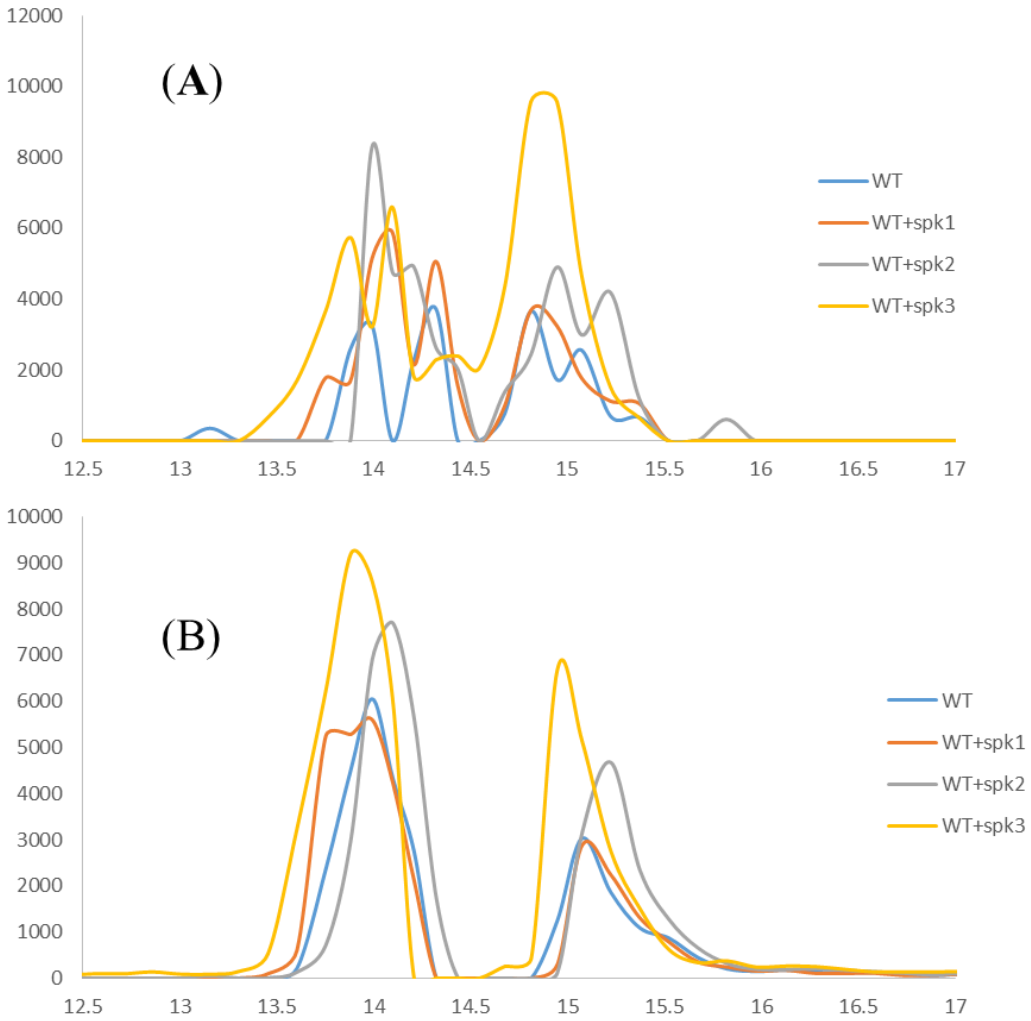

Fig. 5.1.6. Quantification of staphylopine in spent culture media (A) HILIC/ESI-MS extracted ion chromatograms (XIC) of complex in full mass 385.06 (A) HILIC/ESI-MS extracted ion chromatograms (XIC) of complex in MS/MS 341.07.

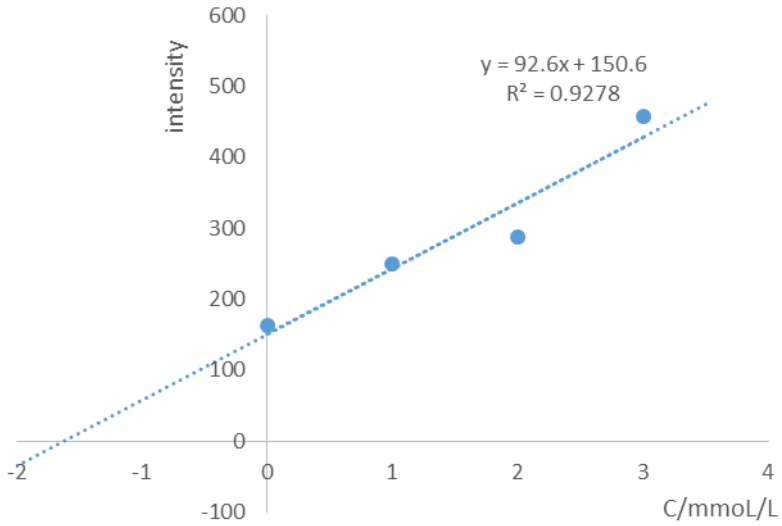

Fig. 5.1.7. Calibration curve of the staphylopine determination by HILIC –ESI MS using the method of standard additions.

5.1.6. Evaluation of the affinity of staphylopine to different metals

We tested metal affinity of staphylopine by mixing the standard compound with different metals (Fe (II), Fe (III), Cu, Zn, Co, Ni) and direct analysis by ESI-MS. It was found that metal affinity for staphylopine was in the following order: Cu (II) > Ni > Co > Zn > Fe (II) > Mn (II), which is identical to that observed for nicotianamine. Fe (III) affinity for staphylopine relative to other metals is pH dependent and, whereas it has a higher pKd value than Cu (II), Fe (III) has a poor affinity for staphylopine at neutral pH, a phenomenon already described for nicotianamine.

Stability constants for staphylopine:metal complexes were estimated by metal competition experiments with nicotianamine. Mixtures of nicotianamine:staphylopine: metal were analyzed in physiological conditions (pH = 7) by infusion ESI MS. The complex of staphylopine with metal is only observed as a 1:1 complex during ESI MS analysis, as it is also the case for nicotiamine. The structure, affinity constants and the 1:1 stoichiometry of the formation of complexes with metals suggest a strong similarity of staphylopine to nicotiamine. A putative model for metal:staphylopine complex can then be proposed (hexadentate structure with 3 amino groups (the ones spaced by 3 carbons) and the 3 carboxylic groups, **Fig. 5.1.8**).

A

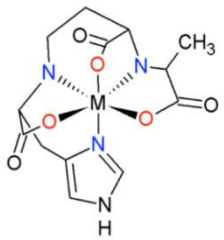

B

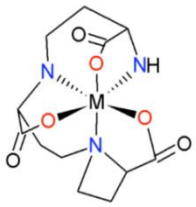

C

	pKd	
	Nicotianamine (*49*)	Staphylopine (this study)
Cu^{2+}	18.6	19.0
Ni^{2+}	16.1	16.4
Co^{2+}	14.8	15.1
Zn^{2+}	14.7	15.0
Fe^{2+}	12.1	12.3
Mn^{2+}	8.8	9.1

Fig. 5.1.7. Putative structure and estimated pKd for staphylopine by comparison with nicotianamine. Putative chemical structure of staphylopine-metal complex (**A**) and nicotianamine-metal complex (**B**). (**C**) pKd values for staphylopine complexes were estimated by metal competition experiments with nicotianamine by ESI MS.

5.1.7. Effect of the cntL gene determination

CntL gene used to be considered involving in staphylopine synthesis so to confirm effect of the cntL gene in this duration, We set experiment sought to determine the effect of the cntL mutation with regard to intracellular metal accumulation in various culture conditions: CDM, where metal concentration is rather low, Chelex-demetalated CDM (dCDM) where metal level is even lower, NTA-demetalated CDM supplemented with metalated NTA resin to supposedly mimic a chelating environment (rCDM), and LB where metal concentration is high. We note that the growth of the cntL mutant is nearly identical to that of the WT strain in these media (**Fig. 5.1.8**), therefore indicating that metal content would be attributable to the absence of staphylopine and not to a growth defect. In all these culture conditions we established that the cnt genes,. In CDM and dCDM, the cntL mutation caused a significant decrease in intracellular accumulation of nickel, copper and cobalt as determined by ICP-MS (**Fig. 5.** 1**.8**). Finally, in a metal rich medium such as LB, the cntL deletion mutant accumulated less iron, copper and cobalt. So we can say that this can be an evidence that when the scary metal condition supplied to bacteria cntL start to involving in staphylopine synthesis.

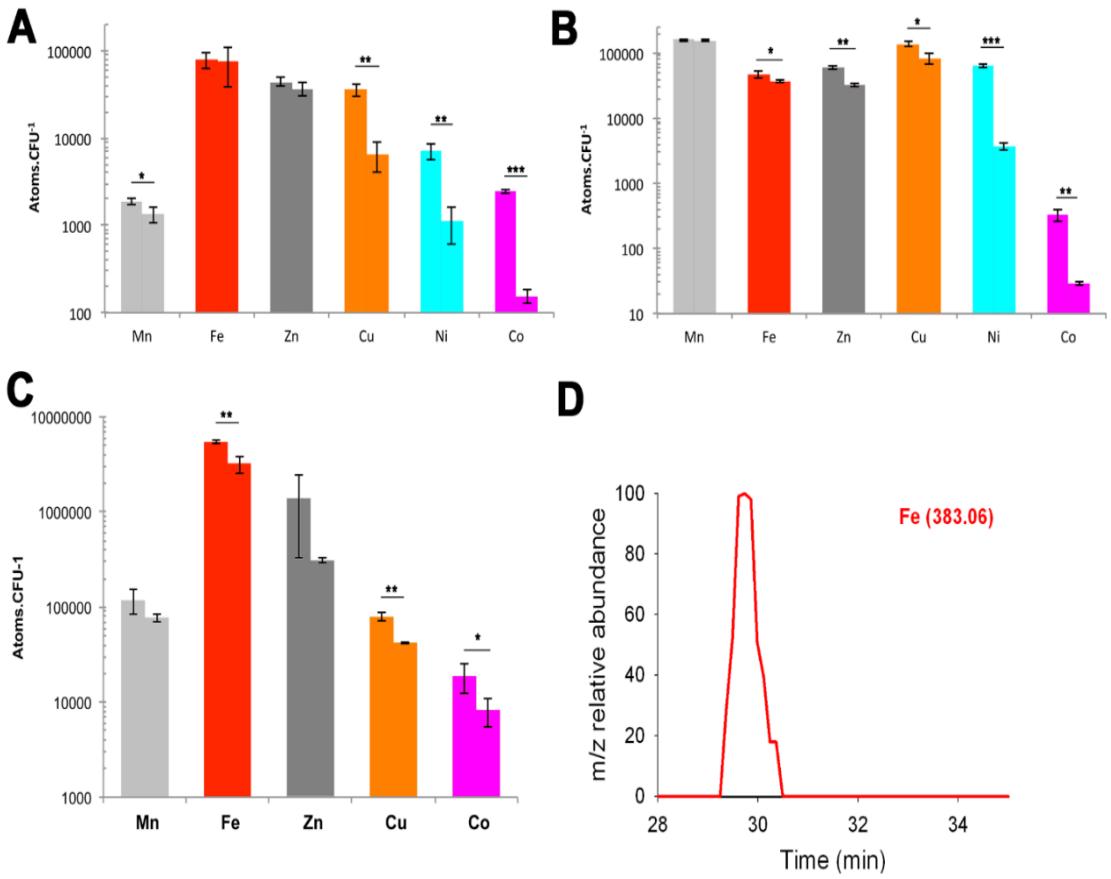

Fig. 5.1.8. Import of divalent metals in various culture conditions. (A) Intracellular metal content determined by ICP-MS of *S. aureus* WT (left bars) and *cntL* (right bars) mutant strains grown in dCDM. Error bars, mean ± s.d. **P*<0.05 and ***P*<0.01. (B) Intracellular metal content determined by ICP-MS of *S. aureus* WT (left bars) and *cntL* (right bars) mutant strains grown in rCDM. Error bars, mean ± s.d. **P*<0.05, ***P*<0.01 and ****P*<0.001. (C) Intracellular metal content determined by ICP-AES of *S. aureus* WT (left bars) and *cntL* (right bars) mutant strains grown in LB medium without further metal supplementation. Error bars, mean ± s.d. **P*<0.05 and ***P*<0.01. (D) HILIC/ESI-MS extracted ion chromatograms (XIC) of the Staphylopine-Fe complex detected in the extracellular fraction of *S. aureus* grown in CDM. Chromatogram was traced using the exact mass of the complex (± 3 ppm). This mass was absent in the extracellular fraction of the *cntL* mutant.

References

1. Flis, P., et al., *Inventory of metal complexes circulating in plant fluids: a reliable method based on HPLC coupled with dual elemental and high- resolution molecular mass spectrometric detection.* New Phytologist, 2016. **211**(3): p. 1129-1141.
2. Remy, L., et al., *The Staphylococcus aureus Opp1 ABC transporter imports nickel and cobalt in zinc-depleted conditions and contributes to virulence.* Mol Microbiol, 2013. **87**(4): p. 730-43.

5.2. Pseudopaline - a metallophore involved in zinc and nickel uptake in *Pseudomonas aeruginosa*

Rich in experience acquired with the discovery and characterization of staphylopine, we investigated another bacterial system *Pseudomonas aeruginosa* in which our co-workers (Arnoux, CNRS, Cadarache) identified an operon responsible for the production of a metal scavenging ligand. The metal-uptake property of the *Pseudomonas aeruginosa* system appears different from that of staphylopine with a predominant effect on nickel uptake, and on zinc uptake in metal scarce conditions mimicking a chelating environment, thus reconciling the regulation of the *cnt* operon by zinc with its function as a zinc importer under metal scarce conditions.

In term of the analytical chemistry approach, a non-denaturing samples preparation applied in the extraction/fractionation cell samples was followed by hydrophilic interaction chromatography (HILIC) with dual detection by inductively coupled plasma mass spectrometry (ICP MS) and high resolution electrospray mass spectrometry (HR ESI MS).

5.2.1. In vivo detection and characterization of a PaCntL-dependent metallophore in the extracellular medium of P. aeruginosa

Our co-works constructed a PA14 mutant strain lacking PaCntL (Δ*cntL*) which presumably control synthesis of pseudopaline and compared the composition of the intra- and extra-cellular contents of wild type and Δ*cntL* strains grown under the previously defined *cnt* inducible conditions. Extracellular samples were analysed by HILIC wityh dual ICP MS and ESI MS/MS detection. HILIC/ICP-MS (a 7-µl aliquot of the supernatant injected) data revealed the presence of a molecule complexed with nickel and zinc in the supernatant of the WT strain, which was absent in the *cntL* mutant strain (**Fig. 5.2.1**).

In order to increase the mass accuracy during HILIC/ESI MS analysis, MS and MS/MS spectra were recalibrated offline using precursor/fragment ions with known formula. Putative metal species were fragmented during a subsequent chromatographic run with collision induced dissociation (CID) mode at 35% energy. Signals were recorded at *m/z* corresponding to pseudopaline complexes with Ni and Zn ($C_{15}H_{20}N_4O_8Ni^+$ and $C_{15}H_{20}N_4O_8Zn^+$ respectively). ESI-MS investigation of the metabolites eluting at this same elution volume

showed unambiguously the presence of typical nickel and zinc isotopic patterns indicating the presence of a free metallophore with a molecular mass of 386 Da (**Fig. 5.2.2**). Using the accurate mass and a molecular formula finder software we proposed the $C_{15}N_4O_8H_{20}$ empiric formula for the ligand in complex with nickel or zinc (**Fig. 5.2.1**, inset for the nickel chelate). This ligand corresponds to a new metallophore produced by *P. aeruginosa* in a *cntL*-dependent manner for which our collaborators coined the name pseudopaline to refer to its origin from *P. aeruginosa* and its belonging to the nopaline family of opine [1].

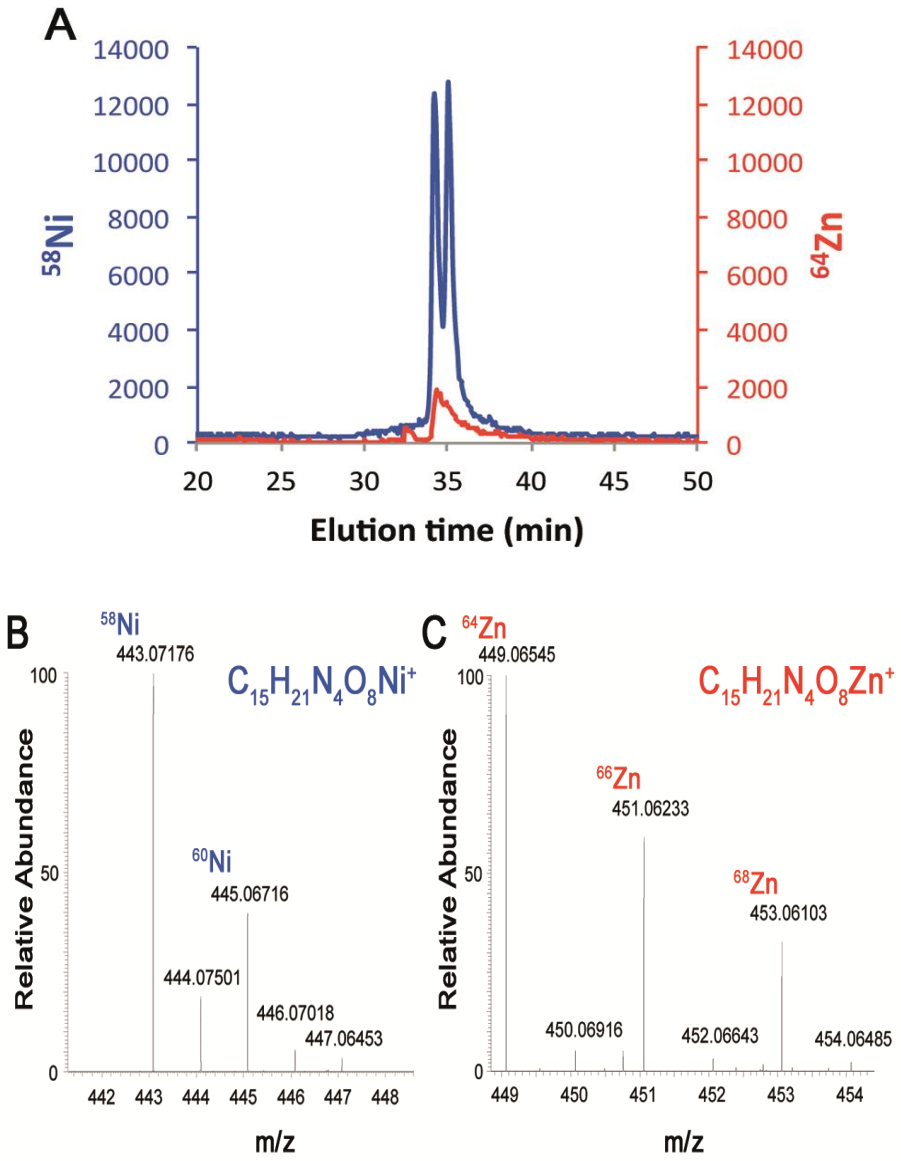

Fig. 5.2.1. In vivo PaCntL-dependent detection of a nickel or zinc-bound metallophore in the extracellular fraction of *P. aeuginosa*. (A) HILIC/ICP-MS chromatogram of metal-bound metabolites. (B) HILIC-ESI/MS mass spectrum of a Ni-metallophore complex in the extracellular fraction of the WT strain but absent in the Δ*cntL* mutant. (C) HILIC-ESI/MS mass spectrum of a Zn-metallophore complex in the extracellular fraction of the WT strain but absent in the Δ*cntL* mutant. The empirical

molecular formula of the CntL-dependant Ni- or Zn-metallophore complexes were deduced from the exact masse.

The comparison of the elemental composition of pseudopaline with that of staphylopine (328 Da) revealed the presence of two additional carbons and two oxygen atoms, suggesting the use of an α-ketoglutarate (αKG) moiety instead of pyruvate as found in staphylopine. The fragmentation of this metallophore in gas-phase confirmed this hypothesis (**Fig. 5.2.2**).

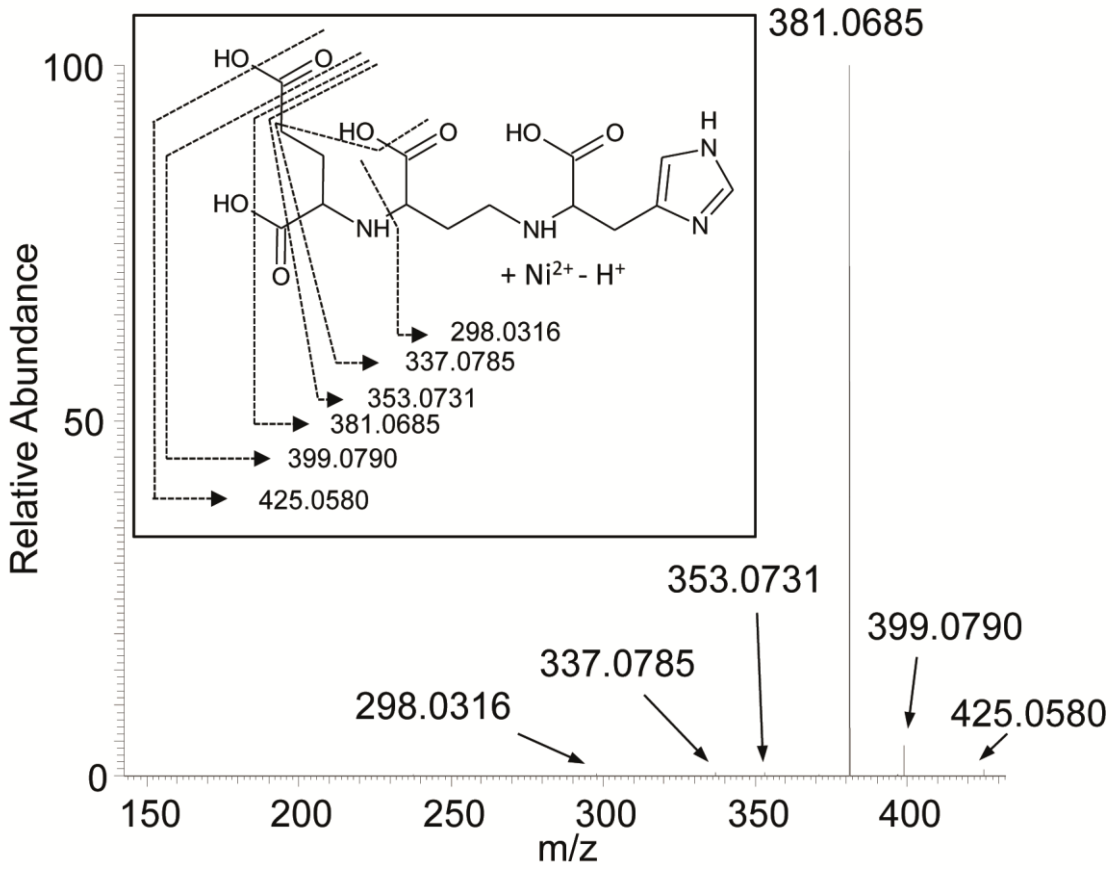

Fig. 5.2.2. MS/MS fragmentation of Pseudopaline-Ni complex. The mass of the ions are indicated as well as their interpretation with the deduced fragmentation scheme shown in the inset.

5.2.2. Involvement of pseudopaline in nickel and zinc uptake

In order to address the involvement of pseudopaline in metal uptake *in vivo*, we compared the intracellular concentration of various metals in PA14 WT, *ΔcntL* and *ΔcntL::cntL* strains. Cells were grown in pseudopaline-synthesis conditions determined above (MS medium) and the intracellular metal concentration was measured by ICP-MS. Under these growth conditions we observed a significant 90% reduction of intracellular nickel concentration in the

ΔcntL mutant strain (**Fig.5.2.3**A), which was mostly recovered in the complemented strain. The levels of all the other metals were not changed in the *ΔcntL* mutant strain compared to the WT strain (data not shown). A similar 90% reduction in intracellular nickel concentration was also observed when the culture was supplemented with 1μM $NiCl_2$ **(Fig. 5.2.3**), thus confirming that nickel uptake was predominantly performed by pseudopaline in these metal-poor media. We were intrigued by the apparent contradiction between the clear *cnt* operon regulation by zinc, and the absence of any effect on zinc uptake. A possible explanation is that the effect of *cnt* could be masked by the effect of a zinc ion importer such as the ZnuABC zinc transport system described in *P. aeruginosa* [2]. In an attempt to discriminate between both transport systems, we sequestered free metal ions by supplementing the growth medium with increasing concentrations of EDTA, a chelating agent for divalent metals. Interestingly, although we did not observe any effect using 10 μM EDTA, the supplementation with 100μM EDTA ultimately revealed a pseudopaline-dependent zinc uptake, with a 60% decrease of intracellular zinc content in the *ΔcntL* mutant strain in comparison with the WT strain (**Fig. 5.2.3B**). The complemented strain accumulated zinc to a level comparable to the WT. In these chelating conditions the pseudopaline-dependent nickel import is abolished (**Fig. 5.23A**), hence proving a direct link between pseudopaline and zinc uptake in metal scarce conditions with competing zinc chelators. These conditions may prevail at the host-pathogen interface where metal binding proteins such as calprotectin are produced by the host[3, 4], or in AMS where metals are complexed in a nutritional immunity framework[5, 6].

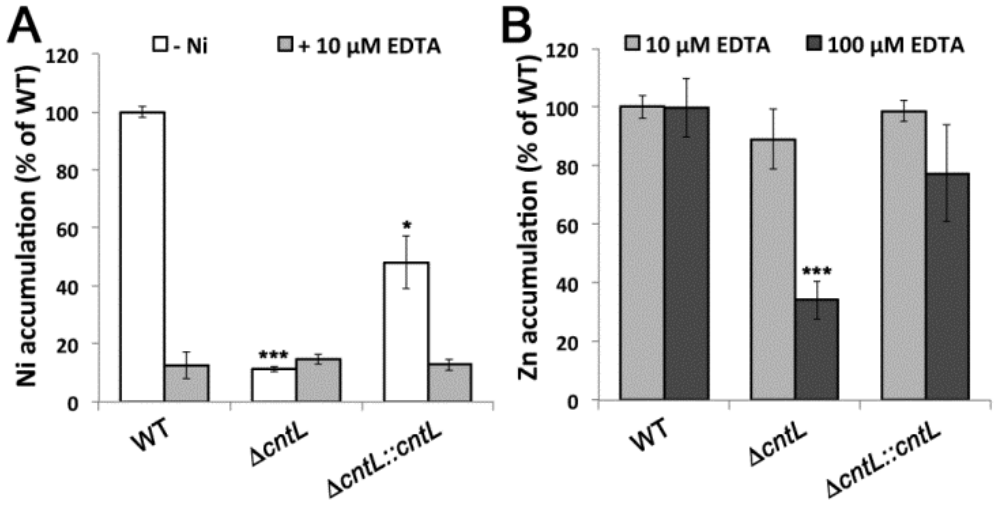

Fig. 5.2.3. Pseudopaline is involved in nickel uptake in minimal media and in zinc uptake in chelating media. Intracellular nickel (A) or zinc (B) levels measured by ICP-MS in WT, *ΔcntL* and *ΔcntL::cntL*

strains grown in MS medium supplemented or not with 10 or 100μM EDTA. Error bars, mean ± s.d. **P*<0.05, ***P*<0.01 and ****P*<0.001 as compared to the WT.

5.2.3. Investigation on pseudopaline biosynthesis

In order to investigate the properties of CntL and CntM of *P. aeruginosa*, our co-workers cloned the corresponding genes, heterologously expressed them in *E. coli* and purified their products for further biochemical analysis. They analysed them by thin layer chromatography (TLC) to follow the carboxyl moiety of a carboxyl-[^{14}C]-labelled S-adenosine methionine (SAM) substrate upon co-incubation with either L- or D-histidine (**Fig. 5.2.4A**). Only the incubation with L-histidine led to a novel band (+) corresponding to a reaction intermediate, tentatively named yNA. HILIC/ESI-MS chromatograms of putative reaction products using PaCntL incubated with L-histidine, revealed the production of the yNA intermediate (top), and a mix of PaCntL and PaCntM incubated with all their putative substrates (SAM, L-histidine, NADH and α-ketoglutarate), revealing the specific detection of pseudopaline in this case (red trace, bottom).

We therefore decided to study the same mixture of PaCntL and PaCntM incubated with all their putative substrates (SAM, L-histidine, NADH and α-ketoglutarate) by HILIC/ESI-MS, following the mass expected for the yNA intermediate and the pseudopaline found in the extracellular fraction of *P. aeruginosa* grown in MS medium. These experiments confirmed that the incubation of PaCntL with SAM and L-histidine led to the formation of the yNA reaction intermediate (**Fig. 5.2.4** top), and most of all, revealed the production of pseudopaline when co-incubating PaCntL, PaCntM and their proposed substrates (SAM, L-histidine, NADH and αKG; **Fig. 5.2.4**, bottom). Co-incubations using alternative substrates of PaCntM (pyruvate or NADPH) only led to the production of yNA. Interestingly, pseudopaline and yNA eluted at the same volume in these HILIC-ESI/MS experiments, showing that their physical properties are very similar.

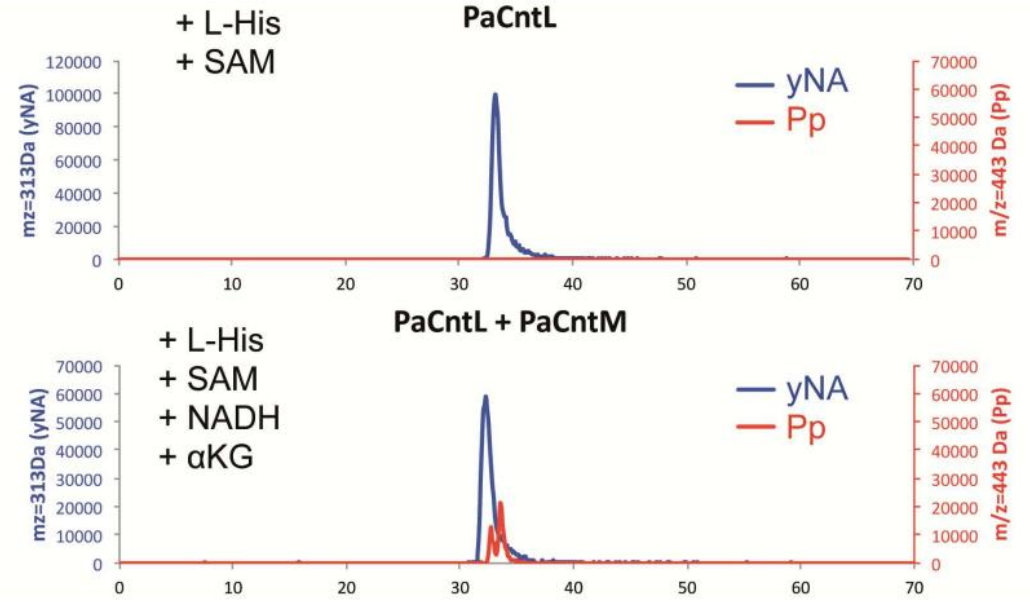

Fig. 5.2.4. HILIC/ESI-MS chromatograms of putative reaction products using PaCntL incubated with L-histidine, revealing the production of the yNA intermediate (top), and a mix of PaCntL and PaCntM incubated with all their putative substrate (SAM, L-histidine, NADH and α-Ketaoglutarate), revealing the specific detection of pseudopaline in this case (red trace, bottom).

Pseudopaline is therefore biosynthesized in two steps: first, a nucleophylic attack of one gamma-aminobutyric acid moiety from SAM onto L-histidine catalysed by PaCntL to produce the reaction intermediate yNA, and second, a NADH reductive condensation of the yNA intermediate with a molecule of αKG catalysed by PaCntM to produce pseudopaline (**Fig. 5.2.5**). Pseudopaline differs from staphylopine by the stereochemistry of the histidine moiety (L- and D- respectively) and by the presence of an αKG moiety instead of pyruvate in staphylopine. The biosynthesis of a specific metallophore by different bacteria recalls the chemical evolution of a large diversity of siderophore in a chemical rivalry to get access to one's own pool of metal[7]. Indeed, once in the extracellular medium, secreted metallophores are a common good, and a privileged access presumably gives a selective advantage.

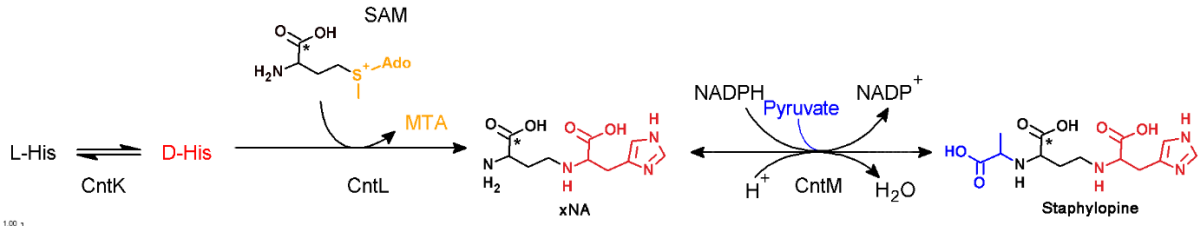

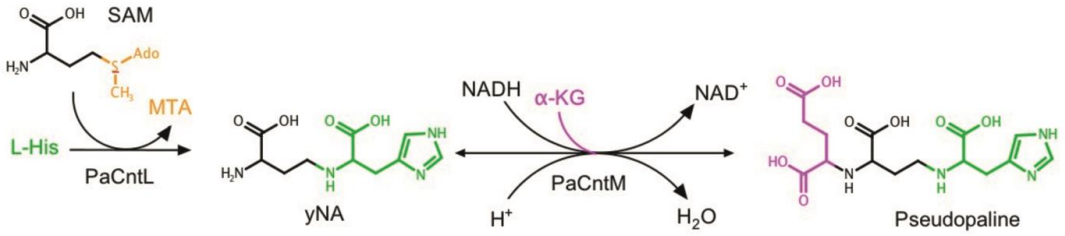

Fig. 5.2.5. Differences in the staphylopine (top) and pseudopaline (bottom) biosynthetic pathways.

5.2.4. Differences and similarities between staphylopine and pseudopaline

It is interesting to note the differences and similarities between staphylopine and pseudopaline and between their respective biosynthetic pathways (**Fig. 5.2.5**). On one hand, pseudopaline differs from staphylopine by the incorporation of a L-histidine instead of a D-histidine moiety in staphylopine, thus explaining the absence of amino acid racemase in *P. aeruginosa.* Another particularity of pseudopaline is the use of an αKG moiety instead of pyruvate as substrate for the second reaction mediated by PaCntM. Together this leads to two species-specific metallophores that might give a selective advantage in a competing environment. The fact that staphylopine and pseudopaline belong to Gram-positive and Gram-negative bacteria has important consequences on their respective transport mechanisms across the two types of bacterial envelopes. Although the transporters of staphylopine are well identified, the outer membrane exporter pseudopaline and inner membrane importer of the pseudopaline-metal complex remains to be discovered (**Fig. 5.2.6**). Recycling of the metallophore could also take place in *P. aeruginosa*, as recently exemplified in the case for pyoverdine[8]. An interesting aspect of this work is the discovery of two different pathways for the export of these nicotianamine-like bacterial metallophores. Whereas *S. aureus* uses a protein belonging to the MFS family (SaCntE) for staphylopine export, *P. aeruginosa* uses a protein belonging to the DMT family of transporters, with PaCntI possessing two predicted EamA domains for pseudopaline export. In the view of their importance in the growth or virulence of these important human pathogens [9, 10], they could emerge as attractive targets for novel antibiotic development.

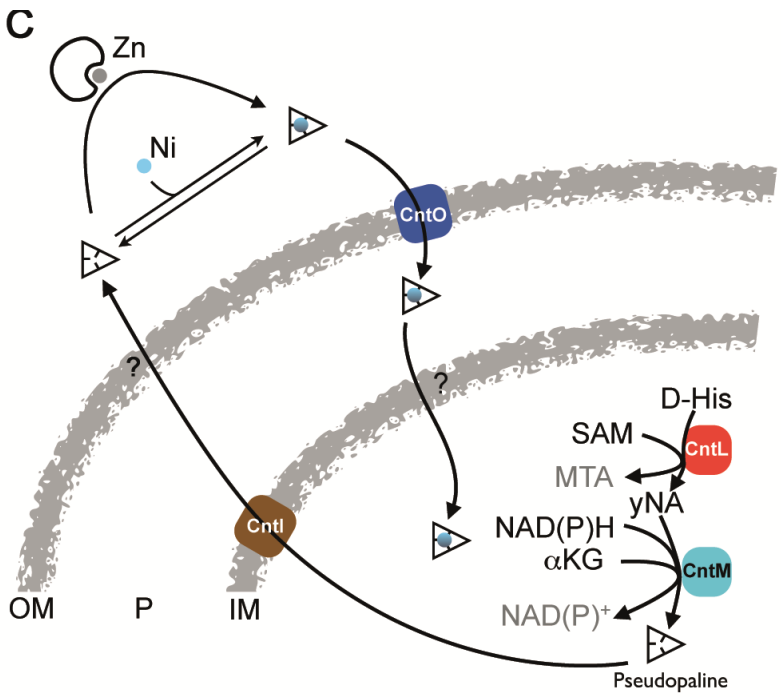

Fig. 5.2.6. Model of pseudopaline production, secretion and recovery of nickel or zinc. Outer membrane (OM), inner membrane (IM), periplasm (P) (proposed by our co-workers: Arnoux *et al*.)

5.3. Conclusions

My work has allowed the development of analytical strategy essentially based on HILIC with dual ICP MS and electropsrya MS detection for the discovery and characterization of a novel a novel metallophore, named pseudopaline. This métallophore is synthesized and exported by *Pseudomonas aeruginosa* and serves for the uptake of nickel in metal poor media, and for the uptake of zinc in metal scarce conditions that mimic the chelating environment. Pseudopaline differs from staphylopine with regard to the stereochemistry of its histidine moiety associated to an alpha ketoglutarate moiety instead of pyruvate. *In vivo*, the pseudopaline operon is regulated by zinc through the Zur repressor. The work illustrated the combination of state-of-the art analytical chemistry and molecular biology approaches.

Reference

1. Thompson, J. and J.A. Donkersloot, *N-(Carboxyalkyl) Amino Acids: Occurrence Synthesis and Functions.* Annual review of biochemistry, 1992. **61**(1): p. 517-554.
2. Pederick, V.G., et al., *ZnuA and zinc homeostasis in Pseudomonas aeruginosa.* Scientific reports, 2015. **5**.
3. Nakashige, T.G., et al., *The hexahistidine motif of host-defense protein human calprotectin*

contributes to zinc withholding and its functional versatility. Journal of the American Chemical Society, 2016. **138**(37): p. 12243-12251.

4. Vignesh, K.S. and G.S. Deepe, *Immunological orchestration of zinc homeostasis: The battle between host mechanisms and pathogen defenses.* Archives of biochemistry and biophysics, 2016. **611**: p. 66-78.
5. Bielecki, P., et al., *In-vivo expression profiling of Pseudomonas aeruginosa infections reveals niche-specific and strain-independent transcriptional programs.* PLoS One, 2011. **6**(9): p. e24235.
6. Hood, M.I. and E.P. Skaar, *Nutritional immunity: transition metals at the pathogen–host interface.* Nature Reviews Microbiology, 2012. **10**(8): p. 525-537.
7. Barber, M.F. and N.C. Elde, *Buried treasure: evolutionary perspectives on microbial iron piracy.* Trends in Genetics, 2015. **31**(11): p. 627-636.
8. Ganne, G.r., et al., *Iron release from the siderophore pyoverdine in Pseudomonas aeruginosa involves three new actors: FpvC, FpvG, and FpvH.* ACS Chemical Biology, 2017. **12**(4): p. 1056-1065.
9. Ding, Y., et al., *Staphylococcus aureus NorD, a putative efflux pump coregulated with the Opp1 oligopeptide permease, contributes selectively to fitness in vivo.* Journal of bacteriology, 2012. **194**(23): p. 6586-6593.
10. Gi, M., et al., *A novel siderophore system is essential for the growth of Pseudomonas aeruginosa in airway mucus.* Scientific reports, 2015. **5**.

Chapter 6. Development of analytical approaches to link iron speciation and bioavailability in maize

Iron (Fe) is essential for virtually all living organisms. Inadequate intake of iron results in iron-deficiency anemia (IDA), especially in children [1], and is a serious problem worldwide [2-4]. The main reason of IDA is the poor availability of iron in foodstuffs of plant origin. Therefore, there is considerable interest in enhancement of the iron bioavailability from staple foods [1].

Maize is the third most important cereal crop in the world, it supplies not only energy in the form of carbohydrates, fat and proteins but also vitamins and many minerals, including iron. However, only 5-20% of the iron in maize can be assimilated by man [5]. Therefore, different breeding and genetic engineering strategies were investigated to increase the bioavailability of iron in maize with the goal of increasing the concentration of iron-binding chelators and proteins, decreasing the concentration of absorption inhibitors and increasing the concentration of absorption promoters [6].

Iron bioavailability is defined as the proportion of iron in a food which is digested, absorbed, and ultimately utilized for normal body functions [7]. Several methods have been developed over time to assess the iron bioavailability in foodstuffs. The chemical balance method is based on the determination of the difference between the iron taken in with food and iron excreted with feces [8]. The solubility approach , based on Caco-2 Cells model, deals with only nonheme iron since heme iron is directly absorbed and enters the enterocyte as heme [9]. The rat hemoglobin repletion method is a standard method used by the Association of Official Analytical Chemist. The isotopic methods which are based on labelling food with an iron isotope intrinsically (biosynthetically) [10] or during the iron absorption measurement [11]. A widely used method to assess the iron bioavailability is based on the use of Caco-2 (human adenocarcinoma) cells [12].

The bioavailability of iron strongly depends on its chemical form. Hence, the description of the bioavailability of iron in food on the molecular level and linking this data with the operational approaches is of potential interest. The relevant analytical approaches are based on chemical fractionation or fractionation under simulated gastrointestinal conditions which are followed by the identification of the released species [13]. Despite several efforts there are several limitations in methodology, especially on the level of the iron species identification, and the truly molecular characterization is seldom achieved [15].

Regarding iron speciation in foods, few works referred to the presence of iron mugineic acid complexes [14], iron – phytate complex which was considered main inhibitors of iron bioavailability [15], and some other amino acid complexes, especially citrate [16]. For maize, there is no information on the distribution of iron amongst its major chemical constituents (e.g. proteins or polysaccharides) nor on the chemical speciation of iron.

The goal of this work was to develop an analytical methodology able to provide information on the fractionation and speciation of iron in maize. For this purpose, the protocols of the enzymatic fractionation were re-visited to provide the first data of the operationally defined iron chemical distribution in this corn. The couplings of hydrophilic interaction chromatography (HILIC) with the parallel detection by inductively coupled plasma mass spectrometry coupling of spectrometry (ICP MS) and high resolution electrospray mass spectrometry (HR ESI MS) were developed to identify the iron complexes. The methods were applied to investigate well characterized genetically modified maize varieties having shown difference in the in vivo bioavailability [17-19] with an attempt to correlate the chemical information with bioavailability data obtained using the Caco-2 cells method.

6.1. Development of iron fractionation method in maize

The objective of the work being to define a chemical molecular signature of iron (association with different molecular fraction and/or speciation) and to attempt to use it to find differences between the different maize varieties investigated.

6.1.1. Total iron determination

The HB, LB, HM and LM varieties were found not to differ in terms off the iron content. Indeed, the iron contents measured (4 individual seeds of each analysed in triplicate) were showing in **Fig. 6.1**.

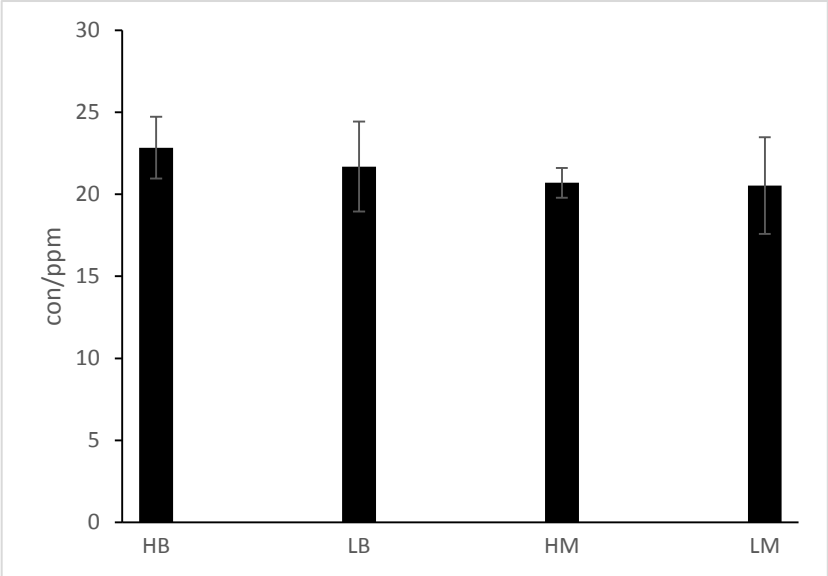

Fig. 6.1. Total concentration of iron in different maize samples. Data represents the average (SD of 4 individual seeds in triplicates analysis)

The iron concentration measured in the NIST8436 Durum Wheat Flour reference material was for the different series of data measured on different days shows in the **table 6.1.**

Table 6.1. Data for standard reference materials

	^{56}Fe (ppm)	^{64}Zn (ppm)	Fe expected value	Zn expected value
WHEAT FLOUR* (50mg)	11.83±0.48	10.55±0.65	14.1±0.5	11.6±0.4

*NIST 8436 Durum Wheat Flour reference material

6.1.2. Development of iron fractionation method in maize

The objective was to solubilize maize completely in the mildest possible conditions without mineralization. According to the literature, maize contains typically: carbohydrate, protein, fat and crude fiber. The rest is moisture and mineral residual to see **Table 6.2** [20].

Table 6.2. Weight loss of each fraction of maize type

	Weight raitio[a]	**Weight raitio[b]**
Protein	5.2-13.7 %	11%
Ether extractable	2.2.-5.7 %	4%
Carbohydrate	66.0-75.9 %	61%

[a] from reference data, [b] from our results [20]

Consequently, a number of procedures targeting the dissolution of the individual components were adapted from literature. They were: extraction of water soluble components with water [21]; fat removal with hexane [22]; starch degradation with α-amylase and amyloglucosidase [23], and proteolysis with pepsin [24]. The capacity of the procedures used independently or in sequence was investigated using weight loss, as an indicator of the efficiency of the approach. The sample used was commercially available maize kernels purchased in a local shop as animal feed. The method of maize fraction were validated by two different ways：the independent procedure fraction and sequential fraction like shows in follow **Fig. 6.2**

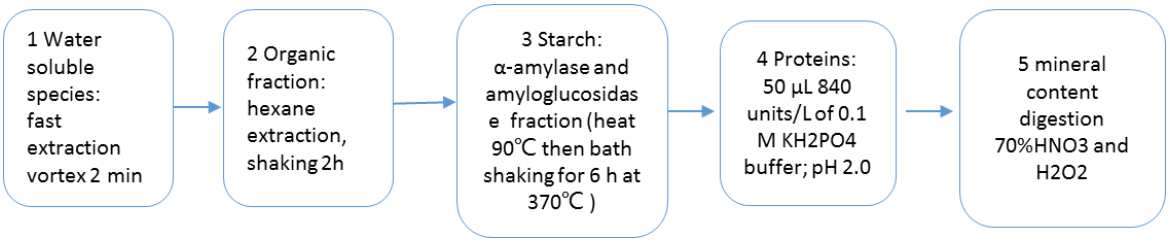

Fig. 6.2. Outline of the procedure which operated on real samples

Both procedure give us details that no mass loss was measured for water extraction. Extraction with hexane resulted in a 5 ± 1% mass loss. The saccharification and proteolysis resulted in a loss of 69.5 ± 0.5 and 11.5 ± 0.5% of mass. Saccharification and proteolysis were independent from each other, in the sense that the same loss of mass was observed for proteolysis of the residue upon removal of starch. In conclusion over 85% of the corn mass was removed after sequential defatting, saccharification and proteolysis. The residue could

was not attacked by phytase although the latter resulted in a mass loss of 10-15% when applied directly on the defatted extract

In parallel, the iron mass balance was controlled (**Table 6.3**). Neither of the extraction procedures when applied individually and directly to the sample allowed the complete recovery of the iron. About 15% of iron could be extracted to water and the most efficient extracting agent was pepsine allowing the recovery of 70% of iron. No iron was found to be associated with the polysaccharide fraction and 15% of iron was observed in the residue. Note that the defatting facilitates the enzymatic attack.

The sequential application of the extraction procedures leads to the recovery of over 90% of iron from the sample (**Table 6.3**).

Table 6.3. Recoveries of iron from maize using the independent extractions and the sequential procedure

Water extraction, %	**Hexane extraction, %**	**Starch degradation, %**	**Proteolysis, %**	**Residue, %**	**Recovery, %**
Individual (independent) procedures					
10.3±2.8				87.0±0.0	97.2±2.8
	7.9±0.9			84.1±18	92.1±17
		<1		90.7±10	92.0±8
			72±17	22.0±4.7	94.0±9
Sequential procedure					
10.3±2.8	7.9±0.9	<1	61.7±10	14.5±1.0	90.6±18

Total Fe content: 21.4± 2.2 µg/g

6.1.3. Iron fractionation in maize

The sequential procedure has been applied to the samples in order to investigate the difference between them in terms of the iron binding forms. Four varieties of maize samples (10 biological replicates and 3 analytical replicates of each) were analysed. The data presented in **Table 6.5** confirms that iron is principally bound to water insoluble proteins (50-70%) or present in the water-soluble extract (15-20%). The fractions associated with fat and starch are

absent within or close to the statistical error.

Table 6.5 Iron release from the genetically modified samples using the developed sequential procedure

Sample	Water extraction, µg/g	Hexane extraction, µg/g	Starch degradation, µg/g	Proteolysis, µg/g)	Recovery, %
HB2	2.6±0.8	≤0.01	1.5±1.4	13.9±2.4	87.4
LB2	4.0±1.2	0.2±0.5	1.9±0.9	14.1±0.7	92.7
HM1	2.6±0.5	0.3±0.1	2.0±0.4	11.0±1.2	69.7
LM1	3.4±1.5	0.4±0.6	1.1±0.4	8.9±0.8	76.7

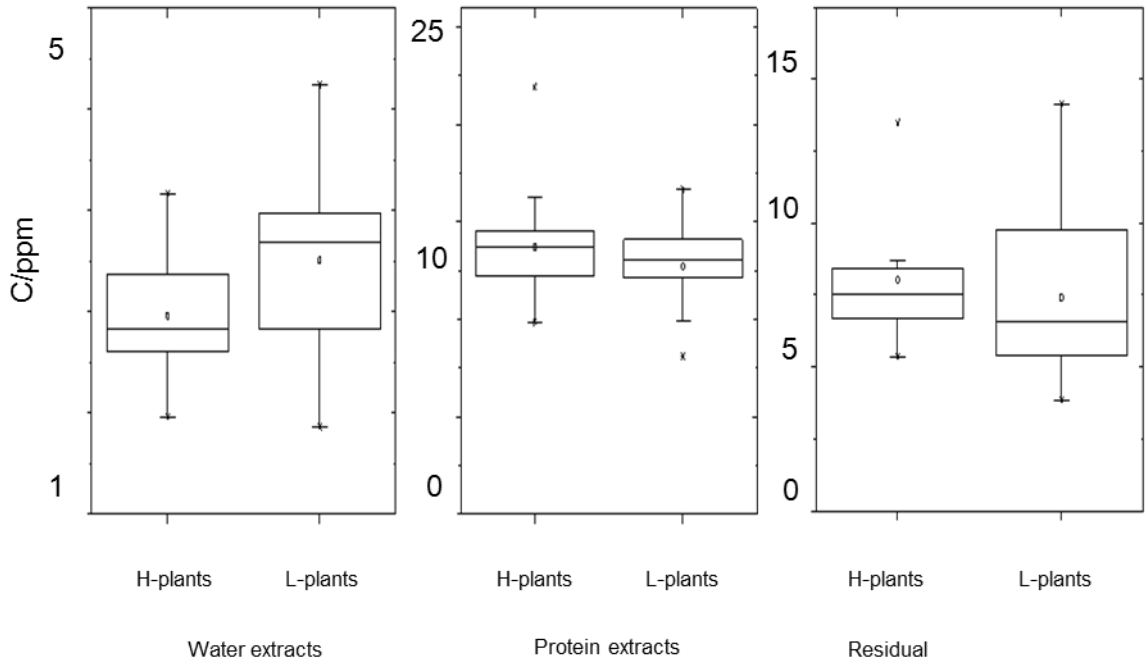

Fig. 6.3 shows the boxplot summarizing the statistical evaluation of the results obtained using the ANOVA method. The variations between the samples are statistically very week. The only statistically difference was observed in the water fraction where the low available varieties showed higher Fe soluble fraction.

6.2. Speciation of water-soluble iron species in maize

The observation of a possible correlation between the maize variety and water-soluble iron lead us to investigate the chemical speciation of iron in this fraction. The two

mechanisms investigated for the separation of iron species included size-exclusion and HILIC. The chromatograms shown in **Fig. 6.4** and **6.5**, respectively, are, to our best knowledge, the first records of the molecular distribution of water-soluble iron in maize.

Size exclusion chromatography with ICP MS detection offers the advantage of fine fractionation of iron species according to the molecular mass using a direct injestion and simple mobile phase thuis reducing the changes in speciation [26]. A representative chromatogram is shown in **Fig. 6.4**. It shows one major and three minor peaks. The major peak coelutes with phosphorous which suggests the presence of phytate. The mass of Fe-phytate is difficult to observe by ESI MS as the coeluting free form is very intense. Note that "Fe-phytate" is frequently referred to as a non-bioavailable form of Fe because of its poor solubility but nevertheless it stays the most concentrated water soluble species of iron. Electrospray mass spectrum indicates the presence of two complexes: phytate-Fe_2 at *m/z* 713.78 and phytate$_2$-Fe at *m/z* 1373.7. The small peak at about 10 min corresponds to water-soluble protein-complex. The remaining two peaks could be identifies by electrospray MS as corresponding to the iron complexes with citric acid and mugeinic acid.

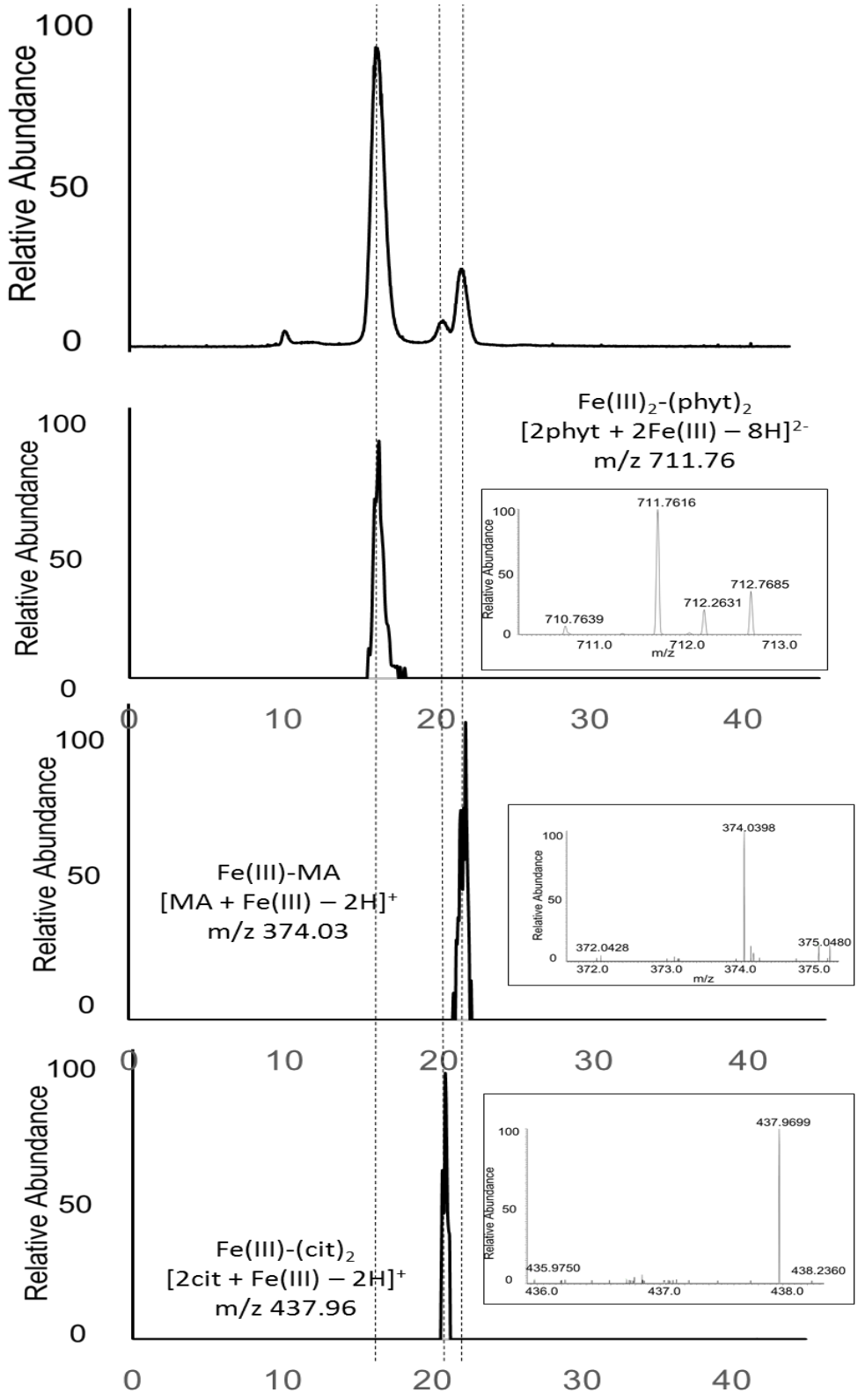

Fig. 6.4. SEC-ICP MS/ESI MS identification of iron species in maize extracts. A- SEC-ICP MS chromatogram, B–Fe-phytate XIC (*m/z* 711.76) , C- Fe-mugeinate ([MW + H^+] 374.03), D – Fe-citrate (([MW + H^+] 437,96); ESI mass spectra are shown in the insets.

HILIC, introduced to speciation analysis by Ouerdane et al.[25]allows the fractionation of metal complexes in biological extracts according their hydrophobicity. The chromatogram in **Fig. 6.5** shows severals peak. First broad and intense peak was identified by electrospray MS as corresponding to thre iron-mugineic acid complex (*m/z* 374.03). The broad massif of peaks in the elution range of hydrophilic compounds corresponds to the complexes with phytate (*m/z* 660.86). There are likely to be several complexes of iron-phytate present, note that ionization of iron-phytate complexes in electrospray does not match, in terms of intencsity the ionization of iron in ICP MS. Note that the phytate may precipitate at the top of the column (90% acetonitrimle) and be subsequently released which can explain the poor peak definition. HILIC – ESI MS confirms the presence of Fe-$(citrate)_2$

The morphology of neither HILIC nor SEC chromatograms acquired for all the studied samples did not show statistically important differences between the H and L-type samples for iron species present in water extract. However, some other detected molecules are of potential interest as they are systematically concentrated in the group of LB and LM plants L but almost absent in their counterpart, HB and HM plants(m/z 296.13 , m/z 441.19, m/z 493.27). (Fig 5) However no significative differences were observed between HH and LL plants.

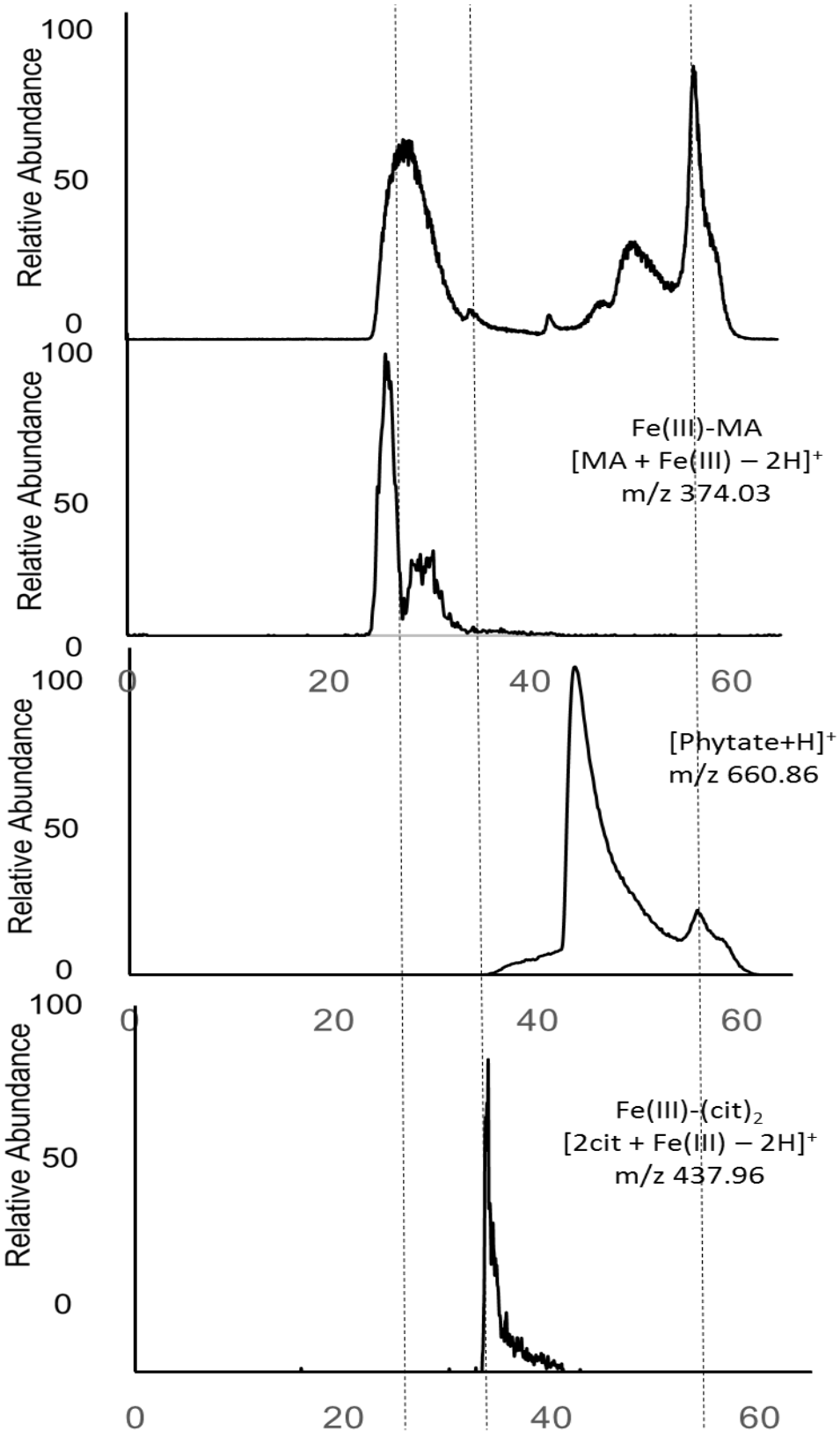

Fig. 6.5. HILIC-ICP MS/ESI MS identification of iron species in maize extracts. A- HILIC-ICP MS chromatogram, B –Fe-mugeinate ([MW + H^+] 374.03), C - phytate XIC (([MW + H^+] 660,86) , D – Fe-citrate (([MW + H^+] 437,96); ESI mass spectra are shown in the insets.

The chromatograms of four kind of maize plants are presented in **Fig. 6.6** for LM, LB, HM, and HB samples respectively.All the chromatograms show a similar pattern with satisfactory reproducibility. However, some samples show the different intensity with generally the same retention times and similar main peak area ratios. Hypothesis that the variation is caused by the heterogeneity of the samples.

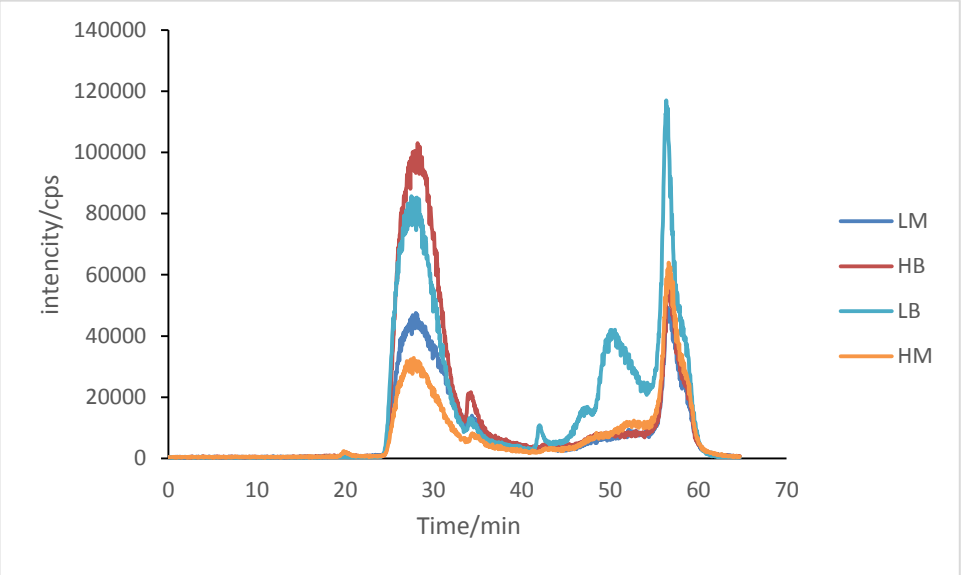

Fig. 6.6. HILIC-ICP-MS chromatograms of iron 56 in maize HB/LB and HM/LM

While comparing the intensities of individual peaks, taking into account of the changes in the sensitivity of ICP MS detection with the changing content of the organic modifier during gradient elution is necessary. Also we checked the sensitivity of Fe in different proportion of water-acetonitrile solution as follows. A series of Fe (and other metals) standard solutions containing different percentage of ACN corresponding to gradient (every 10 %) were prepared. **Fig. 6.7** shows signal intensities as a function of ACN percentage. Then peak area were normalized taking into account the changes in sensitivity during the gradient eluent.

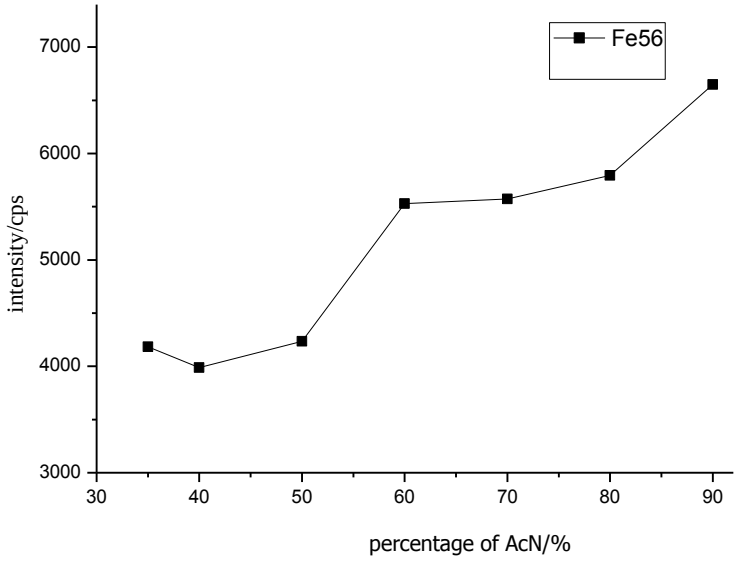

Fig. 6.7. Sensitivity of iron in gradient eluent

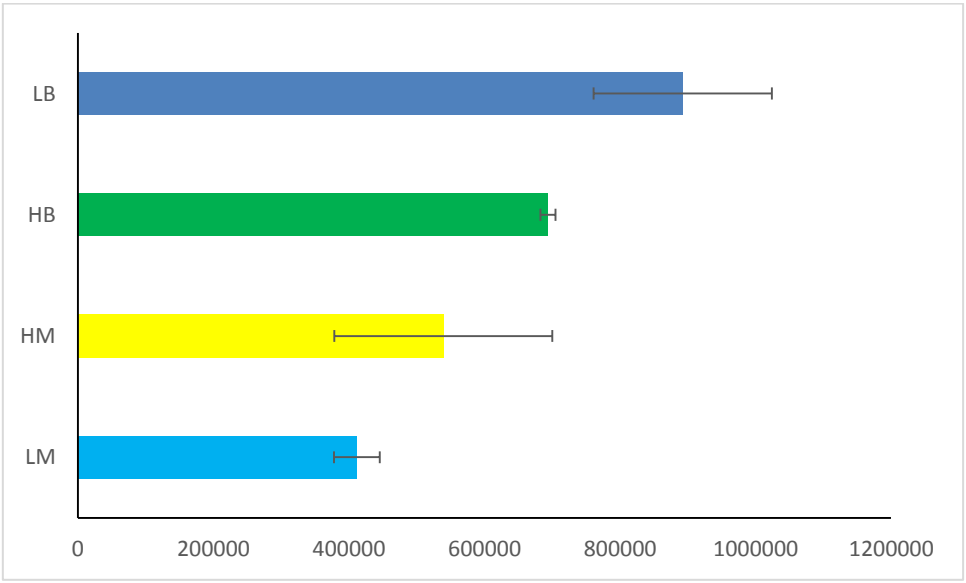

Fig. 6.8. Distribution among the peaks (%)

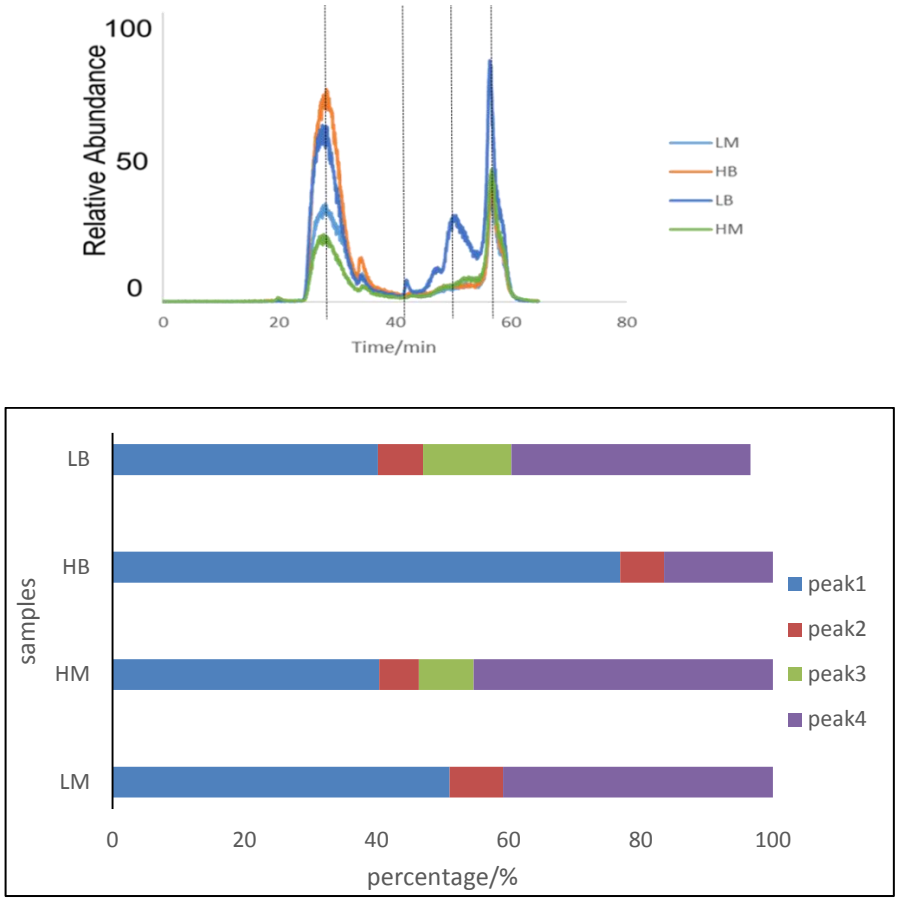

Fig. 6.9. Each peaks of chromatograms attributes to total area (%)

Following these experiments, peak areas were integrated and normalized to determine the contribution of individual peaks. The dominating species elutes as broad peak at the beginning of the chromatogram. The distribution among the peaks in a given sample group shows similar trends. Peak1 in HB plants are significantly higher than in LB plants, whereas HM and LM behave similarly. The next step was the species identification which was carried out by ESI Orbitrap MS using the same chromatographic conditions.

6.2.1. Iron and polyamines

Natural polyamines, such as putrescine, spermidine, and spermine, which are present in maize in large amounts, are assumed to play a role in nonheme iron uptake and iron bioavailability from nutrients [26]. Putrescine was shown to activate Caco-2 cell iron uptake and to induce an increase in the ferritin level. Polyamines can also serve as vectors to form a 3:1 complex with Fe(III) and to be taken up by the polyamine transporter 1900-fold against a concentration gradient. Therefore, polyamines are likely to serve as vectors for the

intracellular delivery of other iron chelators [27].

A search for polyamins by HPLC – electrospray MS chromatograms of the water extracts of L and H varieties indicated (The compound at m/z 493 was found to be much more concentrated in LM and LB group plants (500 to 1000 times less) than in plant of HB and HM groups. The exact compound was tentatively identified as aphelandrine (spermine conjugated to hydroxycinnamic acids and cyclized). The conjugation to hydroxycinnamic acids is known to reduce the capacity of polyamine for iron binding [26, 28] . The presence of these conjugated polyamines in L plants and almost not in H plants could be due to a difference in plant stress response or plant maturation between these two types of plants. It could then result in higher level of plant matrices cross linkages and amine conjugation in LB and LM plants, which could participate to the lower iron bioavailability of this plant group. Indeed free amine molecules like polyamines are known to help Fe assimilation [26], a capacity they lose if conjugated, and, moreover, a denser plant matrix through crosslinkage due to this type of conjugations could lead to iron trapping or, at least, could slow its release.

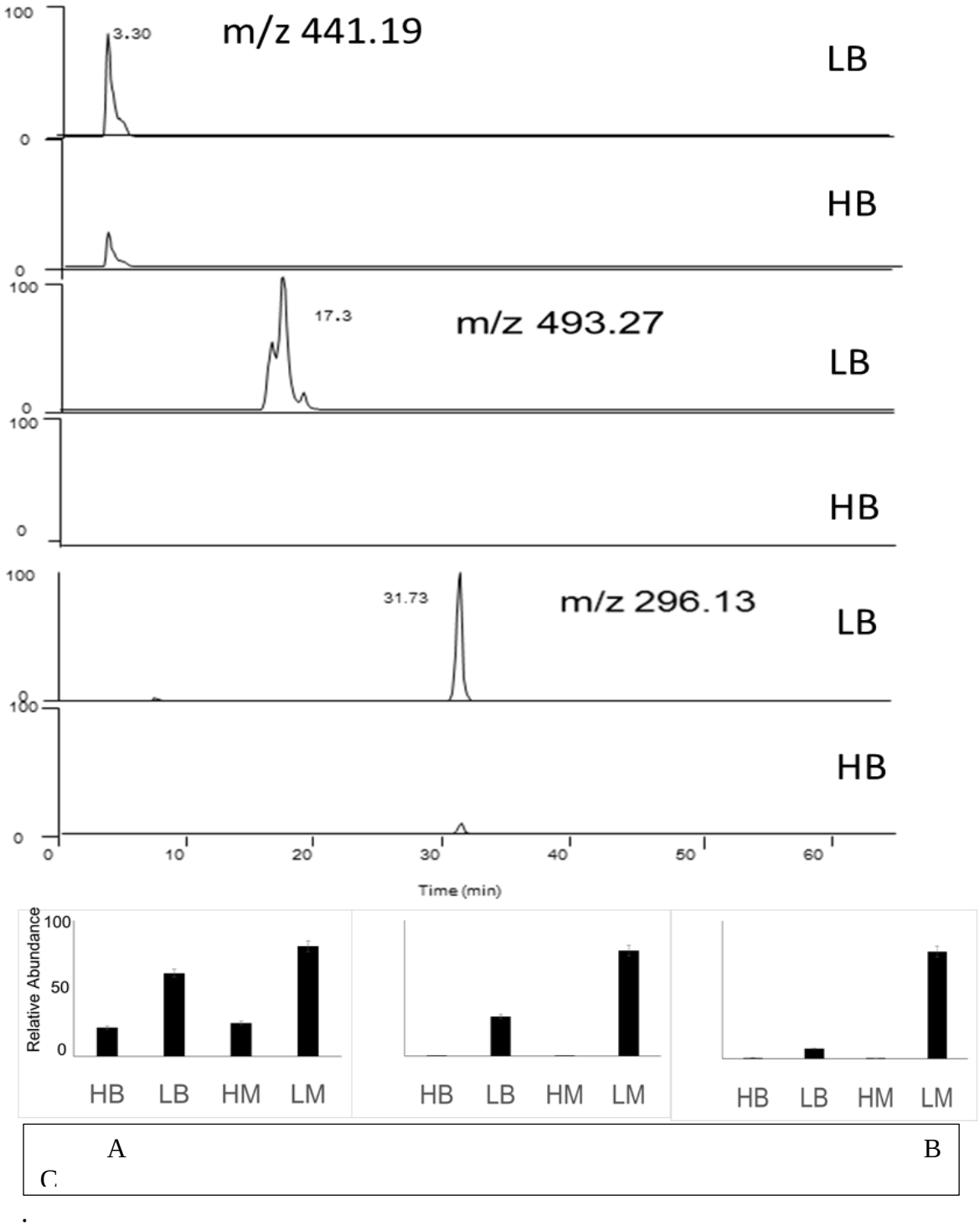

.

Fig. 6.10. Variety s-specific in terms of polyamine content. HILIC (ESI MS/MS) bar chart shows the peak area comparison of each molecular corresponding to the mass spectrum top.

6.3. Iron release in simulated gastro-intestinal conditions

Another attempt to correlate the chemical speciation of iron with the observed difference of iron bioavailability from HH and LL varieties was made using simulated gastro-intestinal conditions. The samples did not show a statistically significant difference in the iron extraction either after the first step (pepsine) or the second (after addition of pancreatinin). The ratio of the Fe/P in the obtained extract was the same for the HH and LL varieties.

An interesting observation is the presence of a Fe-citrate peak in the gastrointestinal maize extracts of the HH line whereas it is absent in the LL line (**Fig. 6.11**)

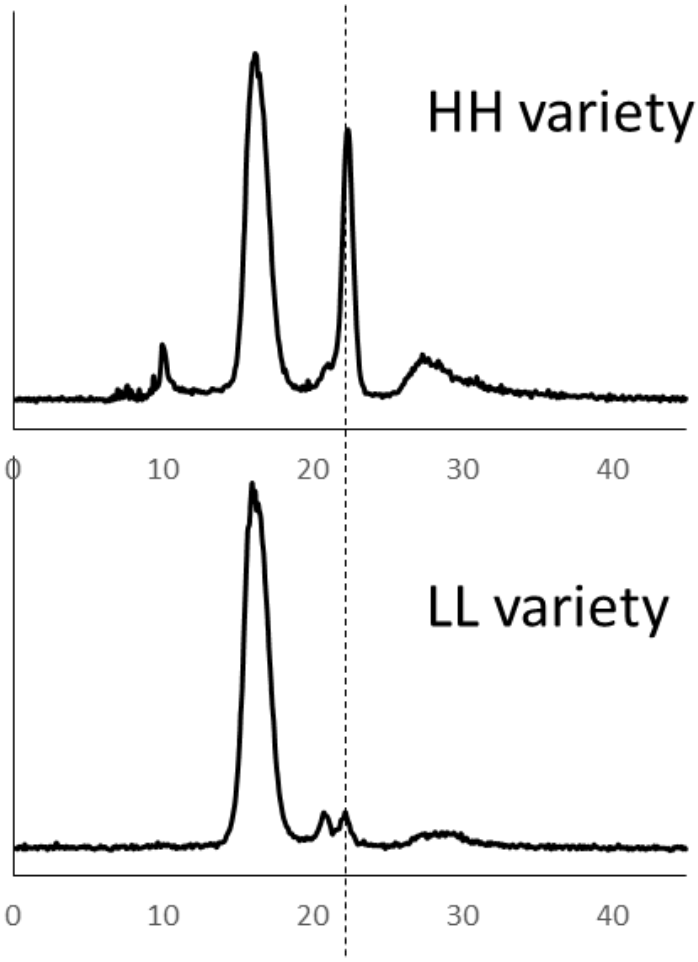

Fig. 6.11. Enrichment of Fe-citrate in HH variety, SEC-ICP MS/ESI MS chromatograms in gastrointestinal maize extracts

A final attempt to discriminate the H and L varieties on the basis of the chemical speciation of iron was based on the comparison of the iron speciation in the gastrointestinal digest. The SEC-ICP MS chromatogram of the LL variety (**Fig. 6.12a**) shows a similar morphology to that of the aqueous extract with a major peak corresponding to the presence of phytate. A comparison of this chromatogram with that of the HH variety shows no significant

difference in terms of the height of the iron-phytate peak, however a fairly intense peak corresponding to the iron citrate appears (**Fig. 6.121b**). Note that the level of free phytate measured as the phosphorus signal in SEC-ICP MS (**Fig. 6.12c**)

Fig. 6.12. Preservation of Fe-phytate complex during gastrointestinal digestion of maize.
SEC-ICP MS chromatogram of sample digests (A- 56Fe, B-31P detection) and standards (C - standard of Fe-phytate complex, 31P detection, D - standard of phytate, 31P detection), and SEC-ESI MS XIC chromatograms of phytate-Fe complexes (E - *m/z* 713.78 and F - *m/z* 1373,7)

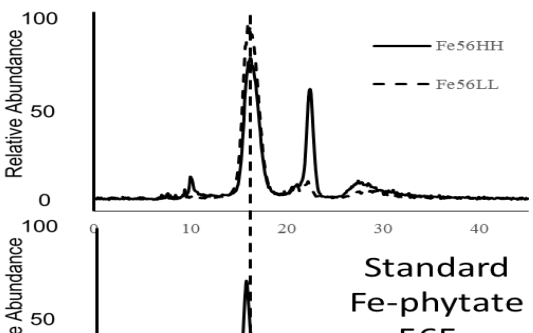

By integrating the peek areas of each peaks of the iron speciation after the gastric intestinal digestion which can illustrate the concentration of each iron species we found that content of mugineic-iron which considered as main bioavailable iron donor higher in H plants than L plants. Whereas phytate-iron which considered as a less bioavailable are less in H plants than L plants as we showed in **Fig. 6.11** and **6.12**.

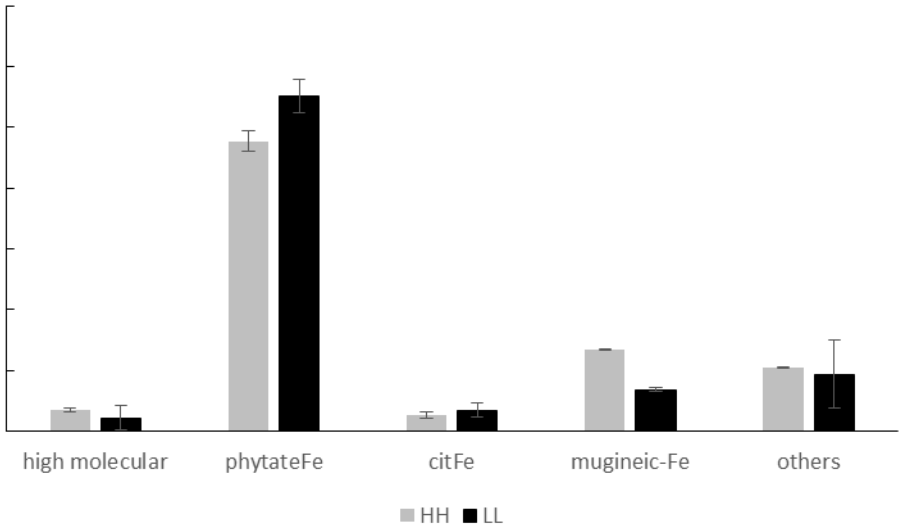

Fig. 6.13. Contribution of each Fe-complex in maize GI digests/by integrating the peak area of size-exclusion chromatography – ICP MS

We also calculated the contribution of each Fe-complex which eluted in SEC-ICP-MS of maize gastrointestinal digests. By integrating the peak area, we could find that Fe (III)-MA gavea significant difference between H plants and L plants after gastro-intestinal digestion in **Fig. 6.13** and **6.14** whereas no change occurred in water extracts. This suggests that gastrointestinal enzymes released more Fe (III)-MA during the digestion. It may be possible that a factor blocks the Fe(III)-MA release in LL plants. Also, the Fe/P ratio (**Fig. 6.15**) showed more iron released in HH plants in comparison with LL plants after GI digests/by integrating the peak area of SEC.

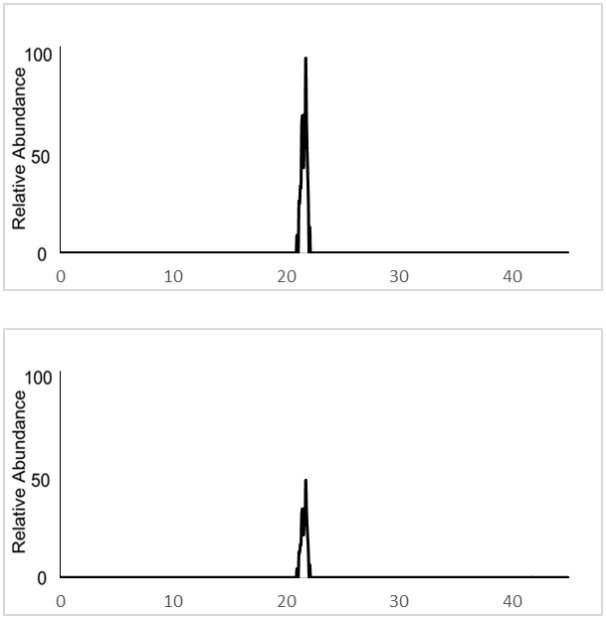

Fig. 6.14. ESI- MS of the mugineic-Fe complex in the digests from HH and LL

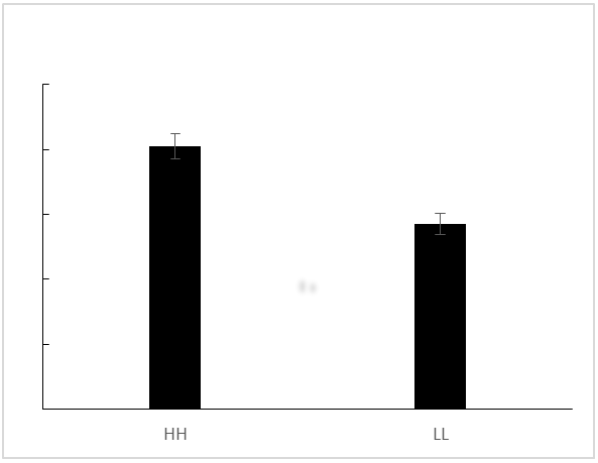

Fig. 6. 15. Fe/P ratio shows more iron released during the gastrointestinal digestion of HH varieties than of LL varieties . Data obtained by SEC - ICP MS

6.4 Kinetics of iron speciation during gastro-intestinal digestion

To monitor the release of iron during gastrointestinal digestion we collected samples as follows: Sample A: 200mg of sample + pepsin solution diluted to 4mL pH 2 after 1h; Sample B: apancreatin solution added, sample brought to 6mL; Sample C: 2 mL 0.1 M HCl added, the solution brought to 8 mL (pH 2) for 5 min and centrifuged; Sample D: 5mL of a 1.25% H_2SO_4 solution added, after 2h at ambient temperature. Sample E: the residues washed with water and dried to detected the total iron concetration.

We could observe that during pepsin digestion less of iron is released in HH plants than

LL plants but after the whole digestion procedure the same concentration of iron was found. Iron would seem to be easier released in intestine for HH than LL plants. To figure out how the pH affects digestion and the total iron released by gastric intestinal digestion, the solution was brought to pH 2 after 3 H. The difference in the released iron concentration normalize for phosphorous for the HH and LL plants is shown in **Fig. 6.15**.

The analysis by SEC-ICP-MS shows the presence of Fe-phytate complex in both the HH and LL plants whereas proportion of the P31/Fe56 is inversed between HH and LL groups. Following the GI digestion, the iron release by three additional extraction steps completed the results. We observed a significant difference between HH and LL plants in terms of iron-to-phosphorus ratio.

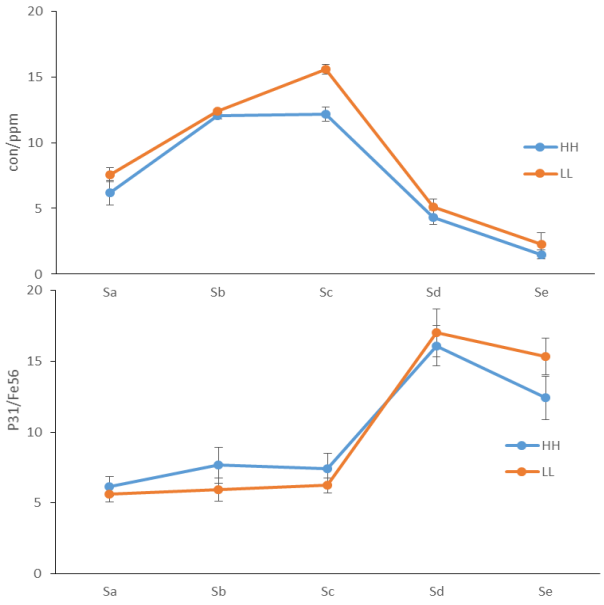

Fig. 6.16 Total concentration of iron during gastric intestinal digestion(left), Fe56/P31 during gastric intestinal digestion(right) Sa>200mg maize+pepsin solution diluted to 4mL pH 2 in 1h. Sb>Adding pancreatin solution bring to 6mL Sc>Adding 2 mL HCl(0.1mol/L) to the solution bring to 8 mL pH 2 extracted 5minCentrifuged. Sd> Adding in 5mL of a 1.25% H2SO4 solution 2h ambient TEMP. Se> the residual were all washed to remove the digests and the dried to detected the total iron concentration.

6.5. Conclusions

A series of analytical methods were developed for an insight into the fractionation and speciation of iron in maize. A sequential fractionation procedure based on (i) water extraction, (ii) hexane extraction, (iii) saccharification, and (iv) proteolysis was developed to provide the first data on the molecular distribution of iron in maize. This was completed by the

operational determination of the iron bioavailability using an in-vito simulated model for gastro-intestinal digestion. The coupling of hydrophilic interaction chromatography (HILIC) with the parallel detection by inductively coupled plasma mass spectrometry (ICP MS) and high resolution electrospray mass spectrometry (HR ESI MS) allowed the identification of water-soluble iron muginate, citrate, and phytate complexes. The procedures were applied to study some well characterised genetically modified maize varieties having shown differences in the iron bioavailability [17-19].

The study allowed the first insight into iron speciation in maize kernels. Iron was found to be principally bound to water insoluble proteins (50-70%) or present in the water-soluble extract (15-20%). The fractions associated with fat and starch did not contain iron. The couplings of HILIC and SEC chromatography with ICP-MS and ESI- Orbitrap MS allowed the detection and identification of iron citrate, mugineate and phytate complexes. These species were detected and compared in genetic varieties of maize known to have different iron bioavailability from Caco-2 cell experiments. The study did not allow the demonstration of the meaningful chemical speciation of iron to explain a 20% difference in bioavailabnility observed using Caco-2 cells. Some findings meriting a deeper investigation include the significant difference in polyamine concentration and the presence of iron-citrate complex in the gastrointestinal extract of high bioavailable variety and quasi-absent in the low bioavailable one.

References

1. Oikeh, S.O., et al., *Assessment of Concentrations of Iron and Zinc and Bioavailable Iron in Grains of Early-Maturing Tropical Maize Varieties.* Journal of Agricultural and Food Chemistry, 2003. **51**(12): p. 3688-3694.
2. Bodnar, A.L., et al., *Iron bioavailability of maize hemoglobin in a Caco-2 cell culture model.* J Agric Food Chem, 2013. **61**(30): p. 7349-56.
3. Eagling, T., et al., *Iron bioavailability in two commercial cultivars of wheat: comparison between wholegrain and white flour and the effects of nicotianamine and 2'-deoxymugineic acid on iron uptake into Caco-2 cells.* J Agric Food Chem, 2014. **62**(42): p. 10320-5.
4. La Frano, M.R., et al., *Bioavailability of iron, zinc, and provitamin A carotenoids in biofortified staple crops.* Nutr Rev, 2014. **72**(5): p. 289-307.
5. Bachir Daoura, G. and C.T. Hash, *Breeding for high grain Fe and Zn levels in cereals.* International Journal of Innovation and Applied Studies, 2015. **12**(2): p. 342-354.
6. Clemens, S., *Zn and Fe biofortification: the right chemical environment for human bioavailability.* Plant Science, 2014. **225**: p. 52-57.
7. Fairweather-Tait, et al., *The Use of Solubility, Dialyzability, and Caco-2 Cell Methods to Predict Iron Bioavailability.* International Journal for Vitamin and Nutrition Research, 2007.

77(3): p. 158-165.

8. Wienk, K.J.H., J.J.M. Marx, and A.C. Beynen, *The concept of iron bioavailability and its assessment.* European Journal of Nutrition, 1999. **38**(2): p. 51-75.
9. Au, A.P. and M.B. Reddy, *Caco-2 Cells Can Be Used to Assess Human Iron Bioavailability from a Semipurified Meal.* The Journal of Nutrition, 2000. **130**(5): p. 1329-1334.
10. Hurrell, R. and I. Egli, *Iron bioavailability and dietary reference values.* The American Journal of Clinical Nutrition, 2010. **91**(5): p. 1461S-1467S.
11. Cook, J.D., et al., *Food Iron Absorption Measured by an Extrinsic Tag.* Journal of Clinical Investigation, 1972. **51**(4): p. 805-815.
12. Fairweather-Tait, S., et al., *The use of solubility, dialyzability, and Caco-2 cell methods to predict iron bioavailability.* Int J Vit Nutr Res, 2007. **77**.
13. Bou Khouzam, R., et al., *Trace element speciation in food: State of the art of analytical techniques and methods.* Pure and Applied Chemistry, 2012. **84**(2).
14. Weber, G., G. Neumann, and V. Römheld, *Speciation of iron coordinated by phytosiderophores by use of HPLC with pulsed amperometric detection and AAS.* Analytical and Bioanalytical Chemistry, 2002. **373**(8): p. 767-771.
15. Persson, D.P., et al., *Simultaneous iron, zinc, sulfur and phosphorus speciation analysis of barley grain tissues using SEC-ICP-MS and IP-ICP-MS.* Metallomics, 2009. **1**(5): p. 418-426.
16. Teucher, Olivares, and Cori, *Enhancers of Iron Absorption: Ascorbic Acid and other Organic Acids.* International Journal for Vitamin and Nutrition Research, 2004. **74**(6): p. 403-419.
17. Glahn, R.P., et al., *Caco-2 Cell ferritin formation predicts nonradiolabeled food iron availability in an in vitro digestion/Caco-2 Cell culture model.* J Nutr, 1998. **128**.
18. Glahn, R.P., et al., *Caco-2 Cell Iron Uptake from Meat and Casein Digests Parallels in Vivo Studies: Use of a Novel in Vitro Method for Rapid Estimation of Iron Bioavailability.* The Journal of Nutrition, 1996. **126**(1): p. 332-339.
19. Glahn, R.P., et al., *Comparison of Iron Bioavailability from 15 Rice Genotypes: Studies Using an in Vitro Digestion/Caco-2 Cell Culture Model.* Journal of Agricultural and Food Chemistry, 2002. **50**(12): p. 3586-3591.
20. *<2992-9068-1-PB (1).pdf>*.
21. Sázelová, P., et al., *Extraction and separation of water‐soluble proteins from Bacillus thuringiensis‐transgenic and non‐transgenic maize species by CZE.* Journal of separation science, 2009. **32**(21): p. 3801-3808.
22. Mullen, C.A., et al., *Analysis and comparison of bio-oil produced by fast pyrolysis from three barley biomass/byproduct streams.* Energy & Fuels, 2009. **24**(1): p. 699-706.
23. Al-Rabadi, G.J.S., R.G. Gilbert, and M.J. Gidley, *Effect of particle size on kinetics of starch digestion in milled barley and sorghum grains by porcine alpha-amylase.* Journal of Cereal Science, 2009. **50**(2): p. 198-204.
24. Mertz, E.T., et al., *Pepsin digestibility of proteins in sorghum and other major cereals.* Proceedings of the National Academy of Sciences, 1984. **81**(1): p. 1-2.
25. Arnaudguilhem, C., et al., *Selenium metabolomics in yeast using complementary reversed-phase/hydrophilic ion interaction (HILIC) liquid chromatography–electrospray hybrid quadrupole trap/Orbitrap mass spectrometry.* Analytica Chimica Acta, 2012. **757**: p. 26-38.
26. Lescoat, G., et al., *Involvement of polyamines in iron(III) transport in human intestinal*

Caco-2 cell lines. Molecular and Cellular Biochemistry, 2013. **378**(1): p. 205-215.

27. Bergeron, R.J., et al., *Polyamine−Iron Chelator Conjugate.* Journal of Medicinal Chemistry, 2003. **46**(25): p. 5478-5483.
28. Petry, N., et al., *Polyphenols and phytic acid contribute to the low iron bioavailability from common beans in young women.* J Nutr, 2010. **140**.

Part V.
CONCLUSIONS

Part V. CONCLUSIONS

The thesis resulted in the development of two types of novel analytical approaches to the speciation of iron in bacteria and plants. The ultimate speciation analysis was achieved based on the couplings of size exclusion chromatography (SEC) and hydrophilic interaction chromatography (HILIC) to either mass spectrometer with ionization in inductively coupled plasma (ICP MS) or LTQ Velos Orbitrap with electrospray ionization (ESI) for elemental and molecular analysis, respectively. The combination and collation of information obtained by high resolution ESI-MS (exact monoisotopic masses, characteristic isotopic signatures recognition and interisotopic mass defect) and with ICP-MS (retention times, shapes and intensities of chromatographic peaks of iron and other elements) resulted in state of the art methodology for speciation analysis in biological samples.

Beyond the coupled techniques, the thesis brought to light the problem of the analysis of solid and largely water insoluble samples for speciation analysis of metal coordination complexes demonstrated on the example of iron speciation and fractionation in maize.

The exploratory analytical approach based essentially on the development of HILIC with ICP MS and electrospray MS detection allowed the discovery of two new metallophores, named staphylopine and pseudopaline in two types of bacteria staphylococcus *aureus* and pseudomonas *aeruginos*a, respectively. The metallophores were exhaustively characterized in terms of their structures and multi-metal complexation behavior. Their biological function was extensively investigated by the combination of state-of-the art analytical chemistry and molecular biology approaches in frame of a joint project funded by the French National Research Agency (ANR). Metal uptake is vital for all living organisms. In metal scarce conditions, a common bacterial strategy consists in the biosynthesis of metallophores, their export in the extracellular medium and the recovery of a metal-metallophore complex through dedicated membrane transporters.

Staphylopine is a metallophore distantly related to plant nicotianamine that contributes to the broad-spectrum metal uptake capabilities of *Staphylococcus aureus*. Pseudopaline is a staphylopine-like metallophore involved in the biosynthesis and trafficking in *Pseudomonas aeruginosa. It is principal function is to serve* for the uptake of nickel in metal poor media, and for the uptake of zinc in metal scarce conditions that mimic the chelating environment that presumably prevails within a host. It differs from staphylopine with regard to the stereochemistry of its histidine moiety associated to an alpha ketoglutarate moiety instead of pyruvate. The iron-uptake property of the pseudopaline system appears to be secondary in comparison with its effect on nickel uptake, and on zinc uptake in metal scarce conditions.

The development of the combined approaches using the couplings of HILIC and SEC chromatography with ICP-MS and ESI-Orbitrap MS detection allowed the identification of iron citrate, mugineate and phytate complexes in water extracts of maize kernels and the methodology is likely to be extended to other biological samples. These species were detected and compared in genetic varieties of maize known to have different iron bioavailability from Caco-2 cell experiments. However, as the water-soluble iron accounted for 15-20% only, it was necessary to develop a procedure for the insight into iron forms in the water insoluble part. For this, a series of a sequential fractionation procedure based on (i) water extraction, (ii) hexane extraction, (iii) saccharification, and (iv) proteolysis was developed to provide the first data on the molecular distribution of iron in maize. This was completed by the operational determination of the iron bioavailability using an in-vito simulated model for gastro-intestinal digestion.

The procedures were applied to study some well characterised genetically modified maize varieties having shown differences in the iron bioavailability. Iron was found to be principally bound to water insoluble proteins (50-70%). The fractions associated with fat and starch did not contain iron.

Despite the state-of-the art speciation analytical methodology the study did not allow the demonstration of the meaningful chemical speciation of iron to explain a 20% difference in bioavailability observed using Caco-2 cells. Some findings meriting a deeper investigation include the significant difference in polyamine concentration which is quasi-absent in the high bioavailable one and the more abundant presence of iron-mugineic acid complex in the gastrointestinal extract in high bioavailable variety, possibly indicating that iron-mugineic acid can be associated to proteins and released during gastrointestinal digestion.